NAP to EVRS

a re-evaluation of the Dutch input and its impact on the realization of the European Vertical Reference System.

by

K.A.J. Speth

to obtain the degrees of Master of Science at the Delft University of Technology,
to be defended publicly on Thursday October 27, 2016 at 11:00 AM.

Student number:	4019393	
Thesis committee:	Prof. R. Klees,	TU Delft, chair
	Dr. D. C. Slobbe,	TU Delft
	Dr. G. G. Drijkoningen,	TU Delft
	Prof. F. Wellmann,	RWTH Aachen

An electronic version of this thesis is available at `http://repository.tudelft.nl/`.

TU Delft — Delft University of Technology

NAP to EVRS

a re-evaluation of the Dutch input and its impact on the realization of the European Vertical Reference System.

Master of Science Thesis

for the degree of Master of Science in Applied Geophysics at
Delft University of Technology
ETH Zürich
RWTH Aachen University
by

K.A.J. Speth

to be defended publicly on
Thursday October 27, 2016 at 11:00 AM.

Department of Geoscience & Engineering · Delft University of Technology
Department of Earth Sciences · ETH Zürich
Faculty of Georesources and Material Engineering · RWTH Aachen University

Delft University of Technology

Printed in The Netherlands, Switzerland, Germany

Abstract

In 2004, Rijkswaterstaat provided geopotential differences between the benchmarks of the Normaal Amsterdams Peil (NAP) network to the Bundesamt für Kartographie und Geodäsie (BKG) for the realization of the European Vertical Reference System (EVRS). This data was found to be incorrect, resulting in inaccurate transformations between EVRF2007 and the national height systems of the participating countries. To correct the realization of the EVRS and obtain accurate transformations between the height systems, it is essential that the BKG is provided with correct geopotential information on the NAP network.

In this thesis, a computational procedure has been developed to obtain correct geopotential differences. The final procedure was implemented in a MATLAB software package that was provided to Rijkswaterstaat for future computations. The old results were compared with the newly computed results, in order to obtain insight into the origin of the errors made in 2004. The impact of these errors on realizations of the EVRS was examined as well. Finally, the connection of the NAP levelling network to the neighbouring countries, and thus the Unified European Levelling Network, (UELN) was investigated.

Due to the available data, most steps in the computational procedure were already predefined. Therefore, the main development was a method for predicting gravity at the levelling benchmarks. Observed gravity was reduced to surface gravity anomalies to remove height dependency. This makes accurate 2-D interpolation possible. Four methods were tested for the interpolation of these gravity anomalies: ordinary Kriging, least-squares collocation, cubic spline and biharmonic spline. Biharmonic spline interpolation was selected as the gravity prediction method for the final procedure. For potentially further improvement of the gravity prediction, two gravity corrections were investigated as well: residual terrain modelling and correcting for a global gravity field model. Both corrections were found to cause negligible improvement to the gravity prediction with respect to the uncertainty of the levelling observations. Therefore, these corrections were not used in the final procedure.

Large regional differences were observed between the newly obtained results and those of Rijkswaterstaat. These differences could predominantly be explained by a mistake in sign convention of the surface gravity anomalies when restoring the observed gravity.

In an updated realization of the EVRS, using the new NAP geopotential information, a tilt of several millimetres within the Netherlands and Belgium is observed. When updated data from other countries are also considered, datum points heights varied in the centimetre range.

Finally, there are a total of 28 Dutch-German cross-border observations at 13 locations, evenly distributed along the border. This lead to the conclusion that the connection between the NAP and the German levelling network is strong. The connection of the NAP with the Belgian network is much weaker, with only a single observation currently known at the BKG. Although, from the data used here it seems that more connections should be readily available.

Abstract (Nederlands)

Voor het realiseren van het “European Vertical Reference System” (EVRS) heeft Rijkswaterstaat in 2004 geopotentiaalverschillen tussen de peilmerken in het Normaal Amsterdams Peil (NAP) netwerk aan het Bundesamt für Kartographie und Geodäsie (BKG) geleverd. Het bleek dat er fouten in deze data zitten waardoor transformaties tussen het EVRF2007 en hoogtesystemen van deelnemende landen niet nauwkeurig genoeg zijn. Om een correcte realisatie van het EVRS en nauwkeurige transformaties te waarborgen, is het noodzakelijk dat het BKG beschikking krijgt over correcte geopotentiaalverschillen in het NAP netwerk.

In deze masterscriptie is er een berekeningsprocedure ontwikkeld om deze correcte geopotentiaalverschillen te verkrijgen. De uiteindelijke procedure is in een MATLAB softwarepakket geïmplementeerd en verstrekt aan Rijkswaterstaat voor de uitvoering van toekomstige berekeningen. De oude bestaande resultaten zijn vergeleken met de nieuw verkregen resultaten om inzicht te verwerven over de in 2004 gemaakte fouten. Ook zijn de gevolgen van deze fouten op de realisaties van het EVRS bestudeert. Tenslotte, is de verbinding van het NAP met de buurlanden en daarmee het “Unified European Levelling Network” (UELN) onderzocht.

Door de beschikbare data stonden de meeste stappen in de berekeningsprocedure al vast. Wat nog vastgesteld moest worden was een geschikte methode voor het interpoleren van de zwaartekracht op de peilmerk locaties. Waargenomen zwaartekracht is omgerekend naar oppervlakte zwaartekrachtanomalieën. Dit neemt de hoogte afhankelijkheid van de zwaartekracht weg, waardoor nauwkeurig 2-D interpolatie mogelijk is. Vier methodes voor de interpolatie van deze zwaartekrachtanomalieën zijn hier getest: Ordinary Kriging, kleinste-kwadraten colocatie, kubistische spline en biharmonische spline. Er is gekozen om de biharmonische spline methode te gebruiken in de uiteindelijke procedure. Voor mogelijke verdere verbetering van de interpolatie zijn er twee zwaartekrachtcorrecties bekeken: topografische correcties en correctie voor een globaal zwaartekrachtmodel. Voor beide correcties is gebleken dat de interpolatie verbeteringen verwaarloosbaar zijn ten opzichte van de fout in de waterpasmetingen. Beide correcties worden daarom niet gebruikt in de uiteindelijke procedure.

Er zijn grote regionale verschillen tussen de nieuw verkregen resultaten en die van Rijkswaterstaat. Deze verschillen kunnen grotendeels verklaard worden door een fout in het teken van de oppervlakte zwaartekrachtanomalieën bij het terugrekenen naar werkelijke zwaartekracht.

Na een herberekening van het EVRS, met de nieuwe NAP geopotentiaalinformatie, bleek het verschil met de vorige realisatie een kanteling van het referentievlak in Nederland en België van enkele millimeters te zijn. Als de recente bijgewerkte data van andere landen ook meegenomen wordt in de herberekening zijn de hoogteverschillen van de datumpunten in de orde van een centimeter.

Tot slot zijn er momenteel 28 metingen bekend bij het BKG die het NAP netwerk met het Duitse verbindt. Deze metingen zijn verdeeld over 13 locaties, die gelijkmatig zijn gepositioneerd langs de Nederlands-Duitse grens. Hieruit is geconcludeerd dat de verbinding tussen het Nederlandse en Duitse waterpasnetwerk sterk is. Voor de aansluiting met België is echter maar 1 meting bekend bij het BKG, ook al lijken er in de hier gebruikte data meer voor handen te zijn.

Abstract (Deutsch)

Im Jahr 2004 reichte Rijkswaterstaat Differenzen im Geopotenzial zwischen den Knotenpunkten im Normaal Amsterdams Peil (NAP) Netzwerk und dem Bundensamt für Kartographie und Geodäsie (BKG) für die Realisierung des European Vertical Reference System (EVRS) ein. Es wurde herausgefunden dass diese Daten fehlerhaft waren, was zu Ungenauigkeiten in der Transformation zwischen den Höhen des EVRF2007 und den nationalen Höhenreferenzsystemen führte. Um diese Fehler zu korrigieren und eine genauere Transformation zwischen den Höhenreferenzsystemen zu gewährleisten, benötigt das BKG die korrekten Daten aus dem NAP Netzwerk.

Im Rahmen dieser Arbeit wurde ein Verfahren zur Berechnung der genaueren Geopotenzialunterschiede entwickelt. Dieses Verfahren wurde in einem MATLAB Softwarepaket implementiert und an Rijkswaterstaat für zukünftige Berechnungen weitergereicht. Um die Ursachen der Fehler von 2004 genauer zu erörtern wurden die Ergebnisse von 2004 mit den neuen Ergebnissen verglichen. Die Auswirkungen dieser Fehler auf die Umsetzung des EVRS werden ebenso untersucht. Schliesslich wurde die Verbindung des NAP zu den Nachbarländern und damit auch zum “Unified European Levelling Network” (UELN) überprüft.

Aufgrund der vorhandenen Daten waren die meisten Schritte im Berechnungsverfahren bereits vorgegeben. Somit stand die Entwicklung einer geeigneten Methode für die Berechnung der Gravitationsmessungen an den Knotenpunkten des Nivellements im Mittelpunkt. Die gemessene Schwerkraft wurde zu Oberflächenschwerkraftanomalien reduziert um die Höhenabhängigkeit zu entfernen, was eine genaue zwei-dimensionale Interpolation ermöglicht. Vier verschiedene Methoden wurden für die Interpolation der Schwerkraftanomalien zwischen den Vergleichspunkten betrachtet: ordinary Kriging, least-squares collocation, cubic spline and biharmonic spline interpolation. Für die schlussendlichen Berechnungen wurde biharmonic spline interpolation verwendet. Die Effekte von weiteren Korrekturen wie Topographiekorrektur und Verwendung eines globalen Schwerkraftmodells wurden untersucht, jedoch als vernachlässigbar im Hinblick auf die Ungenauigkeit der Nivellementmessungen empfunden. Aus diesem Grund sind diese Methoden in der Berechnung nicht implementiert.

Es sind grosse regionale Unterschiede zwischen den neuen Resultaten und denen von Rijkswaterstaat zu beobachten. Diese Unterschiede können grösstenteils durch einen Vorzeichenfehler beim zurückrechnen der Oberflächenschwerkraftanomalien zur beobachteten Schwerkraft erklärt werden.

Nach einer Neuberechnung des EVRS in dem die neuen NAP Geopotentialunterschiede verwendet wurden, schien der Unterschied zu den vorherigen Realisationen in einer Neigung der Referenzfläche von einigen Millimetern zu liegen. Unter Berücksichtigung von aktualisierten Daten anderer Länder sind Höhenunterschiede in der Größenordnung einiger Zentimeter zu beobachten.

Momentan sind 28 Messungen beim BKG bekannt, die das NAP Netzwerk mit dem Deutschen Netzwerk verbinden. Diese Messungen sind auf 13 Standorte entlang der Deutsch-Niederländischen Grenze verteilt was als ein guter Anschluss der beiden Netzwerke zueinander gesehen werden kann. Die Verbindung zu Belgien scheint weitaus schwächer, da nur eine Messung beim BKG bekannt ist, obwohl die in dieser Arbeit verwendeten Daten suggerieren dass mehrere Messungen vorhanden wären.

Acknowledgements

Hereby, I would like to express my sincere appreciation to my supervisors, Dr. Cornelis Slobbe for keeping me challenged, motivated and always making time, even in his busiest moments and Professor Roland Klees for his unequalled expertise and his incredibly fast, thorough and valuable feedback. For without them this project would not have been possible.

Furthermore, I would like to thank Dr. Bas Alberts from Rijkswaterstaat and Dr. Martina Sacher from the BKG for providing the necessary data, advice on software and answering all my questions, as well as Dr. Guy Drijkoningen and Professor Florian Wellmann for being part of my thesis committee.

Last of all, my greatest appreciation goes out to my family, girlfriend, friends and TU Delft colleagues for their continuous support during the whole duration of this project.

Thanks to all the people mentioned above I have been able to completed this thesis as such.

Contents

List of Figures

List of Tables

List of Abbreviations

AIG	International Association of Geodesy
ALMG	Absolute Local Mean Gradient
BE	Belgium
BHSI	Biharmonic Spline Interpolation
BKG	Bundesamt für Kartographie und Geodäsie
DE	Germany
DEM	Digital Elevation Model
DT	Delaunay Triangulation
ETRS89	European Terrestrial Reference System 1989
EVRF	European Vertical Reference Frame
EVRS	European Vertical Reference System
FAA	Free Air Anomaly
GGM	Global Geopotential Model
GNSS	Global Navigation Satellite System
GOCE	Gravity field and steady-state Ocean Circulation Explorer
GOCO05s	Gravity Observation Combination, Satellite-Only Gravity Model
GRACE	Gravity Recovery And Climate Experiment
GRS80	Geodetic Reference System 1980
INSPIRE	Infrastructure for Spatial Information in Europe
Lat	Latitude
Lon	Longitude
LPM	Local Plane Misfit
LSC	Least-Squares Collocation
LSQ	Least-Squares
NAP	Normaal Amsterdams Peil (Amsterdam Ordnance Datum)
NEVREF	Vertical reference frame for the Netherlands mainland, Wadden islands and continental shelf
NL	The Netherlands
OK	Ordinary Kriging
RD	Rijksdriehoeks (coordinates)
RTM	Residual Terain Modelling
RWS	Rijkswaterstaat
SGA	Surface Gravity Anomaly
SST	Satellite to Satellite Tracking
StDev	Standard Deviation
TBCI	Triangular Based Cubic Interpolation
UELN	United European Levelling Network

List of Symbols

c	Geopotential number
C_{PQ}	Covariance between point P and Q
f_i	Errorless observation
$f(P)$	Predicted value at point P
g	Observed gravity
G_n	Error degree-variances
Δg	Surface Gravity Anomaly
h	Vertical direction **OR** lag distance
H	Orthometric height
$H^{\star}$	Normal height
$\mathcal{L}$	Lagrangian
Δn_i	Levelled height difference
P	Point on Earth's surface
P_n	Nth Legendre polynomial
Q	Point on telluroid
Q'	Point on ellipsoid
r	Geocentric radius **OR** range of variogram
s	Sill of variogram
R_B	Radius of the Bjerhammar sphere
R_E	Radius of the Earth
W	Geopotential
ΔW	Geopotential difference
$\vec{x}$	2-D location (in RD coordinates)
α	Weighting coefficients **OR** free-air gravity gradient
γ	Dissimilarity **OR** normal gravity
λ	Biharmonic operator **OR** Kriging weighting factor
μ	Mean
σ	Standard deviation
ϕ	Green's function of biharmonic operator
ψ	Spherical distance

1 Introduction

1.1. Background

In the past, vertical reference systems were defined per country. Each system is uniquely defined by one or multiple datum benchmarks and the way of handling permanent tide (zero, mean or non-tidal system). Therefore, the definition of height within Europe is not consistent, varying per country and thus location [Rülke et al., 2012].

In order to monitor border crossing processes, natural phenomena or to formulate policies within the European Union standardized cross-border compatible height information is crucial.
For this purpose the International Association of Geodesy (AIG) Reference Frame subcommission for Europe (EUREF) suggested the European Vertical Reference System (EVRS) to the European Commission as the vertical reference for pan-European geo-information. Enabling future simplification in data harmonization and interoperability within Europe for all tasks of vertical positioning by e.g. the scientific community, national mapping agencies and commercial service providers. This forms the basis for a future common European Vertical Reference System as proposed in the INSPIRE Directive (Infrastructure for Spatial Information in Europe) [Ihde et al., 2008].

1.2. Previous Work

The first realization of the EVRS, based on the Unified European Levelling Network (UELN) 95/98, was the European Vertical Reference Frame (EVRF) 2000. This is a set of physical points with precisely determined differences in geopotential relative to a reference potential.
A realization of the EVRS is the result of a least-squares (LSQ) adjustment of geopotential differences between 1^{st} order levelling markers [Sacher et al., 2006]. This adjustment is performed by the Bundesamt für Kartographie und Geodäsie (BKG). All participating countries provide the BKG with geopotential information on their national 1^{st} order markers.

The EVRS is a height reference system fulfilling the following four conventions [Ihde et al., 2008]:

- The vertical datum is the equipotential surface.
- The units of length and time are respectively meter and second (SI).
- Height is expressed in geopotential (numbers) and normal heights (GRS80 normal gravity field evaluated at ETRS89 coordinates).
- The EVRS is a zero tidal system, as recommended by the IAG.

For EVRF2000 the datum is fixed by the geopotential number of a single reference point in the "Normaal Amsterdams Peil" (Amsterdam Ordnance Datum, NAP) network, UELN No. 000A2530/13600. The tidal systems of some national levelling datasets used in the realization of EVRF2000 were not known to the UELN computing center at the time of computation, resulting in a mixed tidal system for the EVRF2000 [Sacher et al., 2009].

A large amount of new and/or updated levelling data which had come available between 2000 and 2006 gave the incentive to update the EVRS, resulting in EVRF2007. Among the updated levelling data was the *5de nauwkeurigheids waterpassing* (5th precise levelling campaign) performed by Rijkswaterstaat (RWS) from which the results were provided to the BKG in 2004 [Sacher et al., 2006].

The datum point of EVRF2000 is no longer included in the current NAP network [Sacher et al., 2009]. For user convenience it was decided to keep the level of EVRF2007 in line with the old NAP/EVRF2000 level. Therefore the geopotential numbers of 13 stable datum points were introduced in the computation of the EVRF2007:

$$\sum_{i=1}^{13}(c_{P_i,2007} - c_{P_i,2000}) = 0 \tag{1.1}$$

Also, the tidal systems of the national levelling data were explicitly taken into account in the realization of EVRF2007 [Sacher et al., 2009].

1.3. Motivation

In the framework of the Vertical Reference Frame for the Netherlands Mainland, Wadden Islands and Continental Shelf (NEVREF) project, financially supported by Technology Foundation STW, it appeared that the geopotential differences which RWS provided to the BKG in 2004 are not correct.
Since the EVRS is realized through a LSQ adjustment, local errors influence and propagate into the whole realization. This makes the transformation between NAP and EVRF2007 inaccurate and influences the transformations between EVRF2007 and other (local) height systems, in particular in Belgium and Germany.

Investigation at Delft University of Technology points to:

- a wrongly assumed tidal system of the NAP network,
- miscommunication of NAP datum point,
- errors in the computation of geopotential differences in the NAP network and
- weaknesses in the connection of NAP to Belgium and Germany [Rülke et al., 2012, p. 345-346].

The issues concerning the tidal system and datum point have been identified and are known at the BKG. However, it should be noted that to avoid this in the future consistent implementation and clear communication between all parties is essential [Sacher et al., 2009].

1.4. Objectives

The identified issues have led to the following research questions and tasks:
1) The errors in the computation of the geopotential differences in the NAP network need to be corrected. This shall be achieved through the development of a computational procedure. The BKG will be provided with a correct set of geopotential differences of the NAP network in a well-defined tidal system.
2) This procedure will be implemented into a fully documented and easy-to-use MATLAB software package that will be provided to RWS.
2b) Along with the development of this procedure it will be investigated whether it is necessary to apply residual terrain corrections to measured gravity in order to obtain accurate geopotential differences in the NAP network.

3) To get insight into the origin of the errors made in the data provided to the BKG in 2004, these geopotential differences will be compared with the geopotential differences obtained with the new computational procedure.
4) After a re-adjustment of the EVRF2007, computed by the BKG with the new geopotential differences, the impact of the errors on the current realization of the EVRS will be quantified.
5) And the connection of the NAP to the neighbouring countries and thus the EVRS will be investigated. Recommendations concerning possible improvements of these connections will be given.

The original project description of the objectives and work packages, as agreed with RWS, is attached in Appendix A.

2

Computation of Geopotential Differences

The procedure for the computation of geopotential differences in the NAP network will be explained in this chapter. Starting with an overview of all (sub)processes and their interactions in Section 2.1 and a description of the used data in Subsection 2.1.1.
The challenges concerning gravity interpolation are discussed in Section 2.2, in which it is examined which interpolation method should be used.
The influence of Residual Terrain Modelling (RTM) on the computation of geopotential differences is addressed in Section 2.3.

After the final computational procedure has been established, Section 2.4 will discuss the recomputed geopotential differences of the NAP network. This result will be compared with the geopotential information provided to the BKG in 2004 in Section 2.4.

2.1. Workflow: From Levelling and Gravity Data to a Realization of the EVRS

The complete process of computing a realization of the EVRS from gravity and NAP levelling/benchmark data is shown in Figure 2.1. The background colours illustrate different physical quantities (e.g. height and gravity) which are mutually related though geopotential.

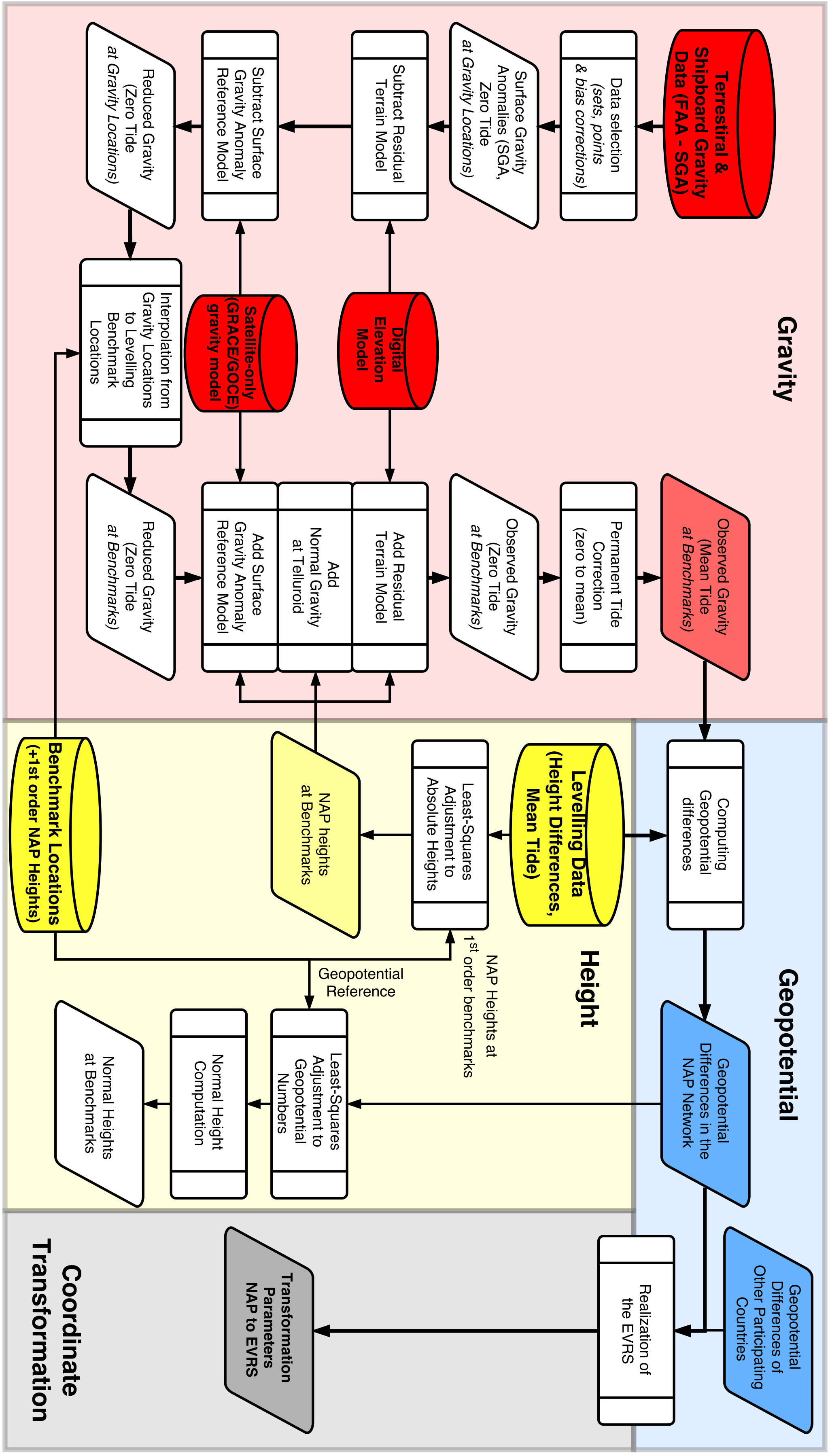

Figure 2.1: An overview of the processes, their mutual connections and steps, needed for the (re-)calculation of geopotential differences in the NAP network, wherewith an update of the EVRS is computed.

As was mentioned in Chapter 1.2 the realization of the EVRS is obtained through a LSQ adjustment of geopotential differences of the 1^{st} order markers of the UELN network. The geopotential information is here (Figure 2.1) divided into information on the NAP network, provided by RWS; and information on other national levelling networks, provided by other participating countries.
The data provided by other countries is not further considered here and will be assumed to be a given fact. The scope of this project is on the geopotential differences of the NAP network.

Geopotential difference is defined as [Hofmann-Wellenhof and Moritz, 2006, Eq. 4-6]:

$$\Delta W_{AB} = W_B - W_A = -\int_A^B g dh, \tag{2.1}$$

where ΔW_{AB} is the geopotential difference in $[m^2/s^2]$, dh the height difference in meter and g the (variable) gravity in $[m/s^2]$ along a path between points A and B.
The implementation of Equation 2.1 in practice is impossible, as it would require continuous gravity measurements along the integral path. Thus for practical use the continuous integral can be rewritten as a discrete sum [Hofmann-Wellenhof and Moritz, 2006, Leismann et al., 1992, Eq. 4-5]:

$$\Delta W_{AB} = W_B - W_A \approx -\sum_{i=1}^{N} g_i \delta n_i \tag{2.2}$$

Here, the geopotential difference ΔW_{AB} is obtained in N steps between points A and B, where g_i is the average value of the gravity at the beginning and end benchmarks for step i and δn_i the corresponding levelled height difference for this step.
The consequences of this approximation can be subdivided into three contributions. The error introduced purely due to the stepwise approach of the continuous integral, shortly discussed below and further examined in Appendix C; and errors in both gravity and height, addressed respectively in Section 2.2 and Appendix C.

For the discretization error it is known that the magnitude mainly depends on the mean altitude difference per kilometer and the mean horizontal gravity gradient along the levelling path [Ramsayer, 1965]. As a reference, in the Alps and Black Forest average discretizations of respectively 6 and 10 kilometer are considered adequate [Leismann et al., 1992]. For flat land no explicit distances could be quoted.
Figure 2.2 gives the cumulative distribution function of the levelling distances used here. This shows that 99.8% of the connections (details on the data are given in Section 2.1.1) are shorter than 10 km and are thus even sampled sufficiently for medium high mountains.
Considering the 0.2% longer levelling lines, these connect across ”het IJselmeer” and a few are running through Germany, see Figure 2.5 and 2.3. The lines on ”het IJselmeer” are unique measurements for which the average altitude difference and horizontal gradient are assumed to be smaller than for the Black Forest, as these measurements are across a lake. However, the lines through Germany are probably derived from German measurements and used for the adjustment of the NAP network. This makes them presumably even unnecessary. Therefore, they will be discussed separately in Chapter 4

Several discretization sensitivity analyses have been performed with the actual data. These are discussed in detail in Appendix C. In summary, given the current discretization of the Dutch NAP network the maximum expected error is in the order of $10^{-3}\,m^2/s^2$. As this is much smaller than the expected levelling errors (Section 2.1.1), the discretization of Equation 2.1 and therewith the usage of Equation 2.2 is justified for the provided data.

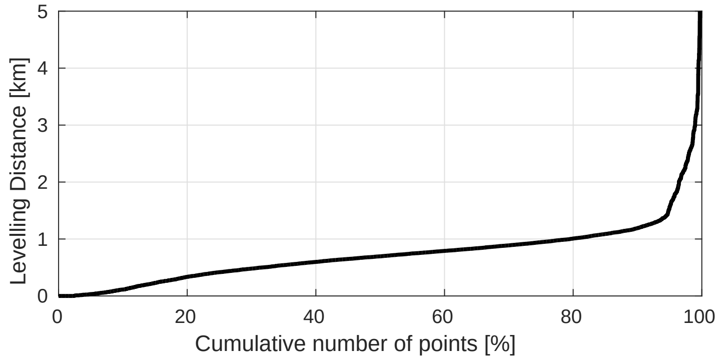

Figure 2.2: Cumulative distribution function of the levelling distances provided in the levelling data.

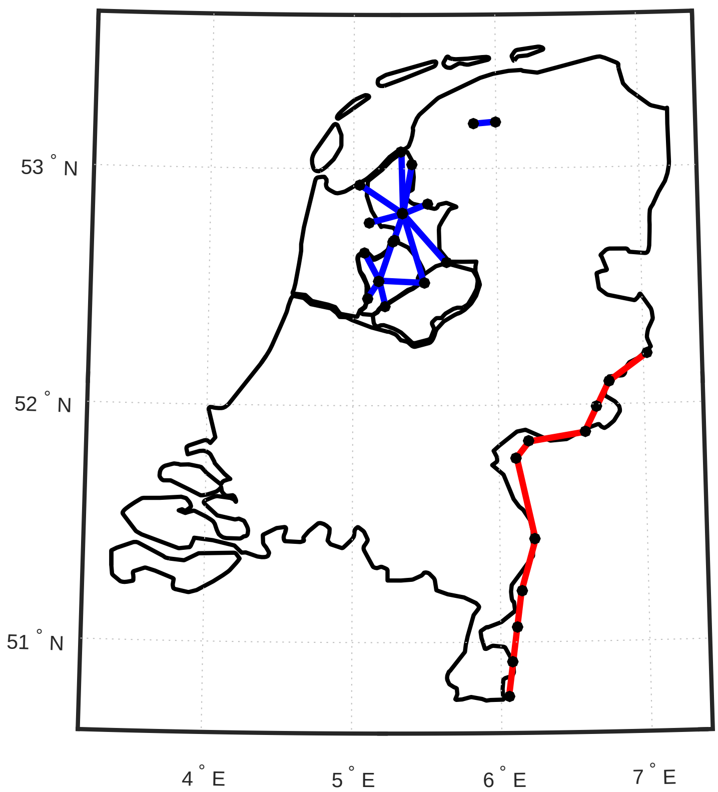

Figure 2.3: Spatial overview of the levelling lines longer than 10 kilometer. The blue lines are completely within the Netherlands. The red lines run (partly) through Germany and might be substituted by more accurate German levelling information.

A large amount of precise gravity measurements is available in and around the Netherlands, however, not at the locations needed for direct use in Equation 2.2. Interpolation is needed to obtain the gravity values at the necessary location.

Because gravity depends on height, accurate gravity interpolation in 3-D is not possible. The observed gravity at the Earth's surface can be reduced to the gravity at an equipotential surface, the geoid for that matter, on which accurate interpolation can be performed on a 2-D surface. After the interpolation the observed gravity at the Earth's surface is restored at the new location. Section 2.2 will explain this procedure, the applied reductions and the interpolation itself in more detail.

Another necessary correction is for permanent tide. Hence, the time average of the tide-generating potentials of the Sun and the Moon are not zero. This influence is called the permanent tide. There are three concepts (e.g. tide-free, mean and zero tidal system) in how to deal with the permanent tide for gravity measurements or the 3-D shape of the Earth [Mäkinen and Ihde, 2009].
The levelling data was provided in mean tidal system, the gravity data in the zero tidal system (details in Sections 2.1.1). In order to obtain geopotential differences in the mean tidal system, consistent with the NAP, the zero tidal gravity measurements need to be transformed to the mean tidal system. This has been performed according to Mäkinen and Ihde [2009], see Appendix E.3.3.

Because height in the EVRS may be expressed as normal heights a transformation routine is added to the software for completeness (Chapter 3.2). This is illustrated in Figure 2.1 as the sub-branch from the geopotential differences in the NAP network. Appendix B provides details on normal heights.

2.1.1. Data Description

For the computation of geopotential differences in the NAP network several datasets were used. In this section their data formats and sources will be described. The following paragraphs corresponds to the datasets shown in Figure 2.1.

Levelling Data

The used levelling data is the same as has been used in the computation of the previous geopotential differences, those provided to the BKG in 2004. This data consists of levelled height differences, mainly between 1^{st} and 2^{nd} order benchmarks of the *5^{de} nauwkeurigheids waterpassing*.
These observations have not been corrected for any permanent tide. Therefore, the mean tidal system emerges after performing a network adjustment, which averages the tidal effects [Brand and Damme, 2004, Mäkinen and Ihde, 2009].
The data consists of 9288 levelling connections, with information on:

- Dutch marker ID of starting point,
- Dutch marker ID of end point,
- levelled height difference (after network adjustment),
- approximate distance of levelling line,
- date of acquisition,
- *mean gravity (of beginning and end point) and*
- *geopotential difference (from 2004).*

The mean gravity and geopotential differences (from 2004) were not used in the computation of the new geopotential differences. They are only used for comparison purposes in Section 2.4.

No benchmark location information is present in the previously described dataset. The locations of the 8890 benchmarks were retrieved via cross referencing with a separately provided benchmark dataset. The horizontal location of the benchmarks is expressed in latitude and longitude in the European Terrestrial Reference System 1989 (ETRS89), based on the GRS80 ellipsoid [Moritz, 1980]. Height is expressed with respect to NAP. Combining these two datasets allows for a spatial representation of the data, shown in Figure 2.5.

From all the benchmarks only the first order benchmarks (000Axxxx) were provided with accurate NAP heights. Several benchmarks, provided later in time, were provided without NAP heights at all. For the restore step after gravity interpolation the heights for all benchmarks are necessary.
In order to acquire the necessary heights at all benchmark locations a LSQ adjustment with the previously described 9288 height difference observations and the accurate heights of 301 1^{st} first order benchmarks was performed.
The computed heights have been compared, where possible, with the provided heights. Figure 2.4 shows a histogram of the differences, which are up to maximum of two centimeters. Assuming a representative value of the free-air gravity gradient of -0.3 $mGal/m$, this height uncertainty translates into a negligible gravity uncertainty as will be illustrated in Section 2.2.

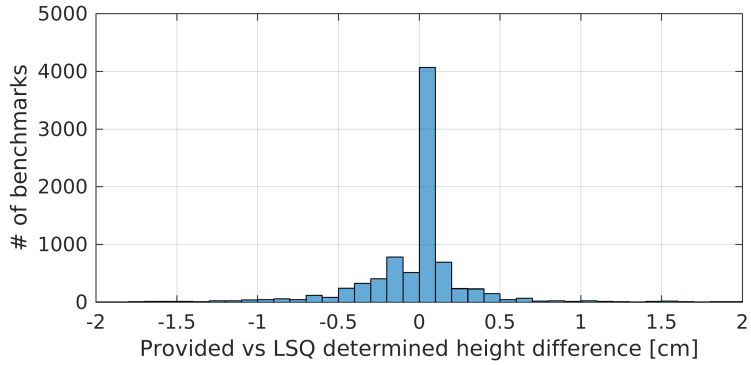

Figure 2.4: Height difference between the provided heights and estimated heights through a LSQ adjustment of the levelling data and NAP heights of 301 1^{st} order benchmarks.

Additionally the ellipsoidal coordinates have been recomputed into Rijksdriehoeks (RD) coordinates(x,y). RD coordinates are the map coordinates used in the Netherlands. These are based on a stereographic projection of a locally best fitting Bessel ellipsoid. This conversion was computed with the RDNAPTRANS-procedure [Bruijne and Brand, 2005], which is described in Appendix E.

Gravity Data

The gravity data used here is a subset of the terrestrial and marine gravity observations used by Slobbe [2013] to estimate and validate the quasi-geoid covering the whole Dutch Continental Shelf and mainland. The definitions and parameters concerning this gravity data were adopted as defined in Slobbe [2013]. A summary is given below.

The gravity measurements are provided in the zero-tidal system and expressed as surface gravity anomalies (SGA):

$$\Delta g = g(P) - \gamma(Q) \tag{2.3}$$

Here, g is the observed gravity taken on the Earth's surface (P) and γ the normal gravity taken on a corresponding point on the telluroid (Q). For the height of point Q the NAP height of point P is used, this is clarified in Appendix B.
The horizontal location of the gravity observations is provided in ETRS89 latitude and longitude and height above NAP.

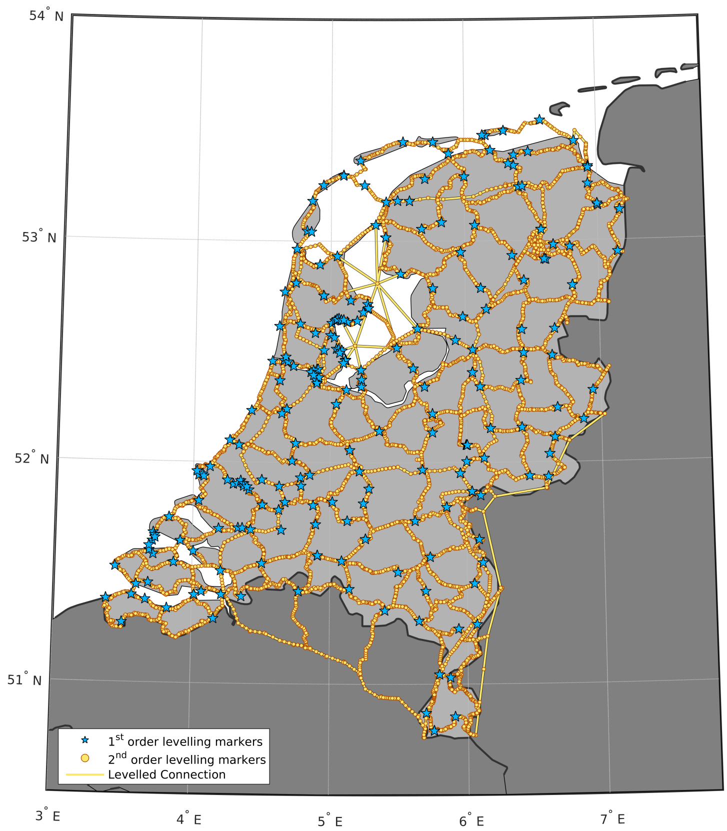

Figure 2.5: Spatial overview of the benchmarks and the levelling lines connecting them as provided by Rijkswaterstaat. The first order benchmarks are known to have accurate NAP heights.

Table 2.1 lists the different gravity datasets which are available for the interpolation. A spatial overview of the different sets is given in Figure 2.6.

Biases were estimated by Slobbe [2013] to account for systematic errors introduced by; inconsistencies in the gravity, vertical and horizontal datums being used, as well as by the application of simplified free-air reduction procedures [Heck, 1990]. These biases between the different data providers and surveys are also given in Table 2.1.
Note, milligal ($mGal$) is a unit of acceleration which is used here to express the magnitude of SGAs as these are usually very small. One $mGal$ equals $10^{-5}\,m/s^2$.

Table 2.1: Overview of available terrestrial and marine gravity observations in and close to the Netherlands. Figure 2.6 gives the spatial distribution of the mentioned datasets, referred to the reference number in the first column.

Ref Fig 2.6	Provider ID	Survey ID	Type	# Points	Bias [$mGal$]	Description
1	1	1	Terrestrial	7815	0	Dutch Mainland
2	1	15	Terrestrial	203	0	Dutch Measurements in Belgium
3	1	13	Marine	1833	0.2028	Waddensea
4	1	14	Marine	525	0.8609	Waddensea (Lines)
5	7	all	Marine	26473	-0.2440	Dutch Offshore
6	9	all	Marine	24371	-0.2440	Dutch Offshore
7	4	5	Terrestrial	16294	0.0680	German Mainland
8	4	6	Terrestrial	16115	-0.1002	German Mainland (Levelling Lines)
9	3	2	Marine	179	-0.2440	German Offshore
10	3	3	Marine	4207	-0.2440	German Offshore
11	13	1	Terrestrial	33282	-0.2020	Belgian Mainland
12	14	1	Terrestrial	567	0.0482	Limburg
13	14	2	Terrestrial	3132	0.0386	Limburg
14	14	3	Terrestrial	276	-0.0470	Limburg
15	14	4	Terrestrial	1283	0.0191	Limburg
16	15	1	Terrestrial	1717	0.1061	Germany (Northwest of Groningen)
17	16	1	Terrestrial	2460	0.0726	Germany (Northwest of Groningen)
18	16	2	Terrestrial	2428	-0.0114	Germany (Northwest of Groningen)
19	16	3	Terrestrial	1340	-0.1027	Germany (Northwest of Groningen)

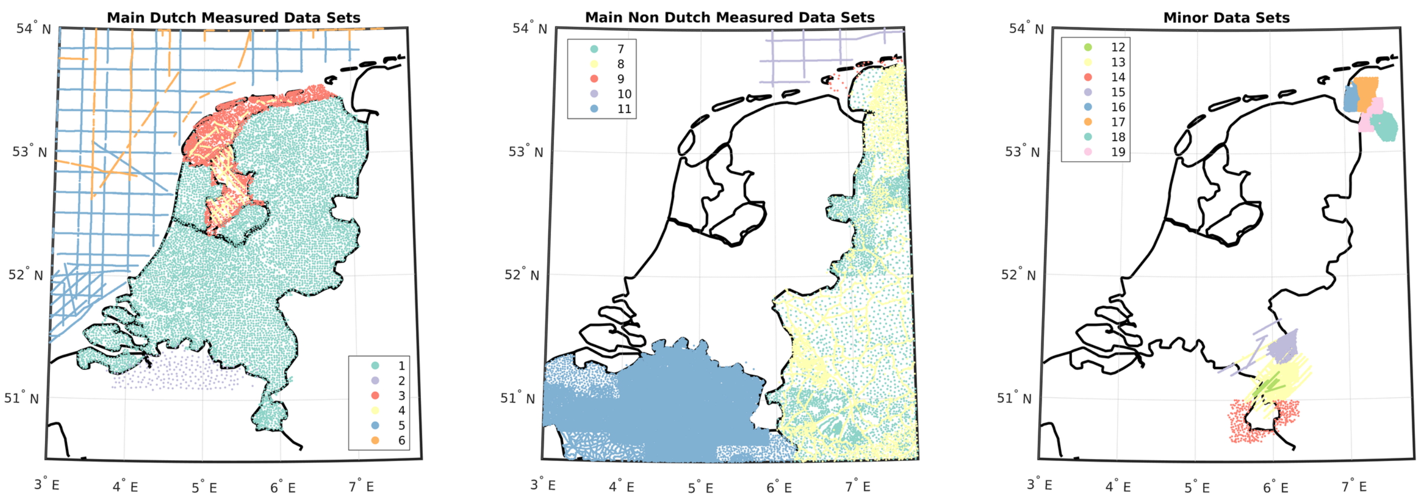

Figure 2.6: Spatial overview of available gravity measurements in and near the Netherlands. Information on the different datasets is given in Table 2.1, in which is referred to the reference number given in the plots.

Satellite-Only (Grace/GOCE) Gravity Model

In order to remove global trends from the observed gravity data a global gravity model was used, further explained in Section 2.2. The Satellite-Only (Grace/GOCE) Gravity Model (GOCO05s) was used here. This is a high-resolution global gravity field model based on data of dedicated satellite gravity missions (e.g. satellite gravity gradient data from GOCE and low-low satellite to satellite tracking (SST) data from GRACE), satellite laser ranging from various laser satellites and high-low-SST from various low-earth orbiters. In this research the regularized static solution is used which is modelled up to a spherical harmonic degree and order of 280 [Mayer-Guerr, 2015].

Digital Elevation Model

For the computation of RTM corrections a digital elevation model (DEM) is necessary. EuroDEM was used here. Released in 2008 with a vertical accuracy of 8-10 meter and a 2 arcseconds (ca. 60m) grid spacing [EurogeoGraphics, 2008]. More details will be discussed in Section 2.3.

2.2. Gravity Interpolation

Equation 2.2 shows the direct relation between gravity and geopotential. Therefore, accurate estimates of gravity at benchmark locations are crucial for an accurate determination of geopotential differences. In this section, it is attempted to find an accurate and robust way for the interpolation of gravity in the Netherlands. Figure 2.7 shows the processes which will be treated in this section.

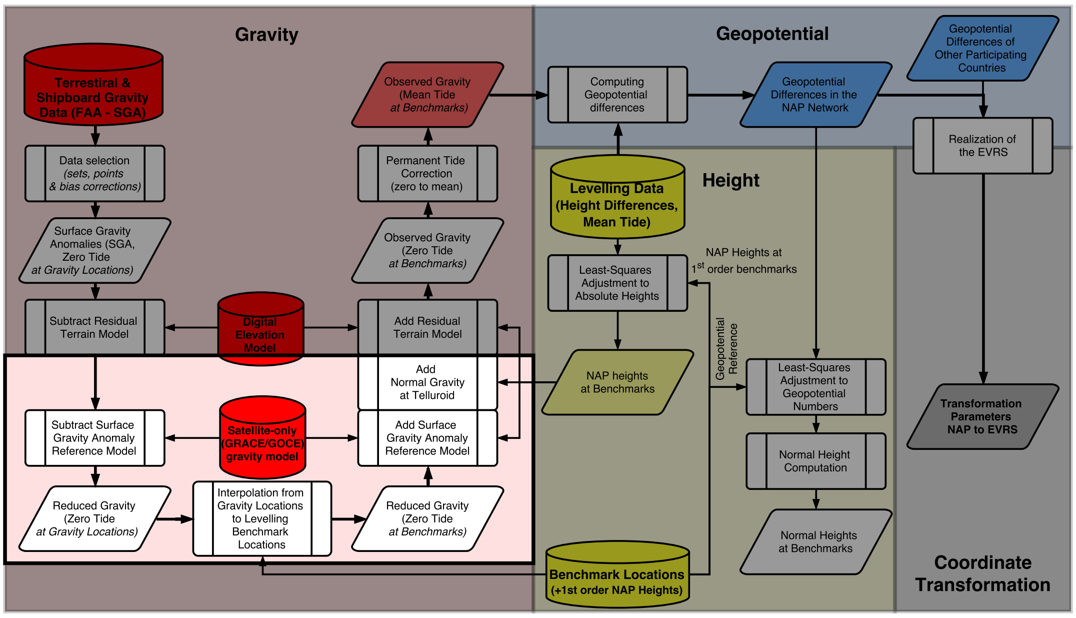

Figure 2.7: Overview of the workflow (Figure 2.1) in which the gravity field interpolation, which will be treated in this section, is highlighted.

2.2.1. Research Set-up

To be able to assess the performance of the different interpolation methods a standard input data set and a control data set were chosen beforehand. The Dutch terrestrial gravity observations (ProviderID 1 and Survey ID 1 & 15, see Table 2.1), as these have no internal biases and cover the whole area of interest, were selected as input for this purpose. This data set consists of 8018 observations.

From these 8018 observations 400 observations, approximately 5%, were randomly selected and left out of the input data set as the control data set. The locations of the input and control observations are shown in Figure 2.8

This amount of control data was presumed to provide enough reference to allow for reliable statistics while not subtracting to much data from the input data set.

To asses the performance of the tested interpolation methods the average precision and accuracy of the predicted gravity at the reference observations, with the remainder (7618 observations) of the standard input data, will be used.

Gravity Field Corrections

Because gravity varies with height, accurate straightforward interpolation of gravity in 3-D is not possible. Gravity reduction translates the gravity values from the Earth's surface onto a equipotential reference surface, which removes its height dependency [Hofmann-Wellenhof and Moritz, 2006]. Re-

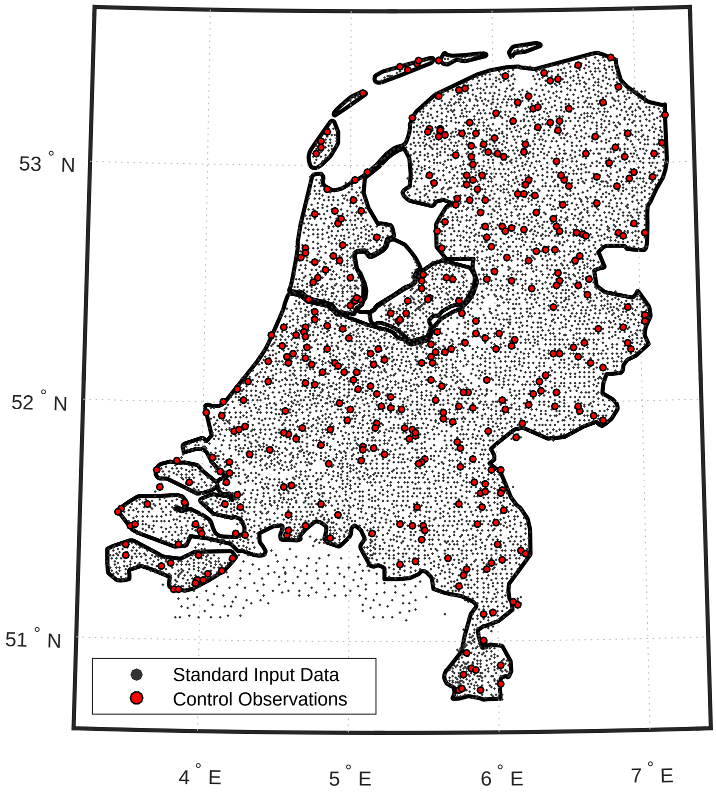

Figure 2.8: Overview of the standard input data and the control data used.

moving the height dependency of the gravity enables 2-D interpolation to be performed on this reference surface. After the interpolation has been executed on the reference surface the previously applied reductions are again restored at the new observation locations to retrieve the wanted observed gravity at the Earth's surface.
The SGA previously introduced (Section 2.1.1, Equation 2.3) are a type of reduced gravity. Making it possible to interpolate gravity as SGAs in a 2-D plane (either on a Cartesian plane or on a sphere). The provided gravity data is already expressed as SGAs. Hence, this reduction step has already been applied. Appendix B elaborates on SGAs.

Another correction, shown in Figure 2.1, is the subtraction of a SGA reference model. A Global Geopotential Model (GGM), in this case GOCO05s, is used to model the long-wavelength information of the Earth's gravity field. The modelled gravity values are reduced to SGAs, with the same procedure as explained previously.
Subtracting the reference SGAs from the observed SGAs removes the long-wavelength information from the provided gravity data. The removal of the long-wavelength information eliminates trends in the data, facilitating the determination of the covariance function needed for stochastic interpolation. The here examined deterministic interpolation methods can capture these trends. Therefore, this step would not be necessary for these methods. However, as it also does not influence their performance, this is illustrated in Chapter 2.3, the correction will be applied for comparison purposes.

In conclusion, the gravity field used to asses the performance of all interpolation methods will be the provided SGAs from the gravity data minus the reference SGAs, modelled with GOCO05s.

Tested Interpolation Methods

Four interpolation methods were examined. Two deterministic and two stochastic methods:

1. Biharmonic Spline Interpolation (BHSI, deterministic),
2. Triangular-Based Cubic Interpolation (TBCI, deterministic),
3. Least-Squares Collocation (LSC, stochastic) and
4. Ordinary Kriging (OK, stochastic).

1. Biharmonic Spline Interpolation (BHSI, deterministic)

The general concept behind BHSI is to find the smoothest surface that passes through a set of irregular distributed points. This results in a surface for which the first and second derivatives are continuous. The surface is defined by a linear combination of Green's functions centred at each data point:

$$w(\vec{x}) = \sum_{j=1}^{N} \alpha_j \phi(\vec{x} - \vec{x}_j) \tag{2.4}$$

Here, $\vec{x}$ is a 2-D location in RD coordinates, α_j the weighting coefficients for which j sums over all N data points and ϕ the Green's function of the biharmonic operator (λ) in 2-D:

$$\phi = |\vec{x}|\, 2\, (ln|\vec{x}| - 1) \tag{2.5}$$

The solution needs to pass through all data points, resulting in the following system of equations:

$$w_i = \sum_{j=1}^{N} \alpha_j \phi(\vec{x}_i - \vec{x}_j) \tag{2.6}$$

Once the system is solved for all α_j's, obtaining predictions at interpolations locations becomes straight forward using Equation 2.4. Therefore, the amount of target interpolation points will not result in time or computation issues. However, solving the system to obtain the coefficients becomes an intensive procedure for large amounts of input data [Sandwell, 1987].

The practical implementation of the BHSI algorithm in MATLAB is straightforward as it is readily implemented in the function *griddata* in which BHSI is referred to as the 'v4' method [MAT, 2015].

Sandwell [1987] points out that: *"...the problem is exactly singular when two data points are located in the same position. Moreover, numerical instabilities occur when the ratio of the greatest distance between any two points to the least distance between two points is large."*.

When using all input data MATLAB returns a warning about duplicate points. The MATLAB standard procedure is to average these points, averaging both locations and values. To examine the influence of this averaging, all observations with neighbours closer than a certain distance were removed from the input data set. When filtering for a minimum observation distance of 100 meter, or more, the warning disappears. As the MATLAB averaging produced better interpolation results than the manual filtering, the standard MATLAB procedure was left untouched.

2. Triangular-Based Cubic Interpolation (TBCI, deterministic)

TBCI is the only method examined here which does not use all input for the prediction of a target location. Via Delaunay triangulation (DT) neighbouring points of the target location are identified. See Appendix D for details on DT. These neighbouring points are used in a cubic spline interpolation. A smart subdivision into sub-triangles ensures continuity of the first and second derivative [Watson, 1992, Yang, 1986]. Due to its local character TBCI is by far the fastest method tested here. However, this is not a concern here since the interpolation has to be performed only once in the final procedure.

Similar to BHSI, the TBCI algorithm is readily implemented in the MATLAB function *griddata*, method 'cubic' [MAT, 2015].
The usage of a DT poses the same sensitivity, as mentioned for BHSI, for observations too close together. As this would result in sliver triangles. Similar to BHSI, MATLAB pre-examines the input data and averages points which are too close together, preventing sliver triangles and making it a robust algorithm.

3. Least-Squares Collocation (LSC, stochastic)

LSC is a well known interpolation technique in geodesy. The underlying basic LSQ interpolation formula is:

$$f(P) = [C_{P1}\, C_{P2} \dots C_{PQ}] \begin{bmatrix} C_{11} & C_{12} & \dots & C_{1Q} \\ C_{21} & C_{22} & \dots & C_{2Q} \\ \vdots & \vdots & \ddots & \vdots \\ C_{Q1} & C_{Q2} & \dots & C_{QQ} \end{bmatrix}^{-1} \begin{bmatrix} f_1 \\ f_2 \\ \vdots \\ f_Q \end{bmatrix} \tag{2.7}$$

Here, $f(P)$ is the predicted value, f_i the errorless observations ($i = 1, 2 \cdots Q$) and $C_{PQ} = C(P, Q)$ the covariance between point P and Q. The LSQ interpolation formula can be used for gravity interpolation by taking $f = \Delta g$. The assumption of errorless data can be generalized to the case in which random measuring errors and systematic parameters can be determined.
Equation 2.7 works with any function $C(P, Q)$ that is symmetric in P and Q, harmonic as a function of P and Q and positive definite. Choosing C as the covariance function makes for the smallest Root-Mean-Square interpolation error. An elaborate explanation can be found in Moritz [1978].

The GRAVSOFT package was used to perform the gravity anomaly interpolation with LSC [Tscherning et al., 1992].
The steps, separate routines, needed to obtain an interpolation result are:

- EMPCOV: in which the empirical covariance function is computed from the input data.
- COVFIT16: in which the analytical covariance function is fitted to the empirical covariance function outputted by EMPCOV.
- SELECT: which takes a subset of the input data.
- GEOCOL11: performing the actual LSC onto the target locations, using the analytical covariance function and (a subset) of the input data.

The empirical covariance was computed with EMPCOV, in bins of 1 arcminute. Because the accuracy of the fitted analytical covariance function at short distances has the largest influence on the inter-

polation performance, the analytical covariance function was fitted through the first 19 values. This corresponds to a distance of approximately 0.32 degrees or 35 kilometre.
There are several admissible analytical covariance functions which ensure positive definiteness of the matrix to be inverted in Equation 2.7. The general gravity anomaly covariance function GRAVSOFT uses is:

$$cov(\Delta g_P, \Delta g_Q) = \sum_{n=0}^{\infty} \sigma_n^2 s^{n+2} P_n(\cos(\psi))/,, \tag{2.8}$$

where ψ is the spherical distance between point P and Q and P_n the Legendre polynomials, σ_n^2 gravity anomaly degree-variances and s is defined as:

$$s = \frac{R_B^2}{rr'} = \left(\frac{R_B}{R_E}\right)^2 \tag{2.9}$$

Here, r and r' are the geocentric radii respectively to points P and Q which are separated by spherical distance ψ. R_E and R_B are respectively the radius of the Earth (6371 km used by GRAVSOFT) and the Bjerhammar sphere.
For the fitting of the analytical covariance function several degree variance models are available in GRAVSOFT. Here gravity anomaly degree-variance model 2 was used [Tscherning, 1994] (equivalent to original model 4 in Tscherning and Rapp [1974]):

$$\sigma_n^2(\Delta g, \Delta g) = A_{\Delta g} \frac{(n-1)}{(n-2)(n+B)} \tag{2.10}$$

where $A_{\Delta g}$ and B are constants. $A_{\Delta g}$ has units of $mGal^2$ and together with R_B determines the fit of the covariance function. B is dimensionless and set to 4.
However, GRAVSOFT expresses all the output as degree-variances of the disturbing potential, not gravity anomalies. The corresponding relations are given below.

A reference field, previously described, was subtracted from the input data. Therefore, the model degree-variances are substituted by the error degree-variances of the reference field, up to the maximum degree of the field. Summarizing the degree-variances of the disturbing potential used by GRAVSOFT:

$$\sigma_{T,n}^2 = \begin{cases} G_n & n = 2, \dots, 280 \\ \frac{A_T}{(n-1)(n-2)(n+B)} & n = 281, \dots, \infty \end{cases} \tag{2.11}$$

Here, G_n are the error degree-variances from GOCO05s and A_T a constant $[m^4/s^4]$. The gravity anomaly degree-variance relate to the disturbing potential degree-variance as follows:

$$\sigma_n^2 = (n-1)^2 R_E^{-2} \sigma_{T,n}^2 \tag{2.12}$$

Note, $A_{\Delta g}$ and A_T do not have the same units. Within GRAVSOFT A_T is given in m^2/s^2 and $A_{\Delta g}$ in $mGal^2$. Transforming between the two fitting parameters using the unit conventions of GRAVSOFT results in

$$A_T = A_{\Delta g} R_E^2 \cdot 10^{-4} \tag{2.13}$$

where R_E is in km. In summary, for the fitting of the analytical covariance function GRAVSOFT returns the fitted parameters R_B and A_T, hereafter simply referred to as A.

With the analytical covariance function fitted, GEOCOL11 performs the collocation. However, when too many observations are provided ($\gtrsim$ 5500) the result become implausible (an example is included in the results, Section 2.2.2). Because the standard input data consists of 7618 observations, a reduction of the number of input data was realized via the SELECT routine. This routine overlays an equiangular grid on the original data, after which only the spatially closest observation per grid point are maintained. The rest of the observations are discarded. This way of thinning ensures that the remaining subset covers the same area as the original data and is evenly distributed. Hence, most observations are removed in densely sampled regions of the original data.
Several choices for the grid spacing were tested. A grid spacing of 0.03 degrees resulted in the smallest interpolation error evaluated at the control points. This grid selected subset consists of 4983 measurements.

4. Ordinary Kriging (OK, stochastic)
There are many different forms of Kriging available. Similar to LSC this family of methods is based on the principle of unbiased minimum error variance prediction of a second-order stationary stochastic process with known, or estimated, covariance function [Menz et al., 2015].
Here OK will be tested, which assumes a constant and unknown mean over the search neighbourhood of the target location. Because of the similarities Equation 2.8 also forms the basic concept for OK. In this case the weights are obtained by solving the following system of equations [Blais, 2010]

$$\begin{bmatrix} \gamma_{11} & \cdots & \gamma_{1N} & 1 \\ \vdots & \ddots & \vdots & \vdots \\ \gamma_{N1} & \cdots & \gamma_{NN} & 1 \\ 1 & \cdots & 1 & 0 \end{bmatrix} \begin{bmatrix} \lambda_1 \\ \vdots \\ \lambda_N \\ \mathcal{L} \end{bmatrix} = \begin{bmatrix} \gamma_{1P} \\ \vdots \\ \gamma_{NP} \\ 0 \end{bmatrix} \tag{2.14}$$

Here, $\mathcal{L}$ is the Lagrangian, λ_i the weight for observation i and γ_{1P} is the dissimilarity between observation 1 and P. These dissimilarity values are obtained from an estimated variogram. Through the variogram the dissimilarities only dependent on the distance between the points.
Note, that for a second order stationary process a simple relation holds between the covariance function and the variogram:

$$\gamma(h) = C(0) - C(h), \tag{2.15}$$

where h is the so called lag distance. The covariance at lag distance zero is the variance.
The practical implementation of OK was realised through a set of MATLAB functions. Which, in analogue with the GRAVSOFT package, first compute an empirical variogram after which the analytical function is fitted. It was found that a spherical variogram model gave the best interpolation results:

$$\gamma(h) = (s-n)\Big[\Big(\frac{3h}{2r} - \frac{h^3}{2r^3}\Big)h\Big] + n \quad for \quad h \leq r \tag{2.16}$$

$$\gamma(h) = s \quad for \quad h > r, \tag{2.17}$$

where r is the range, s the sill or maximum dissimilarity and n the nugget or initial uncertainty [Bohling, 2005].
The fit of the variogram at small lag distance has a bigger impact on the interpolation performance than the fit at larger lag distance, similar as the covariance fit in LSC. However, due to the characteristics of the spherical variogram model the fitting must be performed up to at least the distance of the range. On inspection of the empirical variogram the range seemed to be around 90 km, therefore the fit of the analytical variogram was performed up to 100 km.
The analytical variogram serves as input for the actual Kriging routine. Al locations and distances in the OK routines are computed and expressed in RD coordinates.

2.2.2. Results

It should be noted here that Gal is a unit of acceleration used in the science of gravimetry, defined as cm/s^2. For convenience, gravity in this sections will be expressed in $mGal$, which is $10^{-5}\,m/s^2$ [Leismann et al., 1992].

Covariance/variogram Fit

Before interpolation results with the stochastic methods could be generated, the analytical covariance function and variogram needed to be estimated. The computed empirical covariance function and variogram, with their corresponding fits, are shown in Figure 2.9. The covariance function is computed by the COVFIT16 routine in spherical distance. For comparison purposes the spherical distance has been converted to kilometers at the Earth's surface (radius of 6371 km).
For the covariance fit, Figure 2.9a, the estimated value for A is 246795 m^4/s^4 and for $R_E - R_B$ 7.79 km. For the fit of the variogram, Figure 2.9b, a sill of 63.9 $mGal^2$ and range of 88.8 km were estimated. No nugget effect was observed.
Equation 2.15 was used to compute the empirical covariance function from the empirical variogram to be able to compare the obtained covariance function and variogram. The variance, $C(0)$, value used was 53.88 $mGal^2$, as observed in the covariance function.

Interpolation

Table 2.2 shows the basic statistics for the different tested interpolation methods. The corresponding histograms are shown in Figure 2.10. The histograms are plotted for values -2 and 2 $mGal$. An overview of the spatial distribution of the interpolation errors is given in Figure 2.11.

Using all the data in LSC produced errors two orders of magnitude larger than the original input. Therefore, LSC was also performed with a subset of the input data, as described above. Using the subset produced plausible results, in line with the other methods. To have a reference for the influence of the subset on the interpolation result, BHSI has also been performed using this same input subset.

When LSC with all data is not considered for a moment, all interpolation methods perform quite similar. The average misfit being smaller than 0.1 $mGal$ and standard deviations of around 0.5 mGal, slightly higher for the stochastic methods and slightly lower for the deterministic methods.
All results are bounded between errors with a maximum of about 4 $mGal$ and the minimum of less than -3 $mGal$. With the exception of OK, which has negative outliers of -6.13 $mGal$, more than twice the size of the others methods.

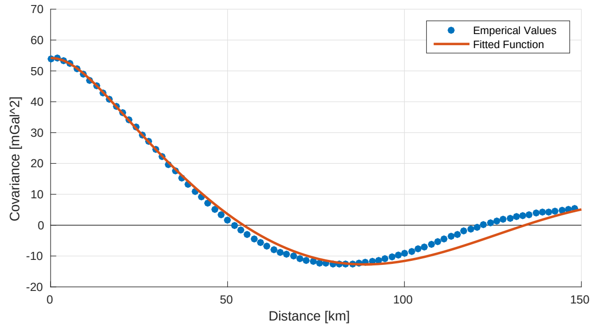

(a) Covariance function fit.
A: 246,795 m^4/s^4, depth R_B: 7.79 km

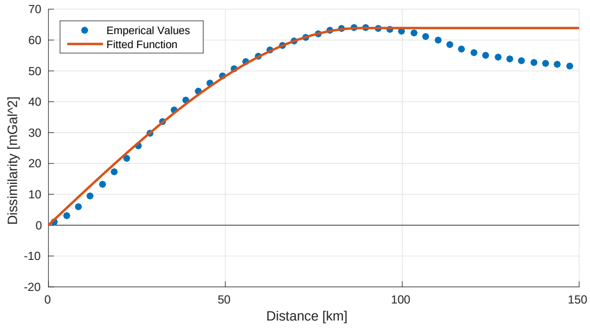

(b) Variogram fit.
Sill: 63.9 $mGal^2$, range: 88.8 km.

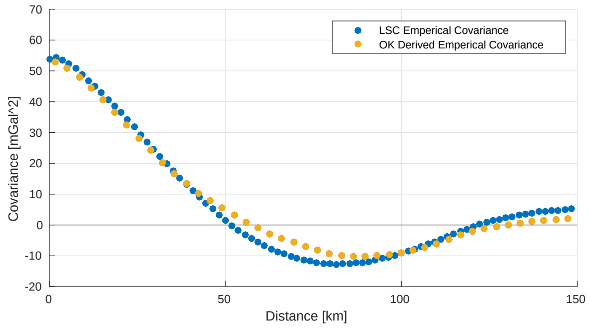

(c) Empirical covariance function and covariance function computed from variogram with Equation 2.15, $C(0) = 53.88$.

Figure 2.9: Fitting and comparison of analytical covariance function/variogram to the empirical values.

Table 2.2: Overview of the basic statistics of the interpolation results. Data "all" refers to all Dutch terrestrial gravity data and "0.03 deg" to a sub-sampled input, described in the text

Method	**Data**	**Mean** $[mGal]$	**St.Dev** $[mGal]$	**Min** $[mGal]$	**Max** $[mGal]$
LSC	all	-0.81	16.81	-257.09	89.36
LSC	0.03 deg	-0.02	0.60	-2.85	3.67
OK	all	-0.05	0.69	-6.13	3.69
TBCI	all	0.01	0.52	-2.66	3.88
BHSI	all	0.00	0.51	-2.75	3.71
BHSI	0.03 deg	-0.01	0.50	-2.75	3.71

2.2.3. Discussion

Covariance/Semivariogram Fit

Because the analytical functions have different properties the comparison was made between the empirical functions, Figure 2.9c.

The general shape of the functions agrees well, showing the same amplitude. Although, the function derived from the variogram seems to be slightly more stretched. This might be due to the different coordinate systems in which both functions were computed.

Looking at the fit of the individual analytical function, starting with the covariance function, Figure 2.9a.

The most accurate fit can be seen up to a distance of 40 kilometre. This is expected as this is the region on which the fit has been performed. The general shape of the analytical function follows the empirical values for larger distances as well.
For the variogram, the fit has been performed up to a distance of 100 kilometre to be able to capture the sill. The analytical variogram, cannot capture the oscillation which occurs beyond the range, due to its properties. GRAVSOFT is optimized for gravity computations and so are the implemented analytical covariance models. This is clearly seen from the analytical functions in Figure 2.9.
The oscillation, the so called hole effect, also explains the discrepancy between the variogram sill and the variance, $C(0)$ [Pyrcz and Deutsch, 2003].

Interpolation
Figure 2.11a illustrates the unexpected behaviour of LSC when the full input data set is used. Aside from a huge local anomaly in the north-east of the Netherlands, the results are similar to the subset LSC results.
In order to investigate the source of this anomaly, several additional control data sets were created and tested. Shuffling the input data set was tested as well, i.e. providing the same information in a different order to GRAVSOFT. This anomaly is not stationary when a different control data sets or a shuffled input is used. This unpredictable behaviour vanishes when fewer input observations is provided. For less than about 5500 input observations the results become stable, independent of the arrangement of the input data or control data set used. Therefore, it is presumed that this anomaly must be caused internally in GRAVSOFT, probably due to an overflow or singularity when attempting to solve a too large system.
For BHSI the difference between results obtained with the complete data set compared with the subset are negligible. With this reference, it is assumed that the result obtained with LSC using the subset gives a fair representation of the performance of this method.

When looking at Figure 2.11, it seems that independently of interpolation method there are certain control points which constantly exhibit relatively large errors. Since this does not vary between the methods, it seems these errors are due to inconsistencies of these control points, not the performance of the different interpolations. The similarities of the maximum and minimum values for all the methods, given in Table 2.2, is due to the errors at these control points.
The large minimum values for OK are clearly visible in the results, located in Zeeland south-west of the Netherlands. Why these errors only show up for OK is unclear. Southern Limburg tends to have relatively large errors for all methods. As this is the most hilly part of the Netherlands this is expected to be caused by topography, Section 2.3 will look further into this.

In general all methods perform well, showing a standard deviation of the interpolation error at control point slightly larger than 0.5 $mGal$.
Because the input data is not error free, the misfits can not be solely ascribed to inaccuracies of the interpolations themselves. The observed standard deviation is the combined result of the precision of the gravity data and the interpolation performance, related in the following way:

$$\sigma_\epsilon = \sqrt{\sigma_{grav}^2 + \sigma_{int}^2} \tag{2.18}$$

This shows that the observed standard deviation of the interpolated control data only gives an upper limit of the standard deviation of the interpolation.

The differences in the performances between the methods are small. Nevertheless, the standard deviation of the deterministic methods is slightly better than for the stochastic methods. The deterministic methods have the added benefit of not having to estimate an analytical function prior to interpolation. Making them easy to implement and robust for variable input data.
A disadvantage of deterministic methods is that there are no accuracy measures are co-estimated, which is possible with stochastic methods. However, the previously performed analysis already gives an insight on the accuracy.
Between the deterministic methods the local approach of TBCI is more sensitive to outlier than BHSI, which uses all input information. The longer computation time for BHSI with respect to TBCI is not considered an issue.

2.2.4. Conclusion

In conclusion, the performance of all interpolation methods was satisfactory and good enough to be implemented for gravity prediction in the computation of geopotential differences in the Netherlands. Considering robustness and the slightly better performance in the analysis carried out above, Biharmonic Spline Interpolation (BHSI) was selected as the interpolation method to be utilized in the final procedure.

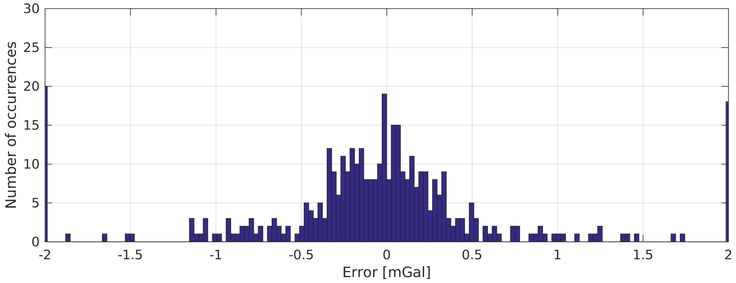

(a) LSC, all data.

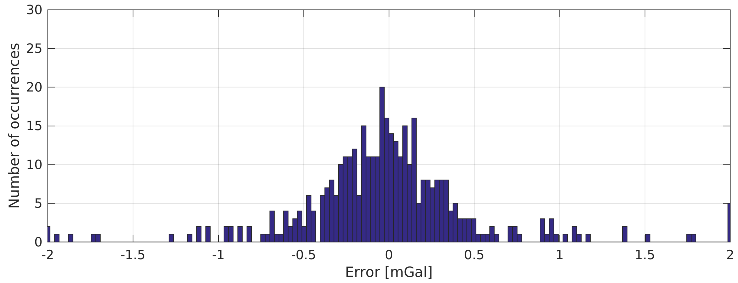

(b) LSC, subset data.

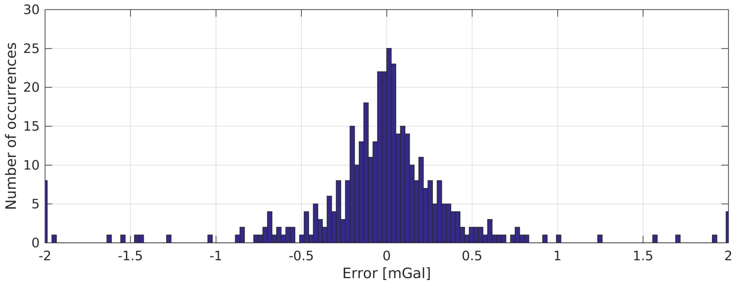

(c) OK.

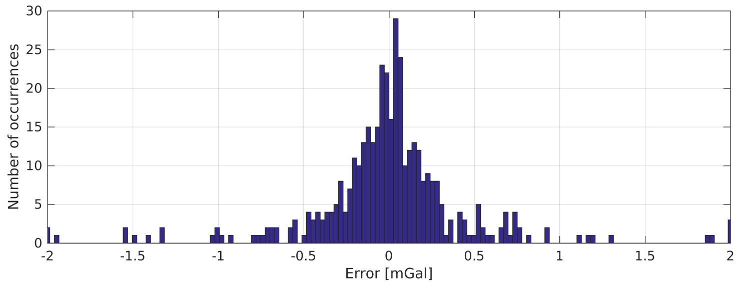

(d) TBCI.

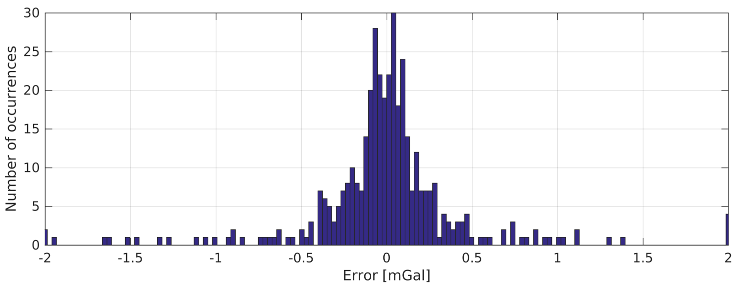

(e) BHSI, all data.

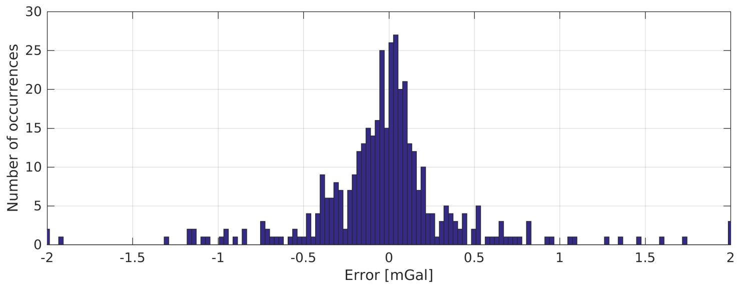

(f) BHSI, subset.

Figure 2.10: Histograms of the different interpolation results. An overview of mean, standard deviation, minimum and maximum errors made is provided in Table 2.2. The spatial distribution of these errors is shown in Figure 2.11.

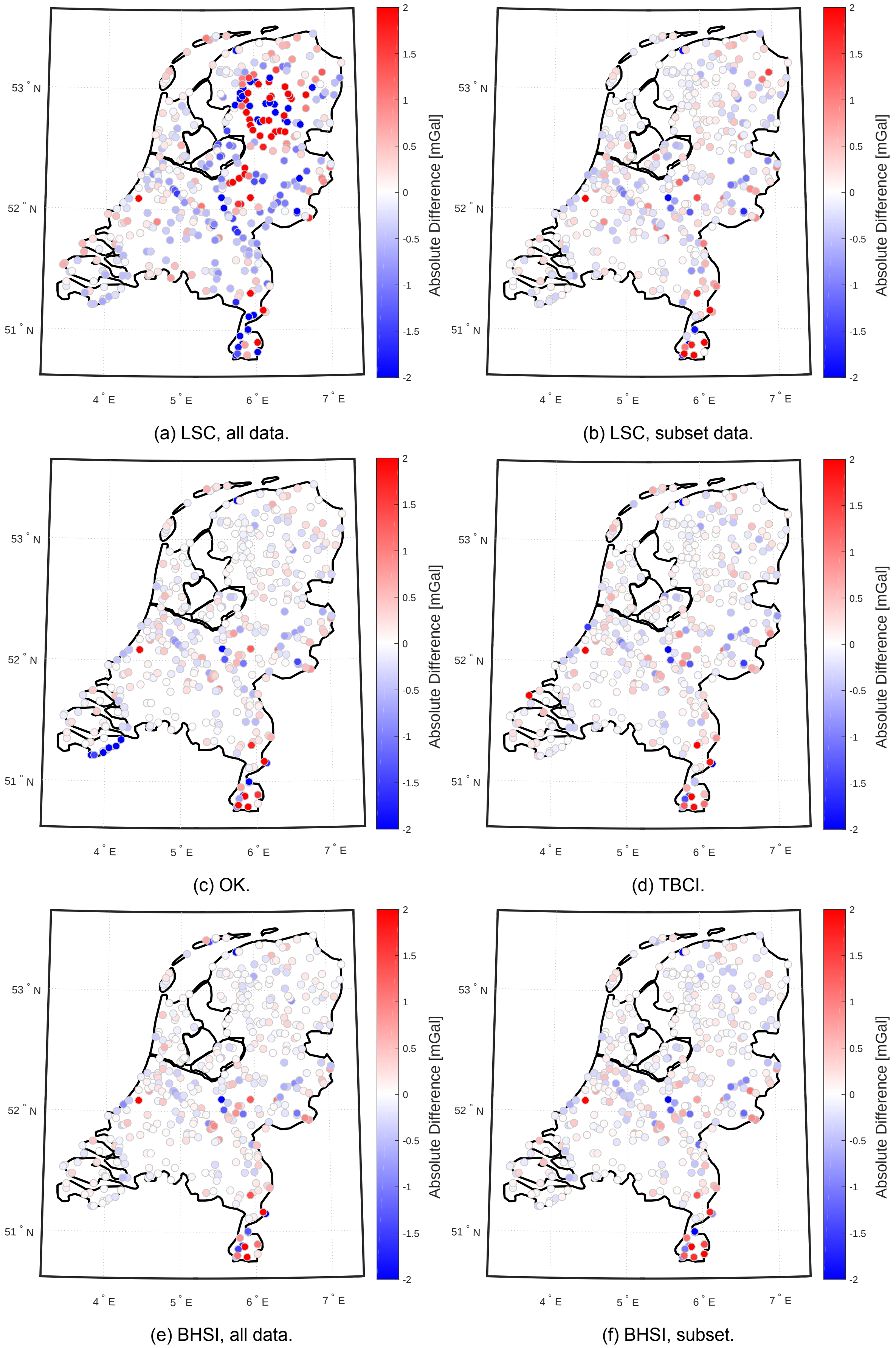

(a) LSC, all data. (b) LSC, subset data.

(c) OK. (d) TBCI.

(e) BHSI, all data. (f) BHSI, subset.

Figure 2.11: Spatial overview of the errors on the control point locations for the different investigated interpolation methods. Table 2.2 gives an overview of the interpolation results. Figure 2.10 gives the corresponding histograms.

2.3. Residual Terrain Modeling

While investigating the gravity interpolation methods, both height dependency and long-wavelength trends in the gravity data were removed.

In this section, the influence of smoothing, i.e. removing the short-wavelength signal, by applying RTM on the interpolation performance will be examined [Farahani et al., 2016]. Figure 2.12 shows the step where RTM is executed in the workflow.

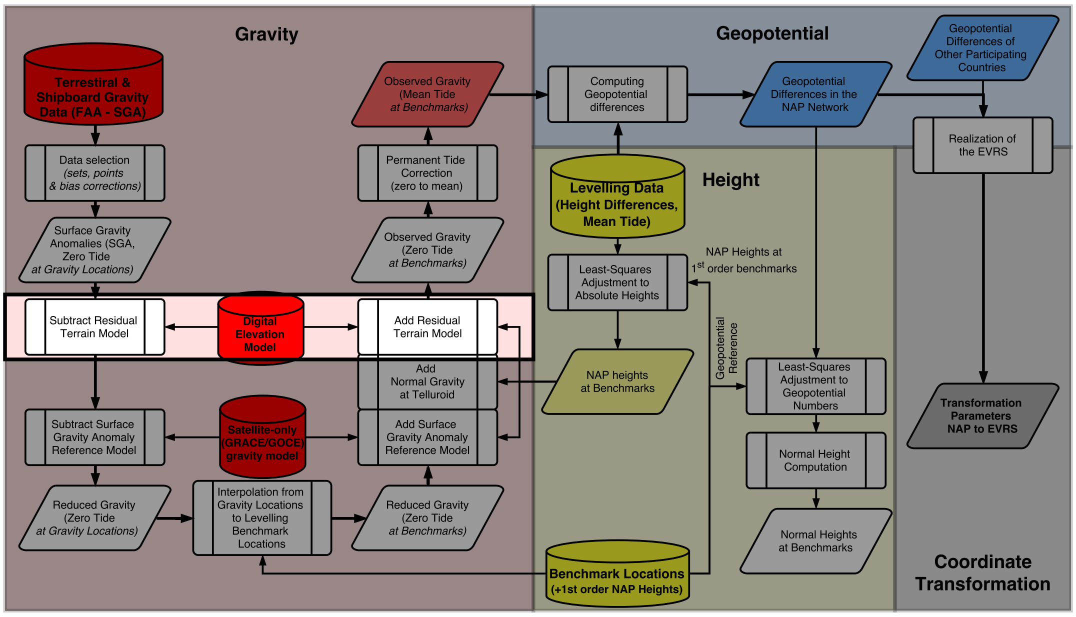

Figure 2.12: Overview of the workflow (Figure 2.1) in which the residual terrain modelling step, which will be treated in this section, is highlighted.

RTM Principle

As rock and soil have higher densities than air, topography causes density anomalies which affect the Earth's gravity field. Corrections for these effects are in general referred to as terrain corrections [Forsberg, 1984]. RTM correction is a specific type of terrain correction, which computationally replaces the topography with a mean elevation surface. Valleys below and masses above this mean elevation surface, or RTM surface, are respectively filled or removed. This is illustrated schematically in Figure 2.13.

In contrast to other topographic corrections, RTM does not influence the long-wavelength information of the data. This is because the RTM surface ensures mass conservation.

2.3.1. Research Set-up

A straightforward comparison of the interpolation results with and without RTM corrections applied will be performed to assess the impact of the RTM correction on the interpolation performance. This procedure is the same as for the interpolation section previously. Using the same control dataset and the same input data, Figure 2.8. In summary, BHSI is performed on the SGAs without the subtraction of the GOCO05s reference field, as was concluded in Section 2.2.

The RTM corrections are computed using the method of Heck and Seitz [2007] and Grombein et al. [2013]. This was performed using the TS software package. TS retrieves the topography information

from EuroDEM, SRTM or Aster GDEM, summed in hierarchical order. For the Netherlands only EuroDEM is used, described in Chapter 2.1.1. The RTM surface is computed for a large area between latitude 40 to 70 and longitude -20 to 20 with a grid spacing of 2 arcseconds, equal to the resolution of EuroDEM. Bathymetry is not taken into account, i.e. heights at sea are set to zero, and density used are 2.670 and 1.023 g/cm^3 for respectively the Earth's crust and water. The results with RTM corrections applied are obtained by subtracting the RTM corrections from both the input as well as the control data.
Additionally, Appendix D elaborates on the effect of RTM on the gravity field smoothness itself, instead of looking at the output effect, i.e. the interpolation quality.

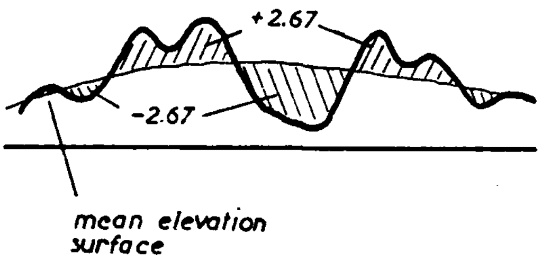

Figure 2.13: Schematic illustration of the topography (thick line) and mean elevation surface or RTM surface. Density effects of areas below the mean elevation surface are filled, areas above are subtracted. 2.67 g/cm^3 is a representable rock density [Forsberg, 1984, Fig. 8D].

2.3.2. Results

Table 2.3 shows the basic statistics of the BHSI with and without RTM correction applied. The corresponding spatial overviews are provided in Figure 2.14a and 2.14b respectively.

Figure 2.15 shows the difference between the interpolation result without RTM correction minus the interpolation result with RTM correction applied, i.e. Figure 2.14b - Figure 2.14a. The corresponding histogram is presented in Figure 2.16.

Table 2.3: Result comparison of the basic statistics of the interpolation results with or without RTM correction applied, as well as the difference in results.

Method	**RTM**	**Mean** $[mGal]$	**St.Dev** $[mGal]$	**Min** $[mGal]$	**Max** $[mGal]$
BHSI	No	0.00	0.51	-2.75	3.71
BHSI	Yes	-0.02	0.44	-3.62	3.57
Difference		0.02	0.38	-2.31	3.26

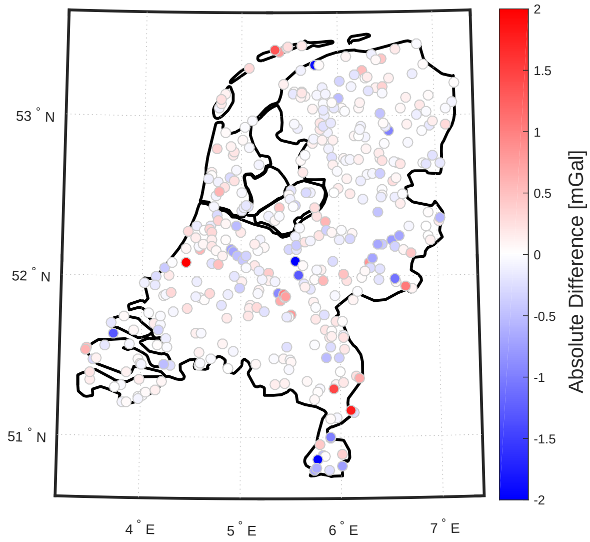

(a) Result with RTM.

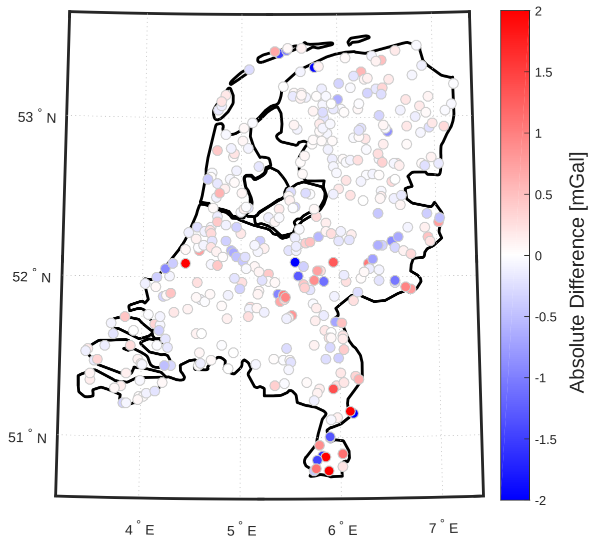

(b) Result without RTM.

Figure 2.14: Spatial overview of the interpolation errors on the control points for the BHSI with and without RTM corrections applied.

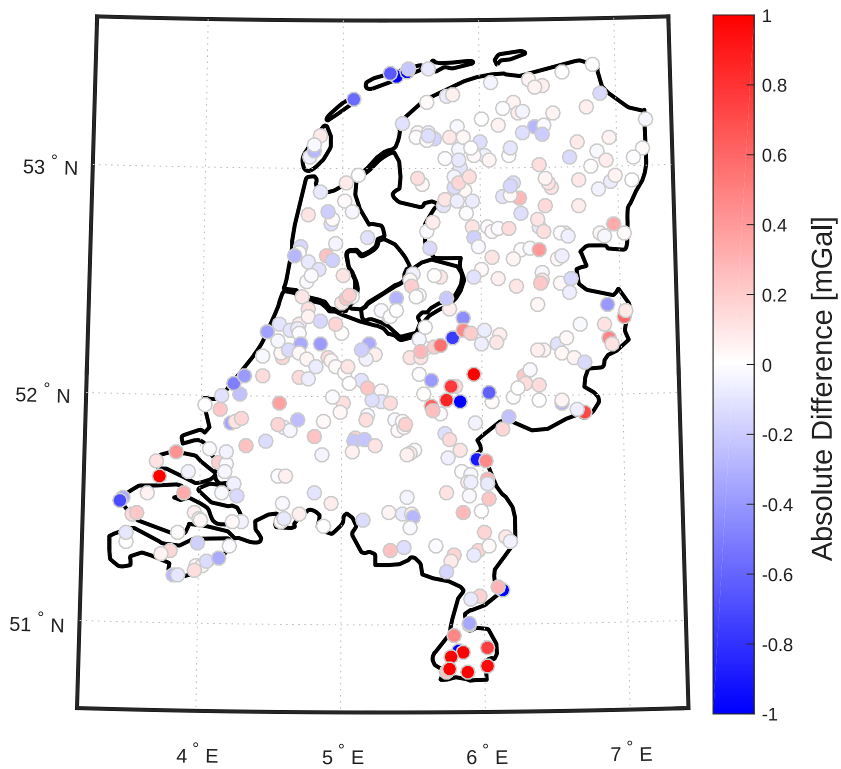

Figure 2.15: Difference between the interpolation results shown in Figure 2.14, results of without RTM minus with RTM corrections applied, i.e. Figure 2.14b - Figure 2.14a.

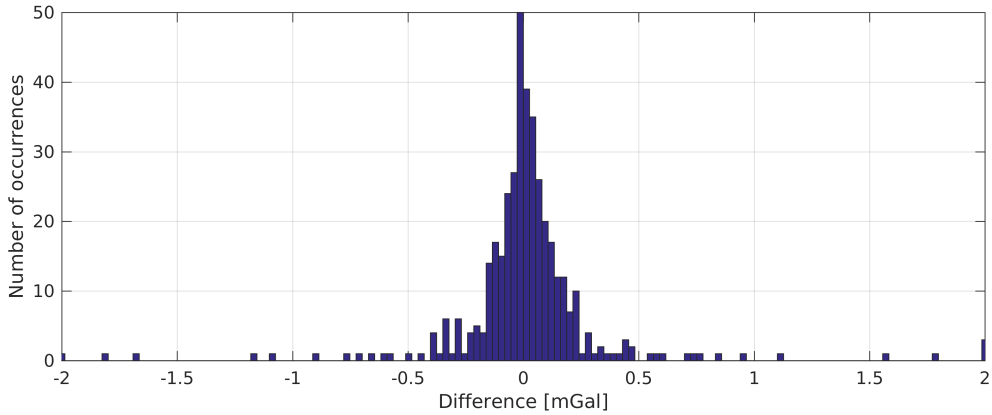

Figure 2.16: Histogram of the difference between the interpolation results with and without RTM corrections, corresponding to Figure 2.15

2.3.3. Discussion

The largest difference in interpolation result is observed in Limburg, where the difference is up to about 2 $mGal$. Also, in the middle of the country differences in the order of 1 $mGal$ are observed. This can be seen most clearly in Figure 2.14. For the rest of the country the differences with or without RTM correction are smaller than 0.5 $mGal$. The location of the larger error is expected given the Dutch topography.

In Limburg, the gravity values were in general overestimated without RTM. Applying RTM improves the quality of the gravity interpolation there. Still, there is one control point in Limburg which is very underestimated, dark blue, when RTM correction is applied. This control point was already underestimated without RTM. Applying RTM correction to this observation, worsens its prediction. However, given the general behaviour of the RTM correction in Limbrug, it is expected that this bad result is due to the control point itself and not the RTM method. Therefore, the minimum values in Table 2.3 are meaningless as this control point is responsible for the large minimum values.

When looking at the differences between the results in the histogram, there are only a few differences larger than $0.5\,mGal$ and the extremes (in Limburg) are approximately 2 $mGal$.
When a height difference of 50 metres over a certain levelling transect is assumed, an error of 2 $mGal$ would influence the geopotential difference about $10^{-3}\,m^2/s^2$. This corresponds roughly to a levelling error of 0.1 mm, given exactly known gravity over this transect. As a levelling error of 0.1 mm is below the expected levelling error, this difference is negligible here.
Also, direct implementation of TS in the software package would be troublesome due to copyright reasons.

Further, the result of the BHSI without RTM (Table 2.3) obtained here is the same as the BHSI results obtained in Section 2.2 (Table 2.2). However, in Section 2.2 the GOCO05s SGA reference field was subtracted, which was not the case here. This confirms the previously made statement that subtracting the reference field does not influence the performance of the deterministic interpolation methods.

2.3.4. Conclusion

The differences between interpolated gravity values with and without RTM correction are almost all smaller than 2 $mGal$. This interpolation improvement was found to be negligible with respect to the levelling errors. Also, the implementation of the RTM routine in the software would be cumbersome. Therefore, it was decided not to use RTM corrections when interpolating gravity in the computation of the geopotential differences for the NAP network.

Furthermore, subtracting the GOCO05s SGA reference field does indeed not influence the performance of the deterministic interpolation methods. Making it also unnecessary to apply this correction when using the BHSI on the Dutch gravity data.

2.4. Re-Computed Geopotential Differences

In Section 2.1 procedure for the computation of geopotential differences in the NAP network has been explained. Figure 2.1 showed a schematic overview of the whole procedure. Several sub-processes were examined in Sections 2.2 and 2.3 or illustrated in Appendices C and D. From this it was concluded that the SGA reference model and RTM corrections are not necessary for accurate gravity interpolation used in the computation of geopotential differences within the Netherlands.
Figure 2.17 shows the computational procedure as it is implemented here. Note, this is a revised version of Figure 2.1.

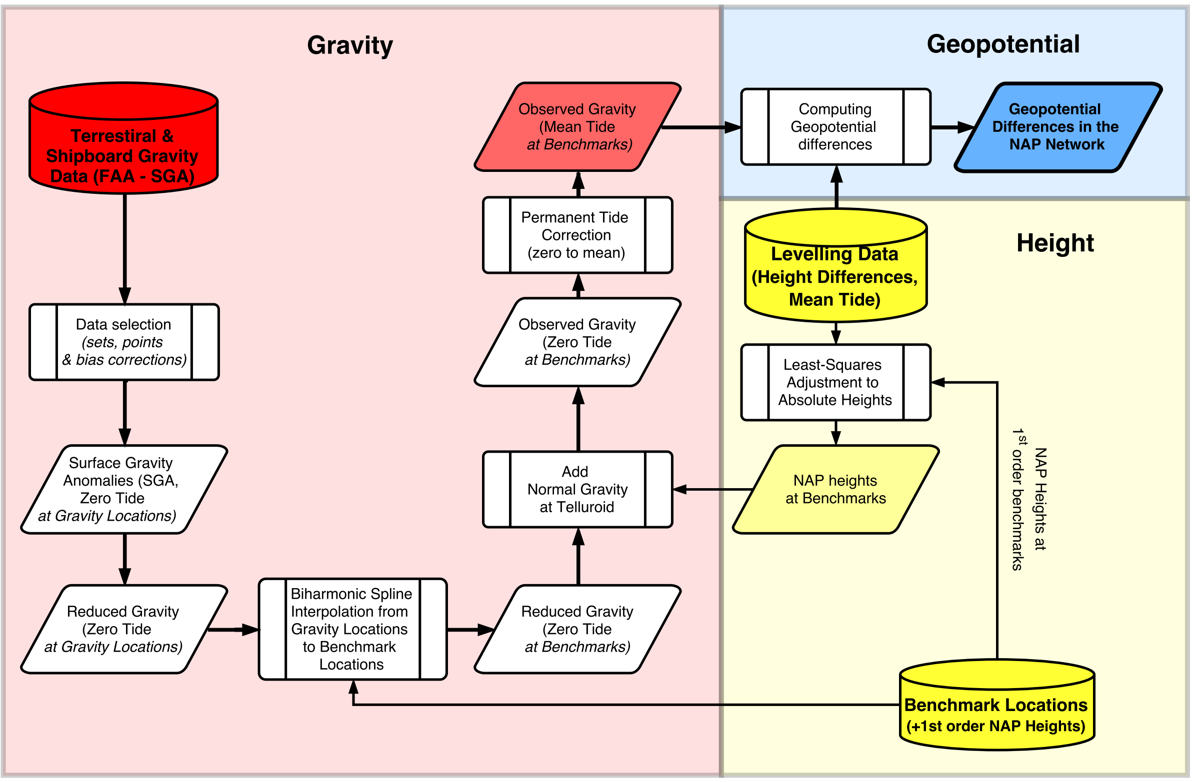

Figure 2.17: Revised and final version of the computational procedure. An overview of the processes, their mutual connections and steps, performed in the re-calculation of geopotential differences in the NAP network. This is the revised and the final version of Figure 2.1.

The newly re-computed geopotential differences between the levelling benchmarks can be found in *'./Data/GeopotentialDifferencesNAP.xlsx'* of the software directory. These results can also easily be obtained by executing the *ComputeNAPGeopotential* example given in Chapter 3.1.

The newly computed geopotential differences will be compared with those computed by RWS in 2004, in order to obtain insight into the origin of the errors made by RWS previously in their computation.

2.4.1. Gravity Comparison

The geopotential differences computed by RWS and those re-computed here are for the same bench-marks, using the same levelled height differences. Therefore, any differences in results must originate from the gravity values used in Equation 2.2. The gravity values used by RWS were also obtained by averaging the gravity of the starting- and end-benchmarks. Hence, the only difference in computational procedure is the gravity prediction at the levelling benchmarks. It was validated that the other steps of the process are exactly the same.

The difference in the gravity values predicted by RWS and those predicted here are shown in Figure 2.18. The histogram shows a noticeable amount of values in the order of $20 - 50\,mGal$. The corresponding benchmark locations are clearly visible in Figure 2.18, as the two red regions in the North and South of the Netherlands. Also ,the levelling line through Belgium shows up due to a slight (negative) difference.

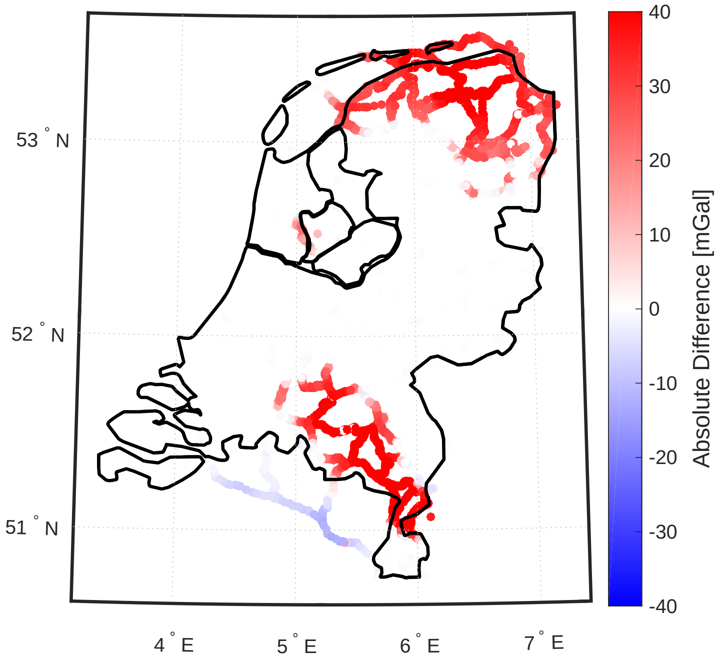

(a) Spatial overview of the differences in predicted gravity.

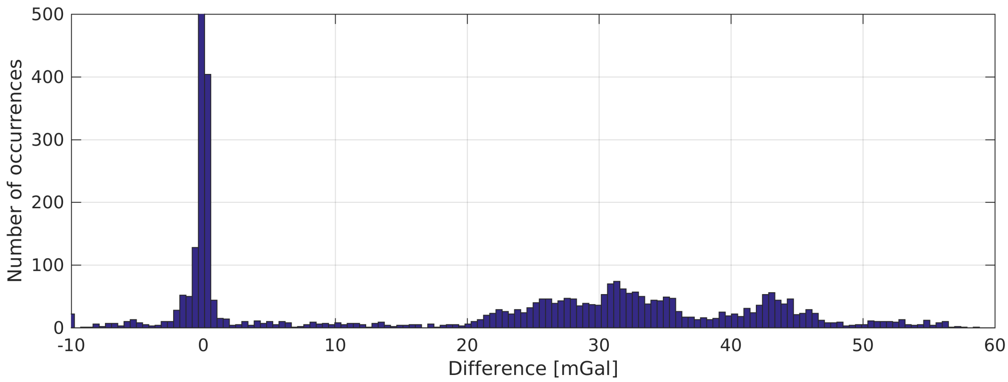

(b) Histogram of the differences in predicted gravity.

Figure 2.18: The differences in gravity predicted by RWS and predicted here. RWS's values minus the re-computed values are shown here.

Figure 2.19 shows the SGA values of all gravity observations used in the gravity interpolation. When compared with the differences in Figure 2.18 there is a certain resemblance. The regions with large negative SGAs correspond with the locations with the large positive difference. The same holds for the positive SGA values in Belgium where the levelling line had a negative difference previously. Further, the magnitudes of the differences in Figure 2.18 is about twice the size of the SGAs in Figure 2.19. This lead to the hypothesis a mistake in the sign convention of the SGAs in Equation 2.3 was made during the computation by RWS.

To test this hypothesis, it was attempted to reconstruct the results from RWS by flipping the SGA sign in Equation 2.3 for the restore-step to obtain observed gravity, i.e. subtracting the SGAs from the mean normal gravity instead of adding them.

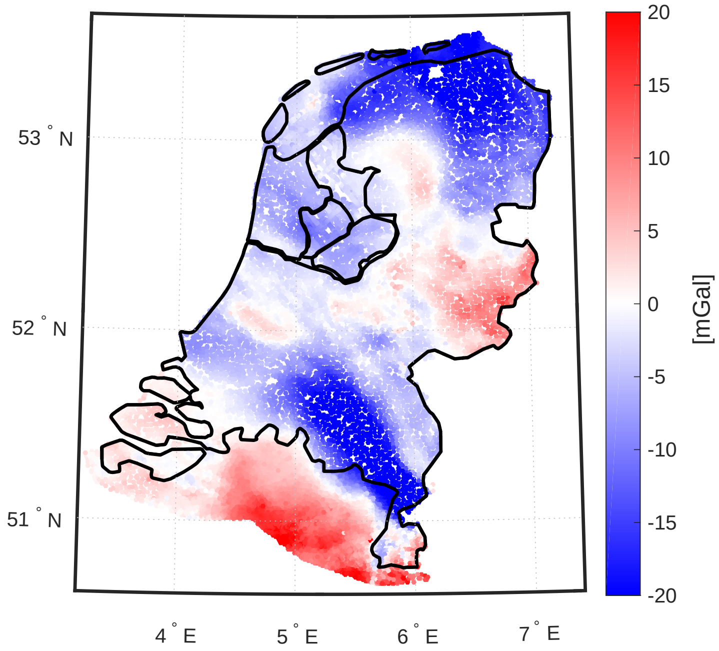

Figure 2.19: The surface gravity anomaly observation used as input for the gravity prediction.

The differences between the attempted reconstruction and the results by RWS are shown in Figures 2.20.
The spatial overview in Figure 2.20 clearly shows that the differences at the previously misfitted areas are now gone. This is also observed in the histogram. However, at all the other benchmarks differences appeared which were not there before. Changing the sign of the SGAs only improved the reconstruction at the previously erroneous locations. For the locations which previously matched, the reconstruction only worsened.

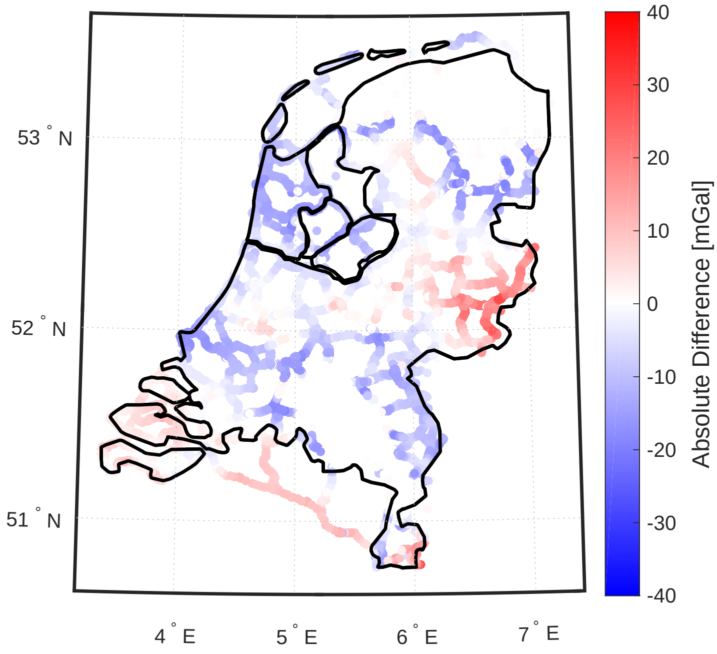

(a) Spatial overview of the differences between the predicted gravity.

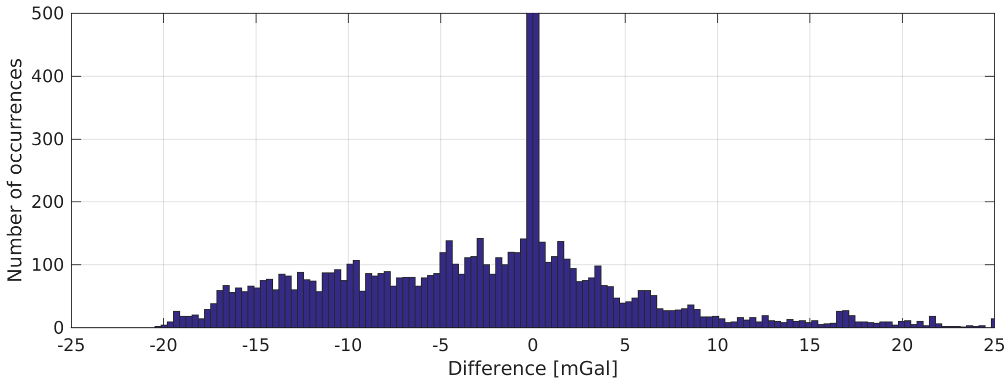

(b) Histogram of the differences between the predicted gravity.

Figure 2.20: The differences between the gravity predicted by RWS and the attempted reconstruction, changing the sign of the SGAs in Equation 2.3. RWS's values minus the reconstructed gravity values are shown here.

The results of selecting the best reconstruction (plus or minus SGA) per benchmark is shown in Figure 2.21. Note, the color bar of Figure 2.21 ranges between $[-5, 5]\ mGal$ instead of $[-40, 40]\ mGal$. Selecting the minimum difference of the two methods examined above results in most differences being smaller than 2 $mGal$, see the histogram in Figure 2.21b. The largest differences left are -12.60 and 12.78 $mGal$, which are located in Belgium. The levelling line through Belgium remains as the largest regional difference between the results. This is probably because RWS did not use gravity measurement in Belgium.

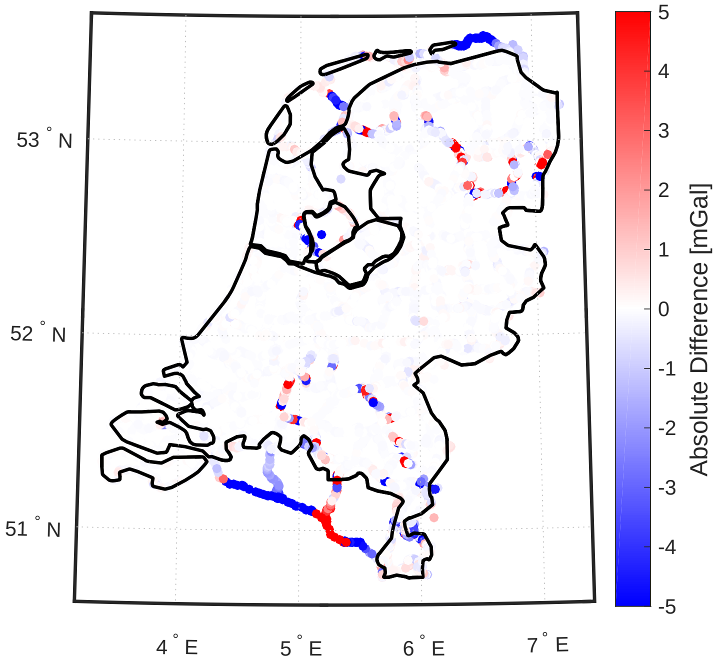

(a) Spatial overview of the difference between the predicted gravity.

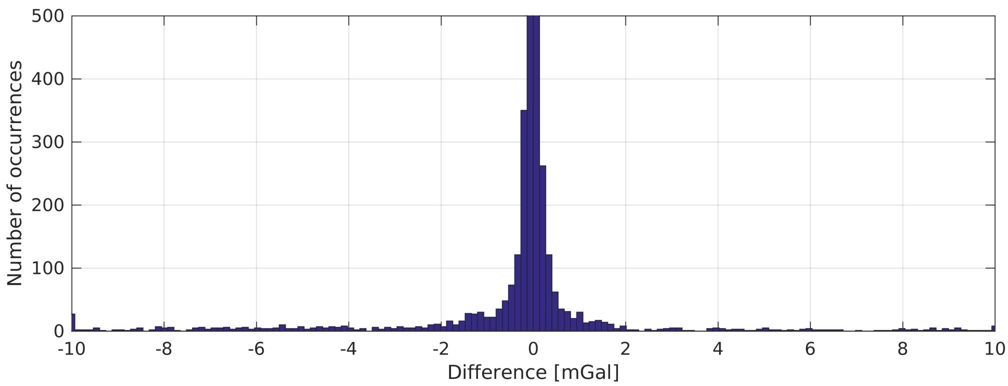

(b) Histogram of the differences between the predicted gravity.

Figure 2.21: The difference between the predicted gravity by RWS and the best reconstruction, i.e. minimum values of Figure 2.18 and 2.20 per benchmark.

However, even when the Belgian gravity measurement were excluded, the differences in Belgium remained large. Therefore, it was presumed also a different interpolation method was used by RWS. Using linear interpolation resulted in the best reconstruction.
This is shown in Figure 2.22, which is a recomputed version of Figure 2.21 using only Dutch gravity measurement and a linear interpolation. The differences in Belgium decreased, as well as resolving a small negative artifact in the north-northeast.

The remaining differences lie on the boundaries of the areas which originally (Figure 2.18) had the largest differences. It was attempted to further improve the reconstruction of RWS's results by testing different approaches for computing the normal gravity. It was examined if errors were made in the heights used here, i.e. using ellipsoidal heights or zero height instead of NAP heights. However, this did not significantly improve the reconstruction of RWS's results.

It is suspected that these minor residual differences could originate from differences in interpolation methods, e.g using ETRS89 coordinates instead of RD coordinates. Or if RWS used free-air anomalies (FAA) instead of SGAs, to allow for 2-D interpolation. Here, slight variations in the variables used would be possible. The relation between SGA and FAA is explained in Appendix B.

Additionally, gravity interpolation was performed using a program freely available on RWS's website, *zwaartekracht.exe* [de Min, 1995]. It was investigated if gravity values obtained with this program reconstructed RWS's results better than has been achieved previously. Just a few benchmarks were tested as only one location at a time could be interpolated by this program. However, the results for these benchmarks were no improvement on the reconstruction.

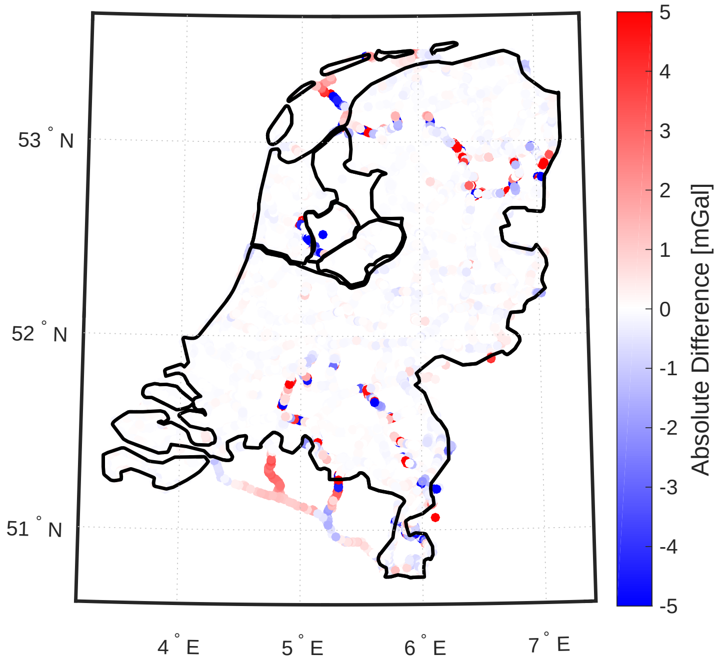

Figure 2.22: Recomputed version of Figure 2.21, using only Dutch gravity measurements and linear interpolation.

2.4.2. Geopotential Comparison

In the previous section, predicted gravity was compared to investigate differences in the procedures to compute geopotential differences. However, the main concern is not the gravity error but the corresponding geopotential difference error caused by these incorrect gravity values.

Geopotential is computed through Equation 2.2, multiplying gravity with levelled height difference. Hence, the magnitude of the geopotential error is the gravity error scaled by the levelling height. Figure 2.23 shows a histogram of the levelled height differences in the Netherlands. Most levelled height differences in the Netherlands are smaller than 5 metre. So given the gravity differences of approximately 40 $mGal$, observed in Figure 2.18b, the expected discrepancies in geopotential difference are expected to be about $2 \cdot 10^{-3}\, m^2/s^2$.

The result of the comparison of the geopotential difference is given in Figure 2.24. Obviously, the

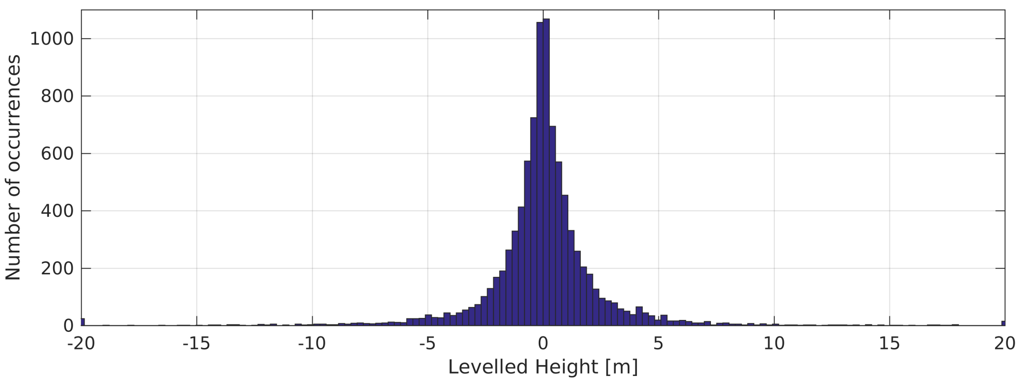

Figure 2.23: Histogram of the levelled height differences of all levelling connections provided by RWS. Absolute maximum levelled height difference is 85.64 m.

locations displaying the differences are still the same as for the gravity comparison. However, when comparing the geopotential histogram with the gravity histogram, Figure 2.18b, it is remarkable that the large outliers which were present in the gravity differences do not show up in the geopotential differences. Hence, due to the small height differences at the locations with the large gravity differences the corresponding geopotential discrepancies are attenuated. Also, because of the sign of the levelled heights this results in a more symmetric histogram.
Figure 2.24 indeed shows that most differences lie within $\pm 2 \cdot 10^{-3}\, m^2/s^2$, as expected. The absolute largest geopotential discrepancy observed is $0.0142 m^2/s^2$. These geopotential values roughly corresponds to height difference of 0.2 mm and 1.42 mm respectively, which is still in the range of expected levelling errors. This is due to the smooth topography of the Netherlands, especially at the location of the largest gravity errors.

2.4.3. Conclusion

The exact reconstruction of the results obtained by RWS in 2004, and thus precise identification of the previously made errors, was not achieved. The major difference in results could be reconstructed using a location dependent SGA sign convention in Equation 2.3. It is suspected linear interpolation was used by RWS for the gravity prediction.
The gravity differences could not be explained completely everywhere. However, as this was not the aim of this project, it has not been further pursued here.

The observed errors in the geopotential differences are approximately $\pm 2 \cdot 10^{-3}\, m^2/s^2$, with a largest difference of $0.0142 m^2/s^2$. This roughly corresponds to height difference of 0.2 mm and 1.42 mm respectively, which is in the range of expected levelling errors. The errors in the geopotential errors were attenuated due to the small height differences in the Dutch levelling data.

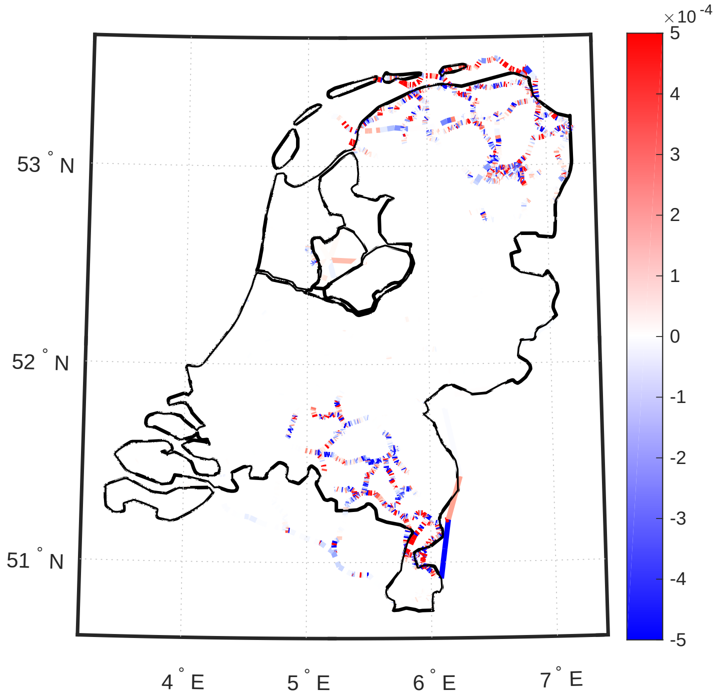

(a) Spatial overview of the geopotential discrepancies.

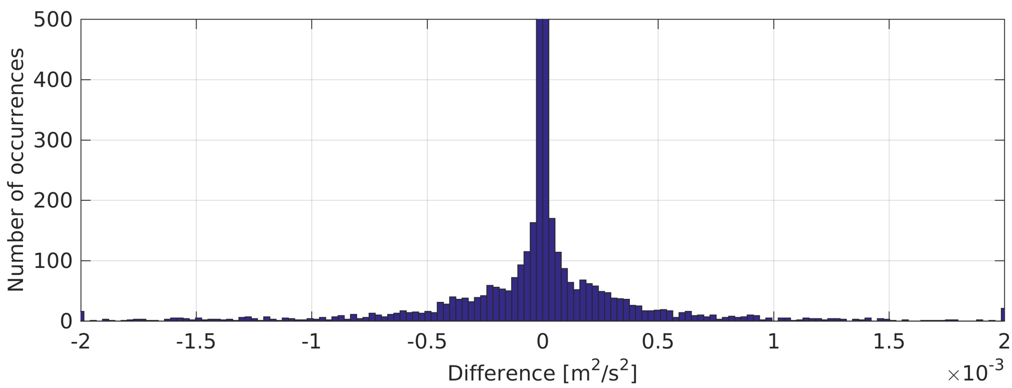

(b) Histogram of the geopotential discrepancies.

Figure 2.24: The differences between the re-computed geopotential differences and those obtained by RWS.

3
Software

For the realization of the EVRS all participating countries have to provide geopotential information on their national levelling networks to the BKG. Rijkswaterstaat is responsible for providing the geopotential differences of the Dutch NAP network.
The workflow to obtain these differences is explained previously in Chapter 2, where Figure 2.17 summerizes the computation of geopotential differences in the NAP network from the available levelling and gravity measurements. To simplify this routinely job, the computation has been implemented into a straightforward MATLAB procedure.

The software routines developed for this purpose and their usage will be explained in this chapter, in- and output are described and minimum working examples are provided. Support and internal routines are described shortly in Appendix E.

All the routines have been provided with a MATLAB help documentation.
The main routines: *ComputeNAPGeopotential*, *ComputeNAPNormalHeights* and *ComputeNormalHeights* can be found directly in the software folder. The user only invokes these routines. The subroutines in the 'misc' folder are only used by these main routines.

3.1. ComputeNAPGeopotential

ComputeNAPGeopotential computes geopotential differences from levelling and gravity data. The development of this procedure was given in Chapter 2 and summarized in Chapter 2.4.
Figure 3.1 shows schematically the steps performed by *ComputeNAPGeopotential*, which corresponds to Figure 2.17. The theoretical steps have been replaced by the sub-routines performing those steps. This illustrates the actions performed by these support routines. They are also described separately in Appendix E.

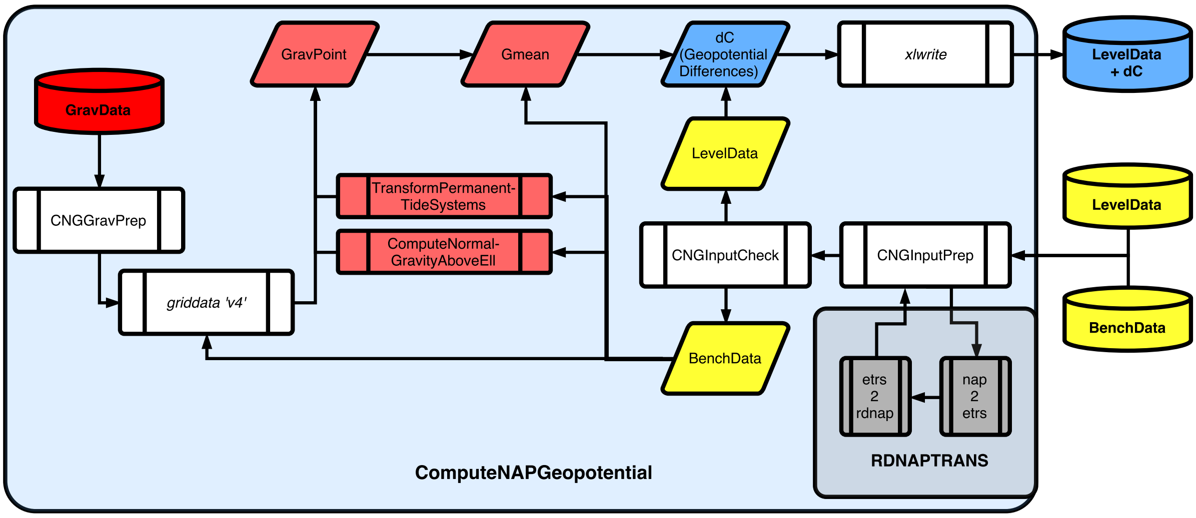

Figure 3.1: Overview of the workflow and support routines used in *ComputeNAPGeopotential*.

3.1.1. Input

The user has to provide information on the individual benchmarks and their levelled connections. The gravity data can be left out as it is embedded in the software.

Information on the individual benchmarks is referred to as BenchData in the software. The necessary information is:

1. IDs
2. UELN IDs (optional)
3. Latitudes [ETRS89, decimal degrees]
4. Longitudes [ETRS89, decimal degrees]
5. Heights [NAP, meter]

Information on their levelled connections is referred to as LevelData in the software. The necessary information is:

1. Starting IDs
2. End IDs
3. Height differences [meter]
4. Distances (optional)
5. Dates of acquisition (optional)

This input can be provided in the form of two spreadsheets (e.g. Microsoft Excel files). The columns of these spreadsheets have to contain the information in the same order as is listed above. A single line header on the first row of the spreadsheet is permitted, but not necessary.

It is also possible to provide the input as MATLAB vectors. This might be convenient if the data is available in another format, allowing more flexibility in loading the data into the MATLAB workspace. Also, for the provided vectors the ordering has to correspond to the previously mentioned lists.

The last two input arguments of *ComputeNAPGeopotential* are optional and reserved for controlling the additional/optional output:

end-1,	Outputfile:	controls if the LevelData spreadsheet, supplemented with computed geopotential differences, is created. The path and name of the output file should be provided as a string. If not provided or an empty array is provided no output file is generated.
end,	plt:	controls if intermediate plots are generated for a quick quality check.

Details on these outputs are described below. By default, when not provided or an empty array is given, no intermediate results are plotted and no output file is created.

3.1.2. Output

The outputs of the *ComputeNAPGeopotential* function are:

1. dC Computed geopotential difference for provided levelling connections.
2. Gmean Mean gravity over the provided levelling connections.
3. GravPoint Predicted gravity at benchmark locations.

These are depicted inside the function in Figure 3.1.

3.1.3. Additional Output

The optional output, controlled by input variable 'Outputfile', is a spreadsheet containing the provided levelling information supplemented with the computed geopotential differences, *LevelData + dC* in Figure 3.1.

Together with the BenchData spreadsheet, including UELN IDs, this output file is the information on the NAP network the BKG needs for the realization of the EVRS.

By default no plots are generated. If input variable 'plt' is set to 'True' three intermediate plots will be generated:

- an overview of the gravity measurements used for the interpolation,
- a cumulative distribution function of interpolation distances between the gravity measurements and the levelling benchmarks and
- an overview of the levelling benchmarks and their connections.

These plots are meant for a quick quality check. To see if the spatial distribution of the gravity measurements covers the area of interest, to make sure interpolation is not performed over very large distances and to see if no major errors have occurred during the handling of LevelData and BenchData.

3.1.4. Example

Folder ”Data” contains example levelling and benchmark input spreadsheets:

- input_levelling_data.xlsx
- input_benchmark_data.xlsx

A minimal working example of *ComputeNAPGeopotential*, using the spreadsheet input format, is given below:

```
InputLevelData = './Data/input_levelling_data.xlsx';
InputBenchData = './Data/input_benchmark_data.xlsx';
Outputfile     = './Data/GeopotentialDifferencesNAP.xlsx';

[dC, Gmean, GravPoint] = ComputeNAPGeopotential(InputLevelData, ...
                         InputBenchData, Outputfile,'False');
```

3.2. ComputeNAPNormalHeights

ComputeNAPNormalHeights computes normal heights in the mean tidal system from the geopotential differences computed by *ComputeNAPGeopotential*.

The steps performed by *ComputeNAPNormalHeights* and its internal support routines are shown schematically in Figure 3.2. These support routines are described separately in Appendix E.

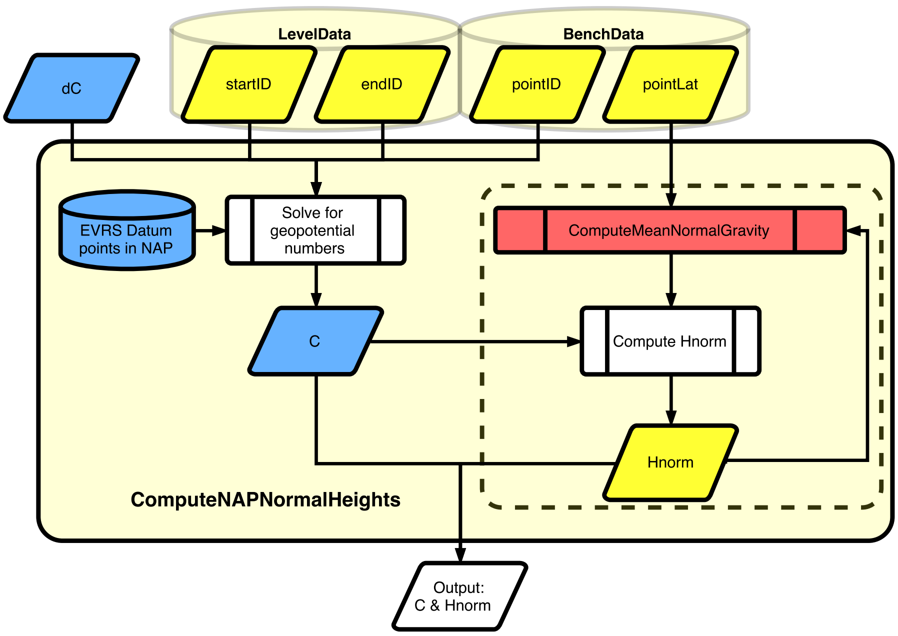

Figure 3.2: Overview of the workflow and support routines used in *ComputeNAPNormalHeights*.

Normal height ($H^\star$) is obtained by dividing the geopotential number (c) by the mean normal gravity between the ellipsoid and telluroid ($\bar{\gamma}$).

$$H^\star = \frac{c}{\bar{\gamma}} \tag{3.1}$$

This is explained in more detail in Appendix B. Because the average normal gravity depends on the corresponding normal height this can be solved iteratively [Hofmann-Wellenhof and Moritz, 2006]. The iteration is shown as a dashed contour in Figure 3.2. The computation is initiated with a height of 0 m. Usually convergence is reached within 10 iterations. If no convergence is reached after 1000 iterations the function is terminated, as a standard safety precaution.

ComputeNAPNormalHeights is designed to compute normal heights given the geopotential differences outputted by *ComputeNAPGeopotential*. Thus, before the previously described procedure can be performed the geopotential numbers of the benchmarks in the NAP network need to be solved for.
The geopotential numbers are obtained by solving a linear system consisting of the geopotential differences computed by *ComputeNAPGeopotential* in a LSQ adjustment. This is similar to the computation of the NAP heights for the missing benchmarks in Chapter 2.1.1. The system of equations can only be defined uniquely if at least one benchmark has a known geopotential number. From EVRF2007 two datum benchmarks, which are located in the NAP network, are used for this. Their details are shown in Table 3.1.

Table 3.1: EVRF2007 datum points used for the determination of the geopotential numbers in the NAP network [Sacher et al., 2009, Table 3].

UELN ID	**NAP ID**	**Latitude [ETRS89, DD]**	**Longitude [ETRS89, DD]**	**GPN EVRF2007 (mean tide) [m^2/s^2]**
913000	000A1013	52.851417	5.518967	57.232
913011	000A1112	52.141733	5.360567	411.084

3.2.1. Input

The following MATLAB arrays are required to compute the geopotential numbers and corresponding normal heights:

1. dC Geopotential differences [m^2/s^2] (output of *ComputeNAPGeopotential*)
2. startID Levelling connection starting IDs (corresponding to dC)
3. endID Levelling connection ending IDs (corresponding to dC)
4. pointID Benchmark IDs (corresponding to pointLat)
5. pointLat Benchmark Latitudes [ETRS89, decimal degrees]

The inputs startID and endID correspond to columns 1 and 2 of LevelData and pointID and pointLat correspond to columns 1 and 3 of BenchData, as previously described for the input of *ComputeNAP-Geopotential*. This is illustrated in Figure 3.2.

3.2.2. Output

The *ComputeNAPNormalHeights* output consists of:

1. C Computed geopotential numbers (mean tidal system) [m^2/s^2]
2. Hnorm Computed normal height (mean tidal system) [m]

The ordering of the output arrays corresponds to input array pointID.

3.2.3. Example

A minimal working example of *ComputeNAPNormalHeights*, using *ComputeNAPGeopotential* to compute dC, is given below:

```
InputLevelData = './Data/input_levelling_data.xlsx';
[~, text, ~] = xlsread(InputLevelData);
startID = text(2:end,1); % startID
endID   = text(2:end,2); % endID

InputBenchData = './Data/input_benchmark_data.xlsx';
[data, text, ~] = xlsread(InputBenchData);
pointLat = data(:,2);      % Benchmark Latitude (ETRS89)
pointID  = text(2:end,1); % Benchmark ID

[dC, ~, ~] = ComputeNAPGeopotential(InputLevelData,InputBenchData);
[Hnorm, C] = ComputeNAPNormalHeights(pointID, startID, endID, dC, pointLat);
```

3.3. ComputeNormalHeights

However, if geopotential numbers are already known the function *ComputeNormalHeights* can be used directly.

ComputeNormalHeights is essentially a stripped version of *ComputeNAPNormalHeights* which performs the steps shown inside the dashed contour of Figure 3.2. The iteration procedure is performed as described for *ComputeNAPNormalHeights*.

This function only needs two input arrays;

1. C the geopotential numbers $[m^2/s^2]$
2. pointLat Corresponding Benchmark Latitudes [ETRS89, decimal degrees]

The output of *ComputeNormalHeights* is the same as the output of *ComputeNAPNormalHeights*.

4

Influence on EVRF2007

New geopotential differences for the NAP network were computed with the computational procedure presented in Chapter 2. The differences between the newly computed and previously provided data were discussed in Section 2.4. In this chapter the influence of the new geopotential differences on the EVRF will be examined.

4.1. Computed Realizations

Since the adoption of EVRF2007 in 2008, several other countries also updated the data of their national levelling networks and provided them to the BKG. The BKG performed the adjustment of UELN using different combinations of old and updated data. Hence, several alternative realizations of the EVRS were computed in order to analyse the impact of the updated data. The different variants computed by the BKG are listed below:

1. **EVRF2007-old**: The current realization of the EVRS, the EVRF2007 as it is in use now. This was already available and is considered the initial state.

2. **EVRF2007-new**: The EVRF2007 recomputed with the updated NAP data, including the correct treatment of the NAP's permanent tide. All other data were left unchanged.

3. **EVRF2016-old**: This is a realization of the EVRS as it would be possible to compute with today's available data. However, instead of the new NAP geopotential differences the old ones, as provided in 2004, have been used here. The permanent tide system of the NAP data has been handled correctly in this computation. Therefore, this realization can be used as the initial state to evaluate the impact of the new computational procedure and the corresponding differences found in Section 2.4.

4. **EVRF2016-new**: Here, The latest data sets have been used.

5. **EVRF2016-new-minus**: Similar to EVRF2016-new this realization uses all the updated data. However, the long levelling lines through Germany, which were discussed in Section 2.1 (Figure 2.3), have been excluded from the NAP data set.

The standard deviation in the EVRF2007(-old) for the Dutch measurements is 0.75 $kgal \cdot mm$. With the new NAP data, EVRF2007-new, the standard deviation is 0.74 $kgal \cdot mm$ and for the adjustment with with the data available in 2016, EVRF2016-xxx, the standard deviation is 0.74 $kgal \cdot mm$. The changes in standard deviations between the realizations are very small, as 1 $kgal \cdot mm$ corresponds approximately to 1 mm.

4.2. Comparison of Realizations

To assess the impact of the updated data, both NAP and others, several comparisons were made. The height difference between realizations were examined at the Dutch UELN benchmarks. There are 1113 and 1115 UELN benchmarks provided for respectively the EVRF2007 and the EVRF2016. Table 4.1 gives an overview of the five comparisons, their basic statistics and the figures showing their results, which will be discussed here.

Table 4.1: Overview of the basic statistics of the height comparison of the Dutch UELN benchmarks for different EVRS realizations. Note, the comparisons are made for ”EVRF 1” minus ”EVRF 2”.

EVRF 1	**EVRF 2**	**Mean** $[mm]$	**St.Dev** $[mm]$	**Min** $[mm]$	**Max** $[mm]$	**Ref Figure**
2007-new	2007-old	0.22	3.66	-9.06	6.87	4.1
2016-new	2016-old	1.10	2.63	-4.42	6.24	4.3
2016-new-minus	2016-new	-0.14	0.50	-6.14	2.87	4.4
2016-new	2007-new	-5.92	4.04	-18.35	6.62	4.5
2016-new-minus	2007-old	-5.83	1.97	-15.08	1.10	4.6

The difference between EVRF2007-new and EVRF2007-old is shown in Figure 4.1. The main difference observed here is a north-south tilt with a magnitude of about 16 mm, from a difference of almost -9 mm in the south to a difference of almost 7 mm in the north.

It is known permanent tide mistakes were made in the realization of EVRF2007-old. The NAP data in 2004 was processed by the BKG as if being tide-free data, while actually being provided in the mean tidal system. The observed trend appears to be latitude dependent. This is a behaviour which corresponds to height differences between permanent tide systems. Figure 4.2 shows the normal height difference between mean tidal system and tide-free system above a zero tidal geoid in the Netherlands. This figure shows a similar tilt.

However, the offset in Figure 4.2 is not observed when comparing EVRF2007-old/new and the magnitude of the tilt is smaller, only 8 mm instead of 16 mm.

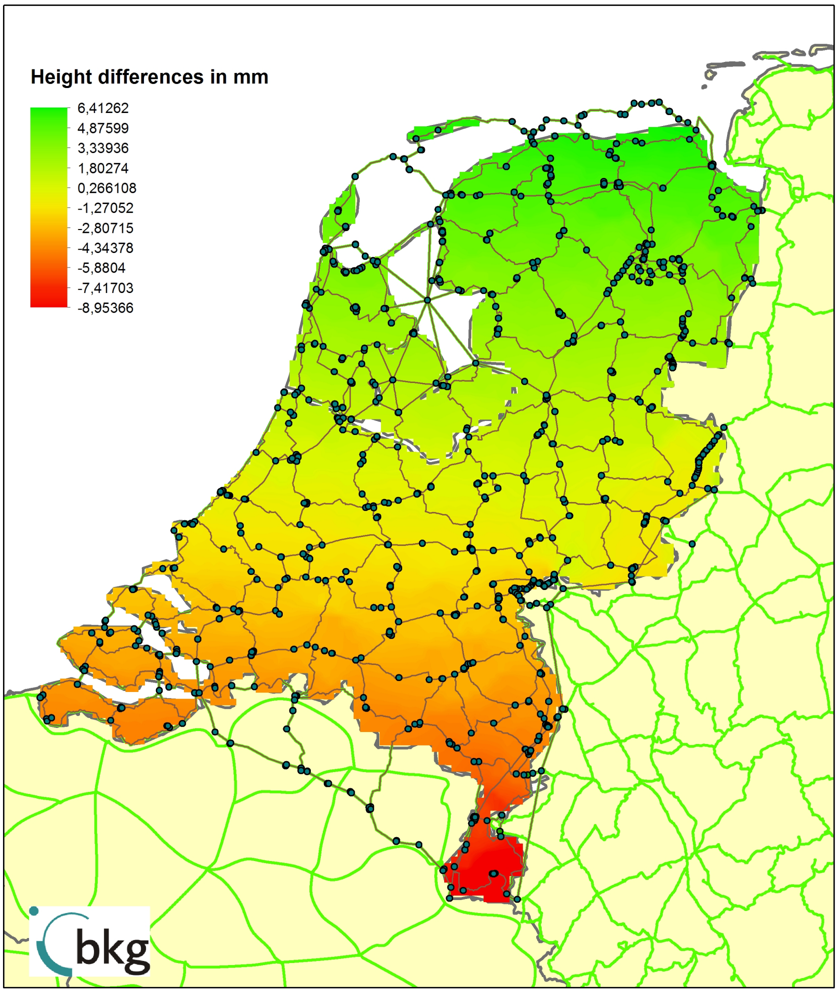

(a) Spatial overview of the height differences of the Dutch UELN benchmarks and interpolated between them.

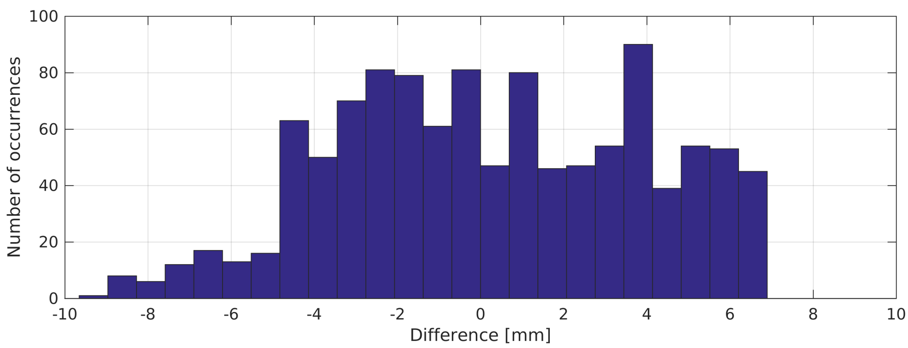

(b) Histogram of the height differences.

Figure 4.1: The height difference between EVRF2007-new and EVRF2007-old, heights at the Dutch UELN benchmarks.

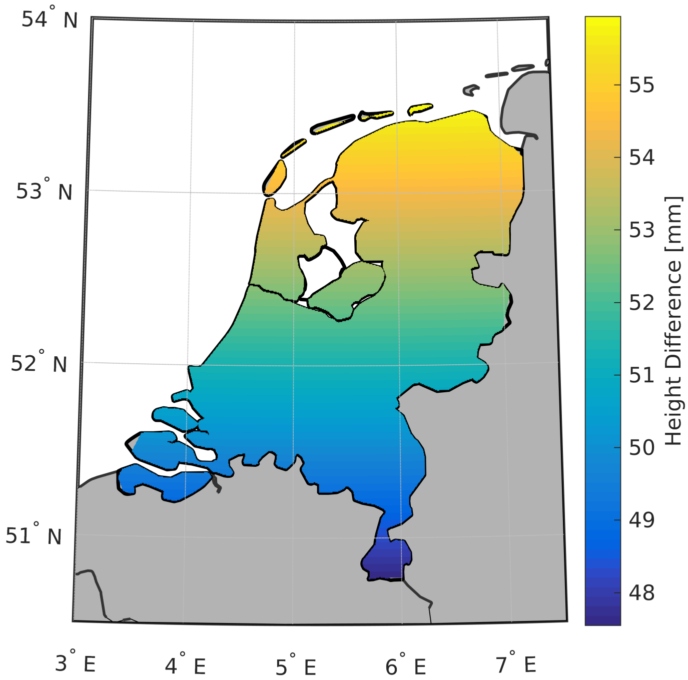

Figure 4.2: Spatial overview of the normal height difference between mean tidal system and tide-free system in the Netherlands. A zero tidal geoid was used.

When comparing EVRF2007-old/new the observed differences are due to both the updated geopotential differences and the treating of the permanent tide system. Comparing EVRF2016-old and EVRF2016-new the observed differences are only due to the updated geopotential difference, as the permanent tide has been treated the same for both these realizations. Thus, in order to isolate the effect of the updated geopotential differences EVRF2016-new is compared with EVRF2016-old. The results are shown in Figure 4.3.
Again a tilt, in the same direction, is observed. The magnitude of the tilt is 7 mm from south to north, which is slightly smaller than observed for EVRF2007-old/new.

Since the data used to compute EVRF2007 is not exactly the same as for EVRF2016, an accurate comparison of the observed effects cannot be made. However, the combined magnitude of the tilts observed for EVRF2016-old/new and the tidal effect do roughly add up to the total effect observed for EVRF2007-old/new. It thus seems the updated geopotential difference and the correct treatment of the permanent tide account in a similar amount to the differences observed in EVRF2007-old/new.

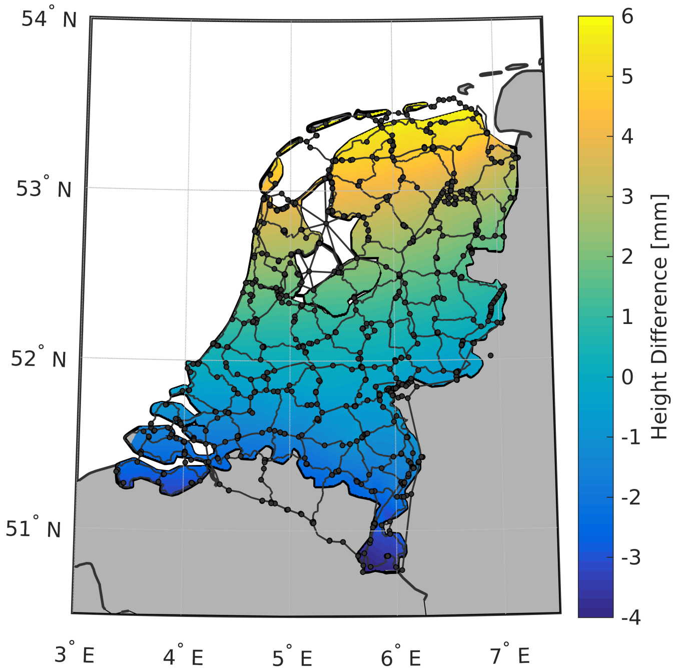

(a) Spatial overview of the height differences of the Dutch UELN benchmarks and interpolated between them.

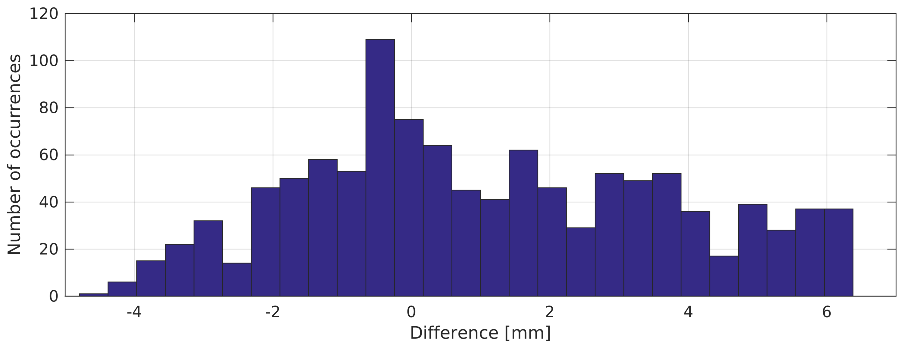

(b) Histogram of the height differences.

Figure 4.3: The height difference between EVRF2016-new and EVRF2016-old, heights at the Dutch UELN benchmarks.

Figure 4.4 shows the difference between EVRF2016-new and EVRF2016-new-minus. EVRF2016-new and EVRF2016-new-minus both use all the updated data. The only difference in the data is that 10 long levelling observations, located along the Dutch-German border, are excluded in the EVRF2016-new-minus realization. Most differences here are smaller than 1 mm. These originate from a very subtle tilt, magnitude of 2 mm dipping north. The more remarkable feature is a local negative difference at latitude 52 at the Dutch-German border.

The long levelling lines excluded in EVRF2016-new-minus are represented in the provided NAP data as a single observation. The observations in the NAP data are mostly already sums of several observations, this is explained in Section 2.1.1. However, what makes the excluded lines different is that they are a sum of German levelling observations. For the adjustment of the NAP these lines have been

incorporated into the Dutch data to strengthen the network along the border. As the NAP is adjusted as purely levelled heights, these lines are perfectly valid height observations. However, the EVRS is realized with geopotential, which introduces some issues. Firstly, the route of the original levelling line is unknown. Therefore, the geopotential difference cannot be computed accurately for this observation, see Appendix C. Secondly, levelling lines in the German network connecting these same benchmarks are available in the UELN adjustment. Hence, this results in correlated observations; the geopotential differences via the German network and the inaccurate geopotential differences provided directly in the NAP data.
These long levelling lines should indeed be excluded for the previously stated reasons. Therefore, the EVRF2016-min-minus realization is here adopted as the best realization of the EVRS given the current data sets.

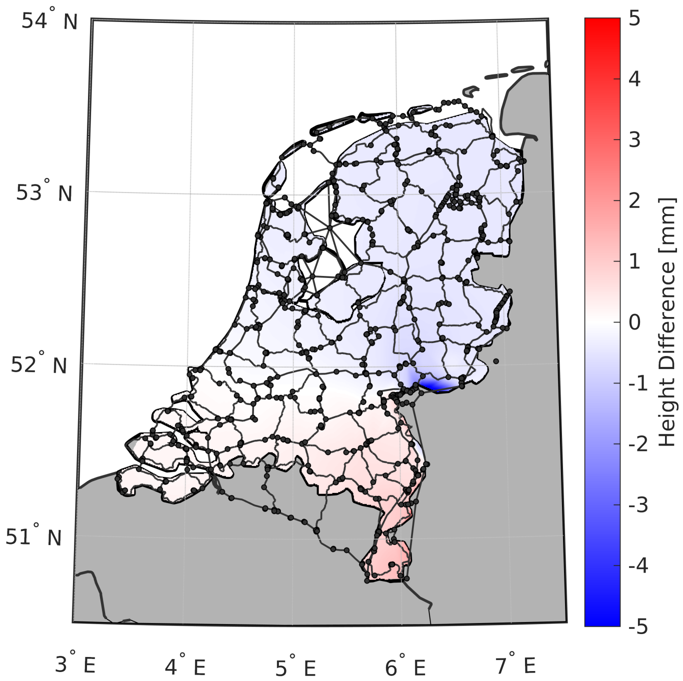

(a) Spatial overview of the height differences of the Dutch UELN benchmarks and interpolated between them.

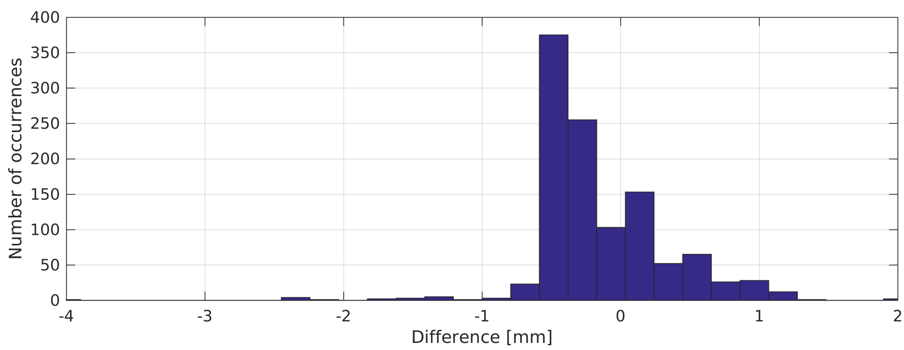

(b) Histogram of the height differences.

Figure 4.4: The height difference between EVRF2016-new-minus and EVRF2016-new, heights at the Dutch UELN benchmarks.

The only influence which has not yet been investigated here, is that of the updated data of other countries. This will be done by comparing EVRF2016-new and EVRF2007-new, shown in Figure 4.5. Again, the main influence is a general north-south oriented tilt. The magnitude is about 20 mm dipping to the north. However, the NAP data is the same for the realizations compared here. This illustrates the influence of updated measurements propagating into the rest of the network, which will be looked into further in the next section. It should be noted that the height differences of the UELN benchmarks here are largely negative, with a mean of -5.92 mm. Additionally, a locally negative difference is observed in the north-east of the Netherlands.

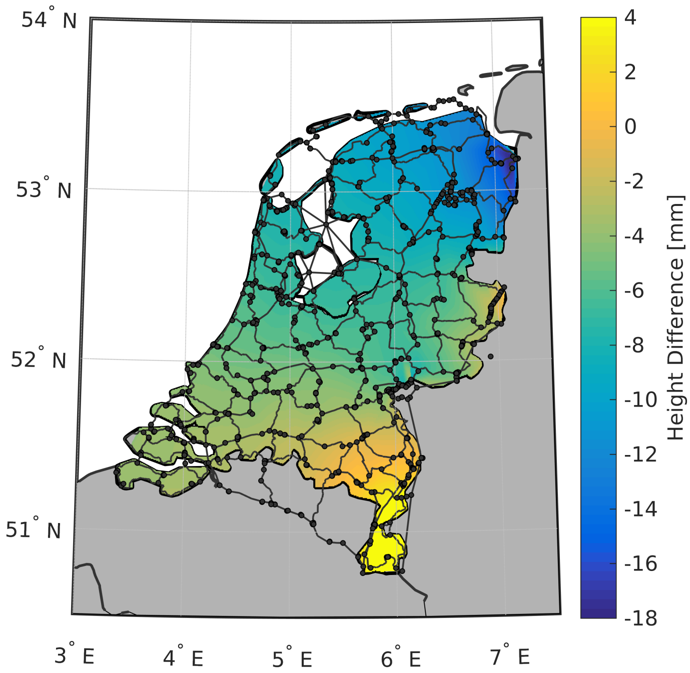

(a) Spatial overview of the height differences of the Dutch UELN benchmarks and interpolated between them.

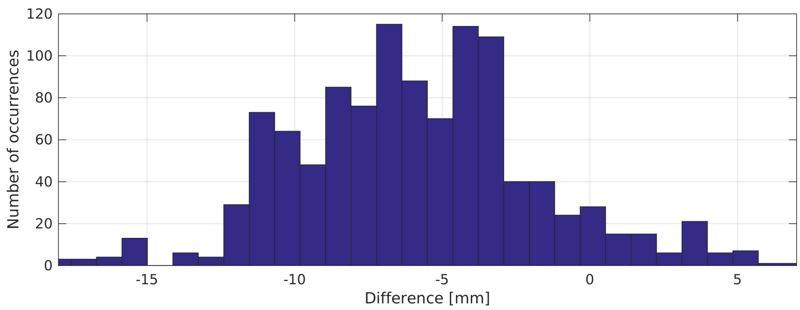

(b) Histogram of the height differences.

Figure 4.5: The height difference between EVRF2016-new and EVRF2007-new, heights at the Dutch UELN benchmarks.

So far only the impact of separate updates, isolating the different contributions, was investigated. The initial EVRF2007-old is compared with EVRF2016-new-minus to visualize the total impact of the updated information, both in the NAP and provided by other countries. This result is shown in Figures 4.6. Here, no obvious tilt is observed. It is expected that the tilt due to the updated NAP data, 16 mm

dipping south, is counteracted by the tilt due to the other updated data, 20 mm dipping north. Since the differences between EVRF2016/2007-new were mainly negative, the remaining signal here also has a negative difference. Hence, in the Netherlands EVRF2016-new-minus is generally lower than EVRF2007-old.

The other noticeable local features, as observed in EVRF2016-new/new-minus and EVRF2016/2007-new previously (Figures 4.4a and 4.5a), are located at the same positions.

It should be noted that the input-output effects in the UELN adjustments are not straightforward, e.g. local errors propagate into the whole network. Still, the general effects of the separate contributions previously identified could be recognized in the observed total difference.

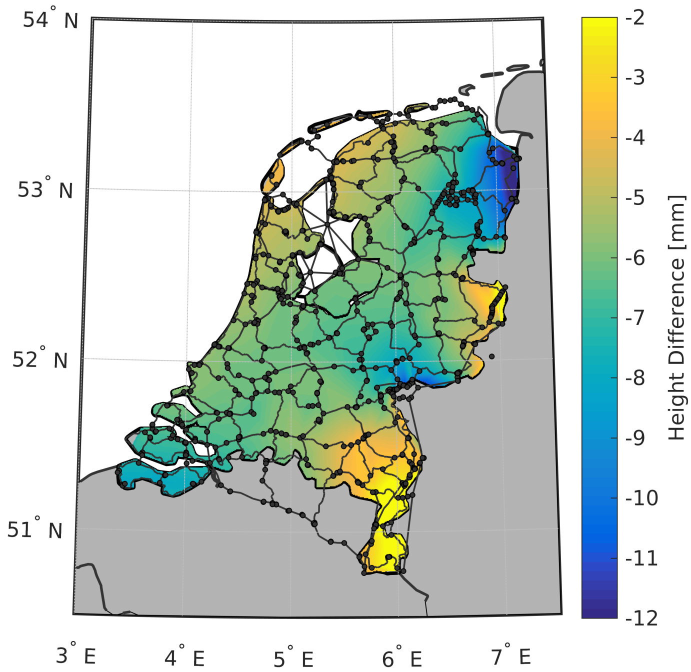

(a) Spatial overview of the height differences of the Dutch UELN benchmarks and interpolated between them.

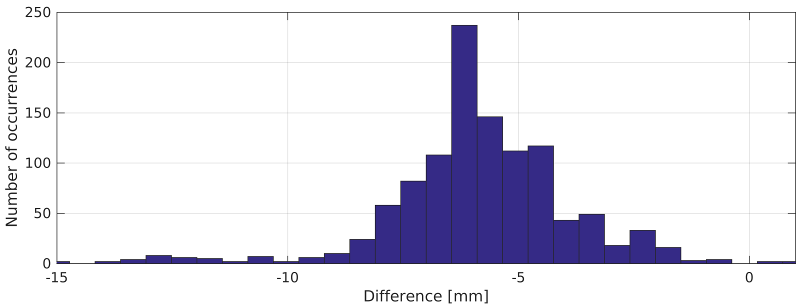

(b) Histogram of the height differences.

Figure 4.6: The height difference between EVRF2016-new-minus and EVRF2007-old, heights at the Dutch UELN benchmarks.

4.3. Influence Datum Points

In the previous section the differences between realizations were examined at UELN benchmarks within the Netherlands. In this section, the impact of updating the NAP, and the other data sets, on the whole network will be illustrated. This impact will be asses by looking at the height difference of the 13 EVRS datum points in different realizations. Table 4.2 gives an overview of all datum points, their locations and heights in different EVRS realizations. Note, the sum of the datum point heights is equal for all realization, satisfying Equation 1.1.

Figure 4.7 shows the change in datum point heights for EVRF2007 when the geopotential differences in the NAP are updated. This is EVRF2007-old minus EVRF2007-new, corresponding to Figure 4.1. The tilt observed in Figure 4.1 is also seen at the two datum points in the Netherlands, as expected. It can be seen this trend continues into Belgium, where the height difference is -2.68 mm. Due to its latitude, the west-German datum point is not influenced by the north-south oriented tilt. As was mentioned in the introduction, heights in Belgium and Germany are effected the most. Further away from the Netherlands the effects decrease and becomes sub-millimetre.

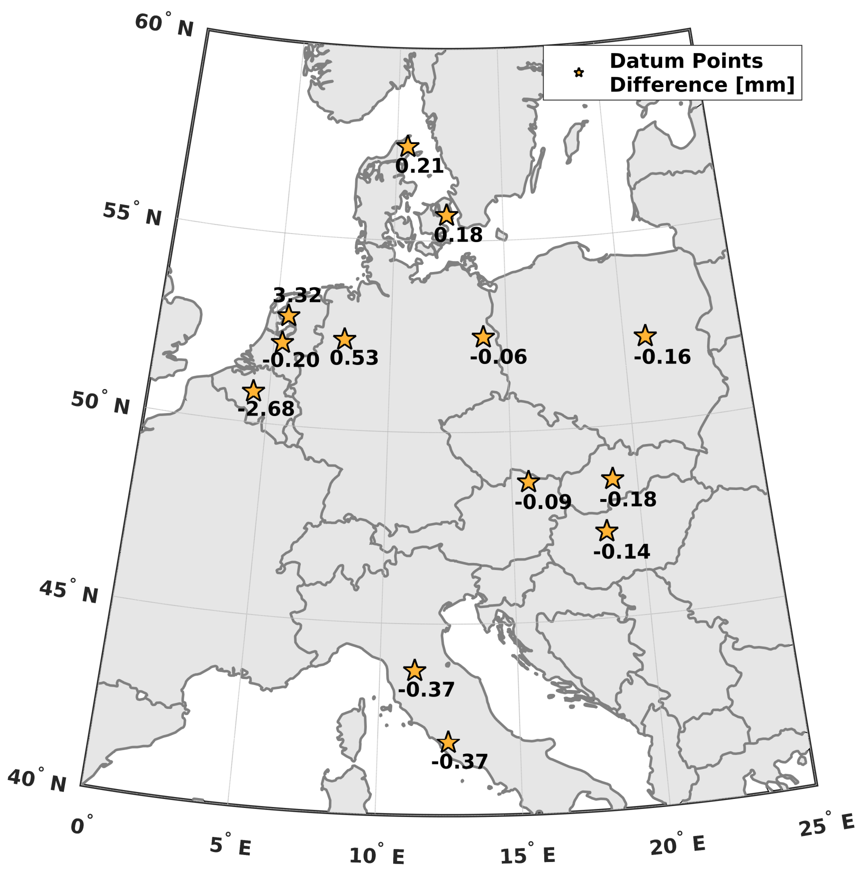

Figure 4.7: Spatial overview of the height difference of the EVRS datum points between EVRF2007-new and EVRF2007-old. A full overview of the datum point information is provided in Table 4.2.

Examining the total impact of all updated data is done by comparing EVRF2007-old and EVRF2016-new-minus. Because EVRF2016-new-minus is thought to be the best realization of the EVRS with the current information, this comparison illustrates the expected difference between the current EVRF2007 and the expected next updated version of the EVRS.

Figure 4.8 shows the change in datum point heights between EVRF2007 and the best EVRS realization given the current information. The changes of the Dutch UELN benchmarks were already shown in Figure 4.6. Here, it was seen that the whole Dutch vertical reference would be lowered by updating the EVRS. When looking at all datum points it seems this lowering of the Netherlands is caused by a Europe-wide north-northwest dipping tilt. With the largest effects in Denmark and Italy, -1.7 and 1.5 centimetre respectively. Hence, a translation of the reference surface is restrained due to Equation 1.1. The change in height of the most datum points is larger than 0.5 cm with extremes in the range of 1.5 cm. These are quite significant changes, which might suggest this is an appropriate moment to adopt an updated realization of the EVRS.

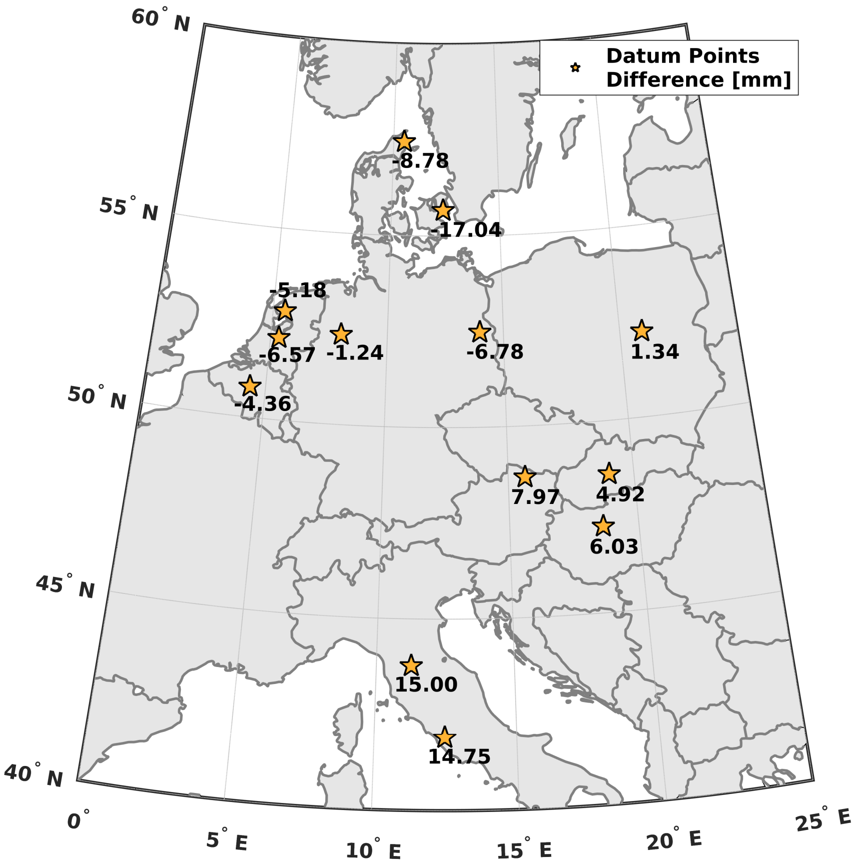

Figure 4.8: Spatial overview of the height difference of the EVRS datum points between EVRF2016-new-minus and EVRF2007-old. A full overview of the datum point information is provided in Table 4.2.

Table 4.2: Overview of EVRS datum points, their heights in the different realizations and differences in heights.

ID		Location			Height [m]					Height Difference [mm]	
EULN ID	Local ID	Country	Lat	Lon	2016 old	2016 new	2016 new-minus	2007 old	2007 new	2007-new 2007-old	new-minus 2007-old
102105	937856	AT	48.664867	15.674783	306.614	306.613	306.613	306.606	306.605	-0.09	7.97
200038	IGNMK	BE	50.799167	4.359400	97.852	97.849	97.850	97.854	97.852	-2.68	-4.36
401110	3614900005 / 5	DE	52.349788	8.015233	94.455	94.456	94.456	94.457	94.457	0.53	-1.24
401658	3549901400 / Hoppegarten	DE	52.480537	13.983619	54.630	54.630	54.630	54.637	54.637	-0.06	-6.78
514004	00204009190 / G.I.2086	DK	55.666017	12.393367	14.294	14.294	14.294	14.311	14.311	0.18	-17.04
514182	05304009619 / G.M.787.1	DK	57.447017	10.511600	16.886	16.886	16.886	16.895	16.895	0.21	-8.78
800432	35 / Firenze	IT	43.776000	11.259883	49.820	49.819	49.820	49.805	49.804	-0.37	15.00
800441	44 / Roma	IT	41.909850	12.476050	17.333	17.333	17.333	17.318	17.318	-0.37	14.75
913000	000A1013	NL	52.851417	5.518967	5.735	5.739	5.739	5.744	5.747	3.32	-5.18
913011	000A1112	NL	52.141733	5.360567	41.802	41.803	41.802	41.809	41.809	-0.20	-6.57
1103000	0000001-1 / Nadap II	HU	47.255750	18.620017	176.403	176.402	176.402	176.396	176.396	-0.14	6.03
1706115	26330081 / 50	PL	52.230100	20.948383	112.817	112.817	112.817	112.816	112.816	-0.16	1.34
1905325	EH-V. / XVI.	SK	48.606500	19.017333	272.785	272.785	272.785	272.780	272.780	-0.18	4.92
				Sum:	1261.43	1261.43	1261.43	1261.43	1261.43		

5

Connection of NAP to EVRS

For the unification of independent height system realizations, the EVRS uses a geodetic levelling approach. Observed cross-border levelling connections enable a common adjustment to estimate an unified height reference frame, i.e. EVRF2007.
While discussing cross-border levelling observations in the EVRF2007 for this purpose Rülke et al. [2012, p. 345-346] mentioned:

> *"A number of cross border observations have been included into the analysis to connect adjacent countries. ... the number of connections to the Netherlands, France, Spain, Portugal and Italy is fairly poor."*

The quality of the realization of the EVRS depends on the quality of the separate national levelling networks and their mutual connections. The current situation of the connection of the NAP with the neighbouring countries will be examined here.

5.1. Current Situation

The BKG is responsible for the computation of the realizations of the EVRS. The necessary information on the levelling networks and their mutual connections should be provided to the BKG by the participating countries. In this section, an overview of the connections, currently known at the BKG, from the NAP to the neighbouring levelling networks will be provided.

At present, there are 29 cross-border levelling observations known at the BKG which connect the NAP to the German and Belgian levelling networks. These observations, between benchmarks in the UELN network, are listed in Table 5.1. For some observations also an intermediate benchmark is provided.
An overview of the locations of these connections is given in Figure 5.1. The areas indicated with the red contours correspond to the areas mentioned in the last column of Table 5.1. Detail plots of these areas, containing one or multiple cross-border connections are provided in Figure 5.2. The legend of Figure 5.1 also applies to all plots in Figure 5.2.

Table 5.1: Overview of all the border crossing connections of the NAP known to the BKG.

	Dutch UELN Benchmark			Conn. Benchmrk	German UELN Benchmarks			
#	UELN-NL	Dutch ID	German ID	Dutch ID	UELN-DE	Dutch ID	German ID	Area
1	900162	008D0022		008D0025	462349	008D0026	2809900014	1
2	914653	008D0128		008D0140	462349	008D0026	2809900014	1
3	411195	000B0105	2809900019	000B0104	401629	000B0103	2809900017	1 (zoom)
4	462349	008D0026	2809900014	n/a	401628	000B0107	2809900021	1 (zoom)
5	913844	013D0009		013D0150	412366	000B0200	3009900502	2
6	908046	018C0143		018C0091	413580	018C0176	3208900320	3
7	913676	029A0093		n/a	401121	029A0059	3508900018	4
8	913682	029A0121		029A0118	401121	029A0059	3508900018	4
9	913719	035A0110		n/a	417260	035A0109	3707900004	5
10	913709	034F0321		035A0039	417261	035A0108	3707900005	5 & 7
11	913716	034G0165		n/a	401284	035A0133	3708900011	5 - 7
12	913655	000B0130		n/a	418806	034G0164	3906900014	6
13	913711	034G0087		n/a	418807	034G0163	3906900015	6
14	913787	041D0018		041D0084	420212	041D0092	4105900026	8
15	920050	PRE0008131		n/a	420212	041D0092	4105900026	8
16	913763	040G0047		n/a	401633	040G0048	4102900007	9
17	920048	PRE0008129		PRE0008130	401118	000B0191	4102900023	9
18	920047	PRE0008128		n/a	421252	000D0002	4202900023	10
19	913796	046B0026	4101900315	n/a	421236	046B0125	4201900002	10
21	917841	046B00059		n/a	421236	046B0125	4201900002	10
22	920046	PRE0008127		n/a	423934	000B0160	4503900017	11
23	913806	052H0025		052H0063	423934	000B0160	4503900017	11
24	913809	052H0057	4503900037	n/a	423934	000B0160	4503900017	11
25	918942	058G0067	4702901001	n/a	427268		4803900008	12
26	918996	060B0076		060D0205	428281	060D0204	4901900148	13
27	919065	060D0200		060D0202	428281	060D0204	4901900148	13
28	900077	000B0180	5202900084	n/a	431756		5202901104	14

	Dutch UELN Benchmark			Conn. Benchmrk	Belgian UELN Benchmarks			
#	UELN-NL	Dutch ID	Belgian ID	Dutch ID	UELN-BE	Dutch ID	Belgian ID	Area
29	913382	047H0030		n/a	200067	053F0101	HH4	15

Not all benchmarks or levelling connections shown in Table 5.1 were represented in the data available here. Therefore, some connections do not coincide exactly with the connections in the levelling data used here. The cross-border connections as presented in Table 5.1 are plotted between the mentioned benchmarks where possible.

The connections in Table 5.1 which appeared to be inconsistent with the data available here are listed below:

4: German UELN Benchmark 008D0026 was already used as a Dutch UELN Benchmark for connections 1 and 2.

11: German UELN Benchmark 035A0133 is not present in the used levelling data. However, a connection between 034G0165 and 035A0113 does exist. It is assumed a typo has been made. In the figures 035A0113 was used instead of 035A0133.

19: Dutch UELN Benchmark 046B0026 is not present in used levelling data. However, a connection between 046B0125 and 046B0126 does exist. It is assumed a typo has been made. In the figures 046B0126 was used instead of 046B0026.

21: Dutch UELN Benchmark 046B00059 is not present in the used levelling data. It is also not according to the usual format of the Dutch benchmark IDs. Benchmark 046B0059 does exist and connects to 046B0125. It is assumed a typo has been made here. In the figures 046B0059 was used instead of 046B00059

24: Dutch UELN Benchmark 052H0057 is not present in the used levelling data. However, a connection between 000B0160 and 052H0063 does exist. It could be that a typo has been made. In the figures 052H0063 was used instead of 052H0057.

25: No Dutch ID was provided for the German UELN Benchmark (UELN-DE 427268). For visualization purposes benchmark 058G0074 was used in the figures.

28: No Dutch ID was provided for the German UELN Benchmark (UELN-DE 431756). No appropriate or plausible connecting benchmark was found in the available levelling data. Additionally, a 000Bxxxx number is expected to be a German benchmark instead of a Dutch one.

29: Note, this observation connects to Belgium instead of Germany.

The UELN IDs as shown in Table 5.1 are not provided in the benchmark and levelling data. Therefore, these apparent inconsistencies cannot be further examined or verified here.

5.1.1. German Connections

To summarize the status of the connection between the NAP and the German levelling network, as it is currently known at the BKG; there are 28 separate observations connecting the Dutch and German levelling networks. These observations are spread over 13 locations (Area 1-6 and 8-14) which are evenly distributed along the Dutch-German border. This border has a total length of 577 km, which results in a connection location roughly every 44 km.

5.1.2. Belgian Connections

The connection of the NAP to the Belgian levelling network is clearly less well known at the BKG. Only one observation (observation 29) connects the NAP to the Belgian levelling network.

The BKG is aware of this situation. It has been mentioned by the BKG that the connection with Belgium was taken from data of 1973. An update of this data has been promised, which is expected to improve the present situation.

5.2. Recommendations

Given the levelling data provided by RWS, the list of cross-border connection points by the BKG and Figure 4.1a, also provided by the BKG, recommendations will be provided in this section.

5.2.1. German Connections

RWS has mentioned that ”000Bxxxx” and ”000D000x” benchmarks in the provided levelling data refer to German underground benchmarks. According to this definition a total of 17 German underground benchmarks are present in RWS’s levelling data. Since only 10 of these reappear in Table 5.1, it might be there are additional connections which have not been explicitly communicated with the BKG yet.

Further on close inspection of Figure 4.1a the levelling loop connecting to observation 1, the most northern Dutch-German connection in Figure 5.1, appears to not be closed. The line which seems to leave to the north from this cross-border connection stops just before it reaches the Dutch benchmark. Figure 4.1a also shows a cluster of UELN benchmarks crossing the Dutch-German border, between area 3 and 4 of Figure 5.1. However, no German levelling line connects to it. This could be looked into.

5.2.2. Belgian Connections

Figures 4.1a and 5.1 clearly show a levelling line in the Dutch network which runs through Belgium. This data was part of the *5de nauwkeurigheids waterpassing* provided to the BKG in 2004.
Figures 4.1a also shows the Belgian levelling network crossing this line at least 5 times. In Antwerp and Maastricht the levelling lines even seem to connect to the same UELN benchmarks. Therefore, it is expected that this levelling line should be, or already is, connected to the Belgian levelling network. The Belgian benchmarks are unfortunately not identified as clearly as the German ones in RWS’s levelling data. The ”000Cxxxx” benchmarks are indeed located in Belgium. However, if these benchmarks belong to the Belgian network is not mentioned explicitly, it is only mentioned that they are used for the mutual connection of hydrostatic levelling. Therefore, no recommendations could be formulated directly from this.

Additionally, Benchmark 000B0180, mentioned in observation 28 and shown in area 14 of Figure 5.1, is located very close to the tripoint where the borders of Germany, Belgium and the Netherlands meet. It would be beneficial for all mutual connections between Germany, Belgium and the Netherlands if there would be a German-Belgian or Dutch-Belgian connection close-by as well. Figures 4.1a shows that the German and Belgium levelling networks almost intersect just south of this point. The German levelling network even extends slightly into Belgium. Unfortunately, there is no connection visible here.

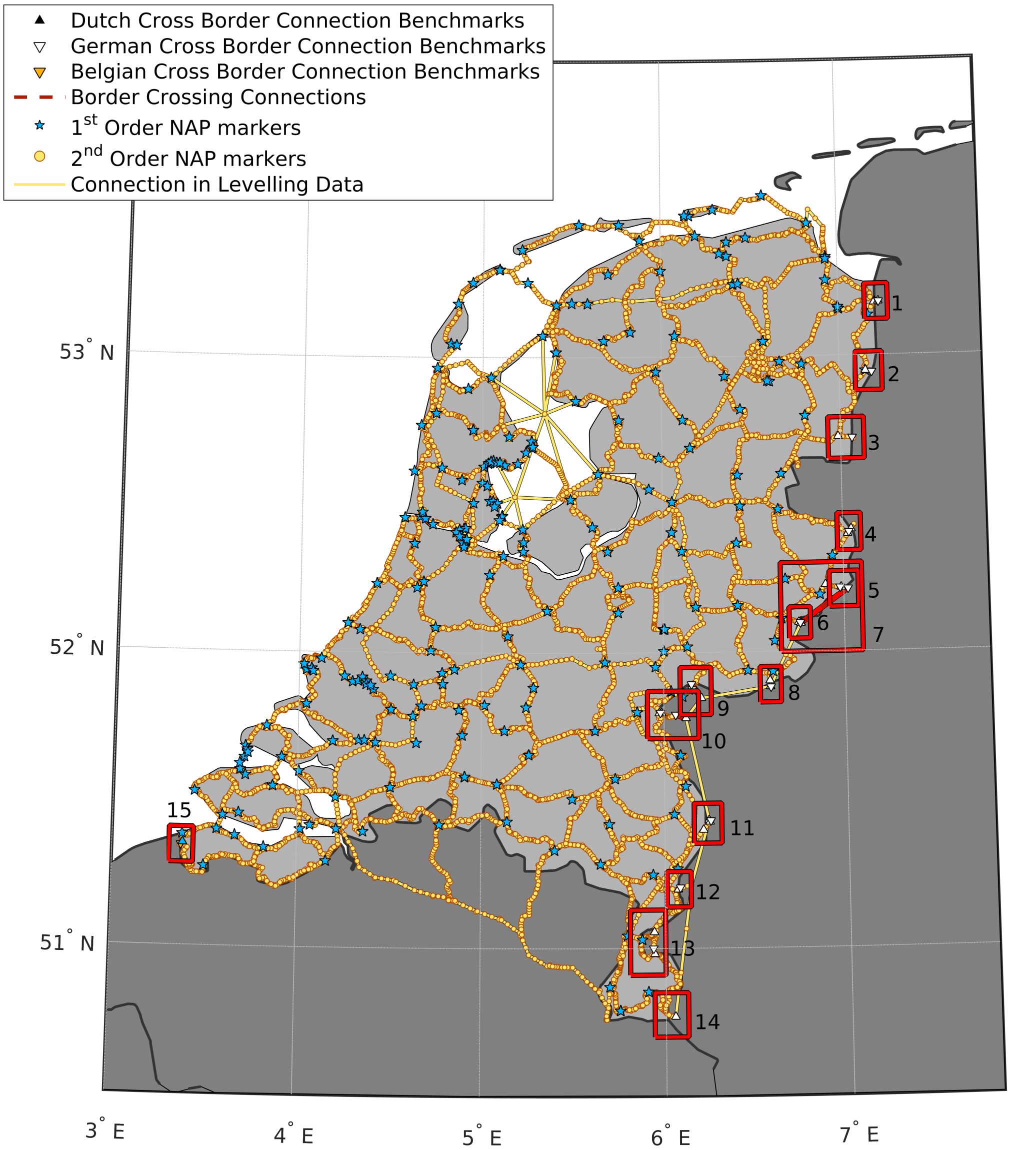

Figure 5.1: Spatial overview of the used benchmarks and their levelling line connections. The cross-border levelling connections and involved benchmarks are indicated here as well. For the indicated areas in the red squares detail plots are provided in Figure 5.2.

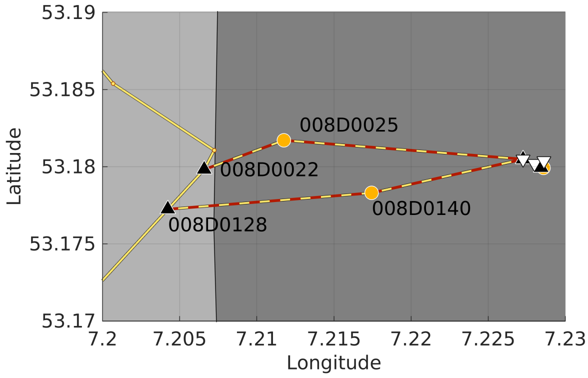

(a) Details area 1.

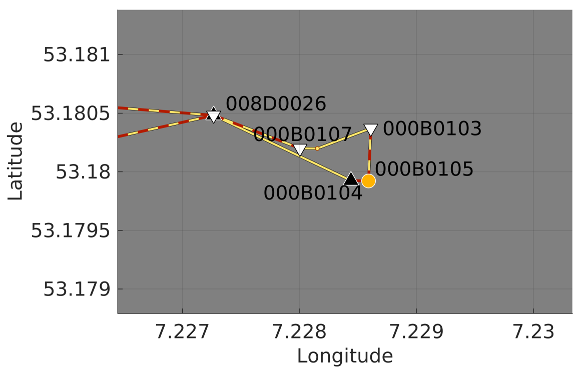

(b) Zoom area 1.

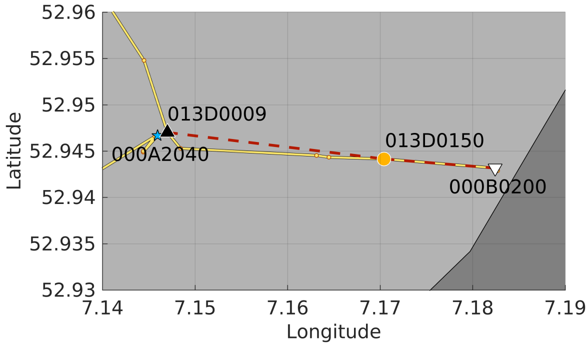

(c) Details area 2.

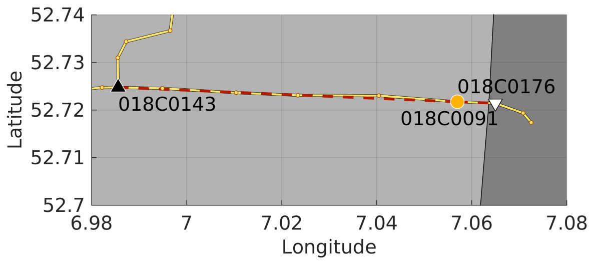

(d) Details area 3.

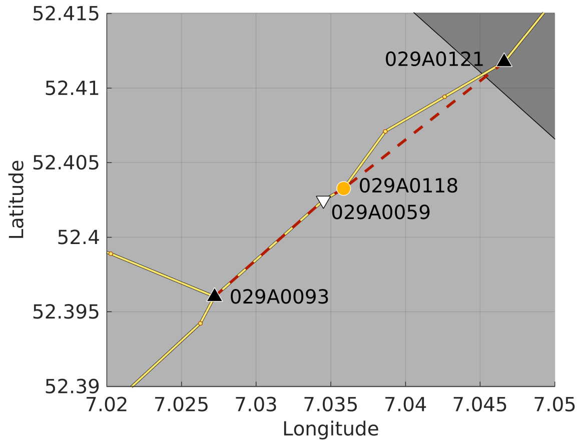

(e) Details area 4.

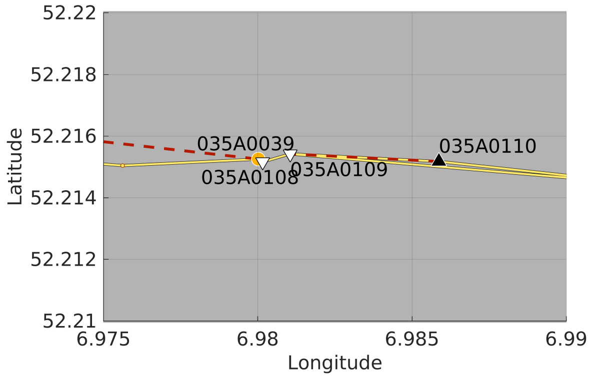

(f) Details area 5.

Figure 5.2: Detail plots for Figure 5.1, the same legend is used. Part 1/3

Figure 5.2: cont'd, part 2/3

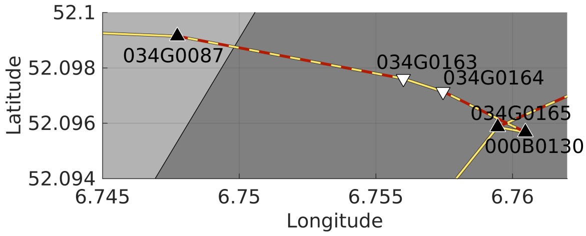

(g) Details area 6.

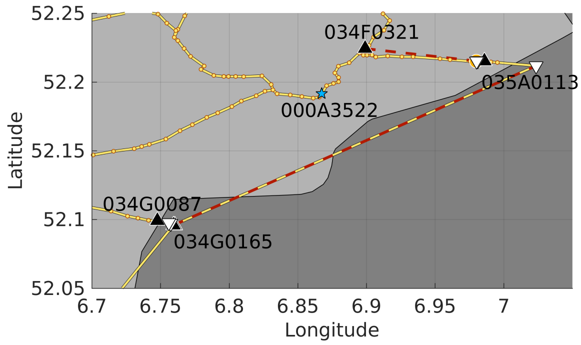

(h) Details area 7.

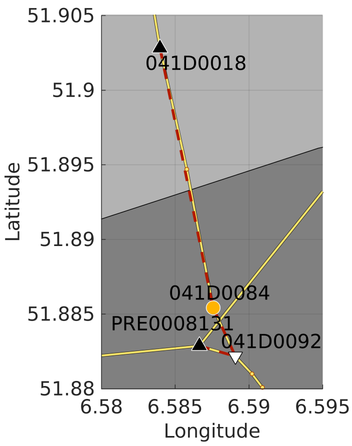

(i) Details area 8.

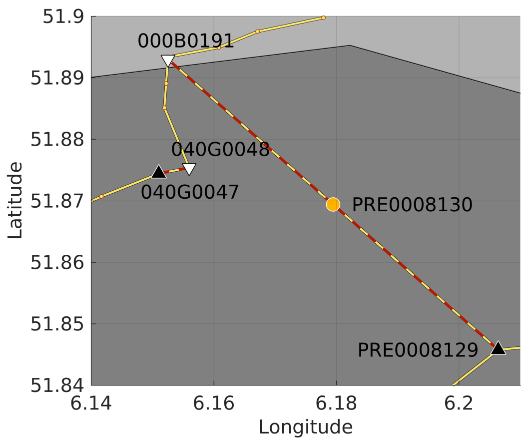

(j) Details area 9.

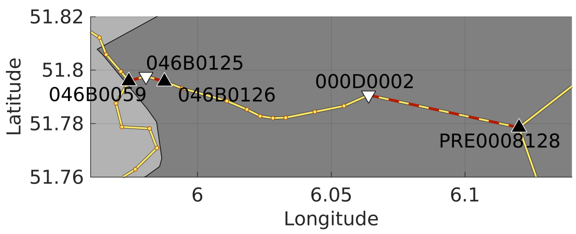

(k) Details area 10.

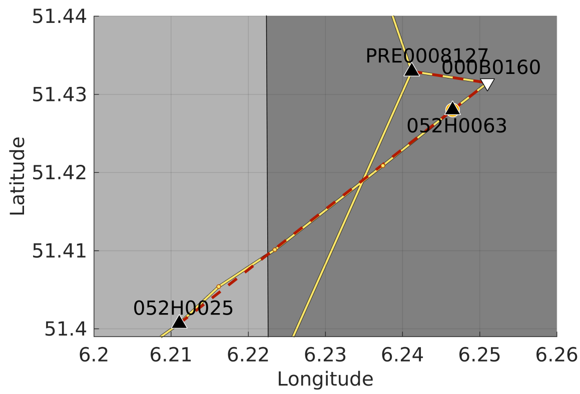

(l) Details area 11.

Figure 5.2: Detail plots for Figure 5.1, the same legend is used. Part 2/3

Figure 5.2: cont'd, part 3/3

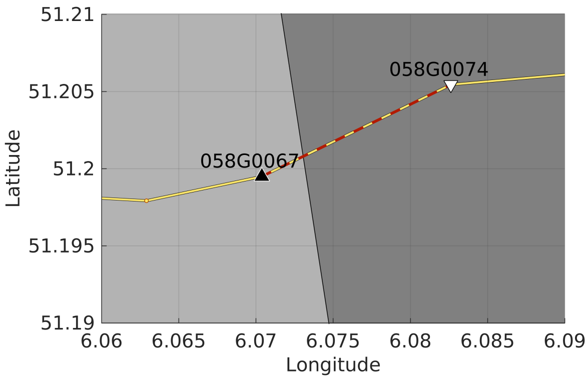

(m) Details area 12.

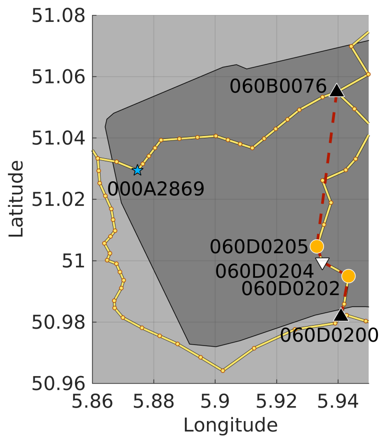

(n) Details area 13.

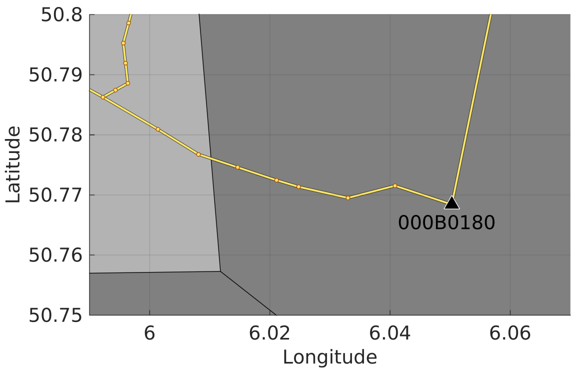

(o) Details area 14.

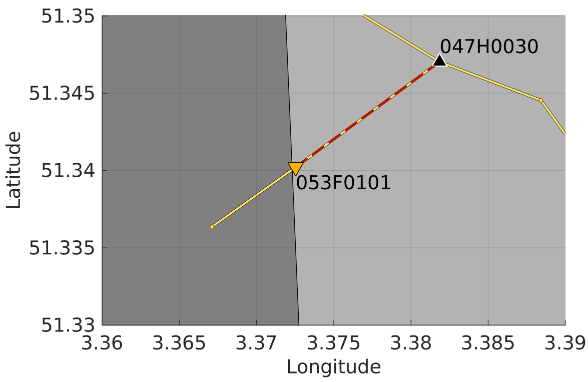

(p) Details area 15.

Figure 5.2: Detail plots for Figure 5.1, the same legend is used. Part 3/3.

6

Summary and Recommendations

In this chapter, the project objectives listed in the introduction will be reviewed. It also includes a brief summary of the conducted research for the development of the computational procedure.

6.1. Computational Procedure

The first two objectives were to correct the errors in the geopotential differences of the NAP network by developing a computational procedure and implementing this into an easy-to-use MATLAB software package. Together with investigating the necessity of RTM for accurate geopotential computation in the Netherlands.
While developing the computational procedure many steps were already predetermined due to the data provided by RWS. This left the determination of an appropriate gravity interpolation method as the essence of the whole procedure development. Besides the interpolation algorithm, the necessity of several gravity corrections were investigated for this purpose as well.

The performance of the different interpolation methods was examined by predicting gravity at a fixed set of 400 control point which had known gravity values. A standard data set, of 7618 terrestrial gravity measurement within the Netherlands, was used as input. Gravity was interpolated as surface gravity anomalies (SGA), in order to remove height dependency, which allows for interpolation in 2-D. Also, a SGA reference model (GOCO05s) was subtracted from the input gravity data to facilitate the stochastic interpolation methods. The following interpolation methods were tested:

- Biharmonic Spline Interpolation (deterministic),
- Triangular-Bases Cubic Interpolation (deterministic),
- Least-Squares Collocation (stochastic) and
- Ordinary Kriging (stochastic).

Biharmonic Spline Interpolation (BHSI) was selected as the interpolation method to be used in the computational procedure. The SGA reference model corrections did not influence the performance of the BHSI, as it is a deterministic method. Therefore, this correction is not applied in the final procedure.

The slight improvement in performance of the gravity interpolation due to RTM was found to be negligible with respect to the levelling errors. Therefore, RTM corrections are also not applied in the final procedure.

All together, the final computational procedure, to compute the geopotential differences in the NAP network, is summarized in Figure 2.17 of Chapter 2.4. This procedure has been implemented into a MATLAB software package. The computation of the geopotential differences is performed by the *ComputeNAPGeopotential* routine in this package. Also, routines which compute normal heights from geopotential numbers or differences were developed.

Possible Further Research

Considering further research which has not been performed during the development of the computational procedure.

Here, adjusted levelling observations were used to compute geopotential differences. However, ideally the geopotential differences should be obtained via original levelling observations, i.e. adjustment of the NAP network in terms of geopotential. Even though, the differences are probably insignificant for the Netherlands, due to the smooth character of both topography and gravity, it would be interesting to look into this.

Similarly, the effect of RTM corrections on the computation of geopotential differences in the NAP network was found to be negligible. Still, it would be interesting to look at the influence of DEM resolution on the RTM corrections. Especially, because the Netherlands is described by a very high resolution DEM, Algemeen Hoogtebestand Nederland (AHN). The AHN has a height measurement for every $0.5 \times 0.5m$, compared to EuroDEM's grid spacing of approximately $60 \times 60m$.

6.2. Error Identification

The third objective was to obtain insight into the origin of the errors made in the data provided to the BKG in 2004. After the development of the procedure, the new geopotential differences were compared with the provided geopotential differences by RWS. The observed differences gave a starting point for retracing the possible origin of the errors made in 2004.

The predetermined steps in the computational procedure were verified to be indeed identical to those performed by RWS. Therefore, the differences in geopotential results had to originate from the gravity prediction. Significant regional differences in the predicted gravity, up to 40 $mGal$, were observed.
These regional features correlated with the SGA field. By changing the sign of the SGA in Equation 2.3 the discrepancies of these regional features were resolved. However, discrepancies at previously correct locations appeared. Selecting the smallest discrepancy per benchmark, i.e. considering both SGA sign conventions, reconstructed the results of RWS within 5 $mGal$.
Gravity prediction with a linear method using only Dutch gravity measurements further improved the reconstruction of RWS's results. However, an exact reconstruction and therewith a complete explanation of the errors made in the data provided to the BKG in 2004 has not been found.

6.3. Impact on EVRS2007

The new geopotential differences were provided to the BKG for the computation of an update of the EVRS. The fourth objective was to quantify the impact of the Dutch geopotential errors on EVRF2007.

Since the adoption of EVRF2007 in 2008, several other countries also updated the data of their national levelling networks. Given these new datasets, the BKG computed 5 different adjustments of the UELN, realizations of the EVRS. The following realizations were computed:

1. **EVRF2007-old**: The current realization of the EVRS, the EVRF2007 as it is in use now.
2. **EVRF2007-new**: The EVRF2007 recomputed with the updated NAP data, including the correct treatment of the NAP's permanent tide.
3. **EVRF2016-old**: A realization of the EVRS as it would be possible to compute with today's available data. However, instead of the new NAP geopotential differences the old data, as provided in 2004, were used.
4. **EVRF2016-new**: A realization with all the updated data.
5. **EVRF2016-new-minus**: Another realization also using all updated data. However, leaving out the long levelling lines through Germany.

The realizations separately are hard to interpret. To look at the impact of the different updated data sets, height differences at the UELN benchmarks in the Netherlands between different realizations were examined. Due to Equation 1.1 there are no translations in the realizations of the EVRS.

The main effects in the Netherlands observed in the realization comparisons are listed below:

- The updated geopotential differences in the NAP network resulted in a north-south tilt, with a magnitude of about 10 mm over the length of Netherlands.
- The correct treatment of the permanent tide system of the NAP also resulted in a tilt, again dipping to the south with a magnitude of about 7 mm.
- Excluding 10 long levelling lines in Germany resulted in a minor tilt and a very local feature in the middle of the Netherlands at the German border.
- The updated data from the other countries resulted in a tilt opposite of previously described. These height differences were largely negative. Also, a large negative local features was observed in the north-east of the Netherlands.

The local feature due to the long lines in Germany illustrated the unwanted impact of these ambiguous lines. They should be left out when realizing the EVRS. Therefore, the EVRF2016-min-minus realization is considered the best realization of the EVRS given the current knowledge.
It should be noted that the input-output effects in the UELN adjustment are not straightforward, e.g. local errors propagate into the whole network. Still, the general effects of all the separate contributions listed above are recognized in the total effect between EVRF2016-new-minus and EVRF2007-old.

The height differences of the 13 datum points between the different realizations were studied to investigate the larger impact of the updated data. For the updated NAP data, the tilt observed in the Netherlands can be also seen in Belgium. The influence outside of the Netherlands decreases fast to sub-millimetre effects.

Considering all updated data currently available, the height difference of most datum points is larger than 0.5 cm with extremes in the range of 1.5 cm for Denmark and Italy. These are quite significant changes. This might suggest it is an appropriate moment to adopt an updated realization of the EVRS.

6.4. Connection NAP to EVRS

The final objective was to investigate the connection of the NAP with the neighbouring countries and thus the EVRS.

Summarizing the connection of the NAP to Germany; there are 28 observations at 13 locations, evenly distributed about every 44 km, currently known at the BKG. This lead to the conclusion that the Dutch-German connection is strong. For the connection of the NAP with Belgium only 1 observation is currently known at the BKG. This is fairly poor and could be what Rülke et al. [2012] meant.

It was investigated if more cross-border connections existed. This was done by inspecting; the levelling data provided by RWS, the list of cross-border connection benchmarks by the BKG and Figure 4.1a also provided by the BKG.
The main information gaps identified are:

- Possible inconsistencies in the cross-border levelling information provided by the BKG with the levelling information provided by RWS.
- Not all benchmarks indicated as German benchmarks (000Bxxxx) in RWS's data are included in BKS's data.
- Figure 4.1a shows two locations where the German levelling network ideally should connect to the Netherlands, but does not.
- The Dutch levelling line through Belgium crosses the Belgian network several times and seems to connect to it as well.
- The Belgian and German levelling networks seem to be easily connected just below the tripoint.

The connection between the NAP and Germany appears to be easily further improved. Also, there already seems to exist more connections between the NAP and Belgium. However, this needs to be communicated clearly between all involved parties.
Ultimately, there should be no gap between existing information and information known/provided to the BKG. This is a mutual responsibility of the BKG and all participating countries.

A

Objectives and Work Package Description of Original Project Proposal

A.1. Objectives

The main goals of the project are i) to identify and correct all errors in the computation of the geopotential numbers of the first order NAP network; ii) to assess the impact of the erroneous and corrected geopotential numbers on the current realization of the EVRS; iii) to investigate whether topographic corrections to measured gravity are necessary to compute the geopotential numbers of the first order NAP network; iv) to develop and document a MATLAB software package that does the computation of geopotential numbers automatically that can be used by RWS for future computation and geopotential numbers. The latter is necessary because providing geopotential numbers at the points of the first order height network is a regular task of all member states of the European Union in order to realize the European Vertical Reference System (EVRS).

A.2. Work Package Description

In order to meet the goals, the following work is necessary:

WP 1. Development of a computational procedure to compute geopotential numbers in the zero tidal system for all points of the NAP first-order network. The following steps are foreseen: i) for each leveling line, the geopotential numbers need to be computed. Input are the official (adjusted) height differences along the main leveling lines and absolute gravity values at the height markers of the leveling lines; ii) the gravity values at the height markers need to be computed from the second-order gravity network (which was established in the 1990s in order to realize the ”De Min Geoide”, and which forms the basis data set of the most recent geoid of the Netherlands, NLGEO2004) by spatial interpolation. It needs to be investigated how many gravity points along the main leveling lines need to be computed in order to preserve the accuracy of the NAP first-order network and to be in compliance with the accuracy requirements of the EVRS; for the spatial interpolation Least-Squares Collocation (LSC) or alternatively, some form of kriging may be used; flat and hilly areas (southern part of the Netherlands) may need to be considered separately; iii) the interpolation of gravity with sufficient accuracy at the height markers of the main leveling lines may require a remove-compute-restore procedure in which the high-frequency gravity signal caused by the topography is removed before interpolation and restored after interpolation. In this way, interpolation may be possible with the necessary accuracy. The remove step requires access to the AHN 2 database. It needs to be investigated, whether topography outside the Netherlands is necessary. For this, the digital elevation database compiled in the framework of NEVREF will be exploited. The computation of topographic reductions will be done using software available at TU Delft.

WP 2. Identification of the errors in the geopotential numbers of all points of the first-order NAP network. For this, we will start with the results of the 5^{e} NauwkeurigheidsWaterPassing, which forms the basis of the current NAP first-order network. New geopotential numbers will be computed using the methodology developed in WP 1. The geopotential numbers will be computed in the zero tidal system, which is the tidal system adopted in the Conventions for the Definition and Realization of the European Vertical Reference System (EVRS) - EVRS Conventions 2007. In this way, a reference set of geopotential numbers will be computed, which establishes the benchmark for the geopotential numbers provided to the BKG in 2004 (they will be provided by RWS). A comparison of the two data sets will provide insight into the origin of the errors in the geopotential numbers from 2004.

WP 3. Quantify the effect of the errors in the geopotential numbers of the NAP first order network on the current realization of the EVRS, the EVRF2007. This will be done by a re-adjustment of a part of the EVRS comprising all leveling lines of the NAP first-order network and selected leveling lines from Belgium and Germany. The re-adjustment will be done by the BKG in Frankfurt. The analysis of the results are part of the project work.

WP 4. Investigation of the connection of NAP to the EVRS, identification of weaknesses in this connection, and suggestions for improvements. This will be done in close cooperation with BKG and the Nationaal Geografisch Insituur in Bruessel.

WP 5. Development of an easy-to-use software package to compute geopotential numbers in the zero tidal system for the first-order NAP network automatically. The software will be implemented in MATLAB. The software will be fully documented and complemented by test input and output data sets. All input data sets for future computations are part of the deliverables. This work will be done in close cooperation with RWS.

B

Normal Heights and Surface Gravity Anomalies

B.1. Heights

Geopotential numbers are a physically the most meaningful way of expressing height. Geopotential numbers are the geopotential difference with respect to the geoid:

$$c = W_0 - W_P \tag{B.1}$$

Because potential is expressed in m^2/s^2, geopotential numbers are not a very intuitive way of expressing height. By scaling geopotential numbers by certain gravity values several types of height can be defined.

Geometrically speaking, orthometric heights are the distance along the plumb-line from the point of interest to the geoid. This is the same as scaling geopotential numbers with the mean gravity along that plumb-line:

$$H = \frac{c}{\bar{g}} \tag{B.2}$$

This can be easily understood by recalling Equation 2.1 and imagining the potential change when moving along the plumb-line. However, to compute the average gravity exactly would require full knowledge on the Earth's internal mass distribution. As this is unknown, orthometric heights cannot be computed exactly in general.

By replacing the true gravity field by a theoretical one (e.g. GRS80) the mean gravity along the plumb-line can be computed exactly and in closed from. Normal heights are defined as:

$$H^{\star} = \frac{c}{\bar{\gamma}} \tag{3.1 revisited}$$

Here, $\bar{\gamma}$ is the average normal gravity between the ellipsoid and the telluroid. The telluroid is a surface for which the normal gravity potential (in Q) is equal to the real gravity potential of the Earth's surface

(in P). The height difference between P and Q is called the height anomaly, ζ. The different relations concerning normal heights are schematically illustrated in Figure B.1.
The distance between the telluroid (Q) and the ellipsoid is thus equal to the normal height for P. The relation between the telluroid and the Earth's surface, is equal to the relation between the ellipsoid and the quasi-geoid. Both are related via the height anomaly. Therefore, the distance between point P and the quasi-geoid is by definition the normal height of point P.

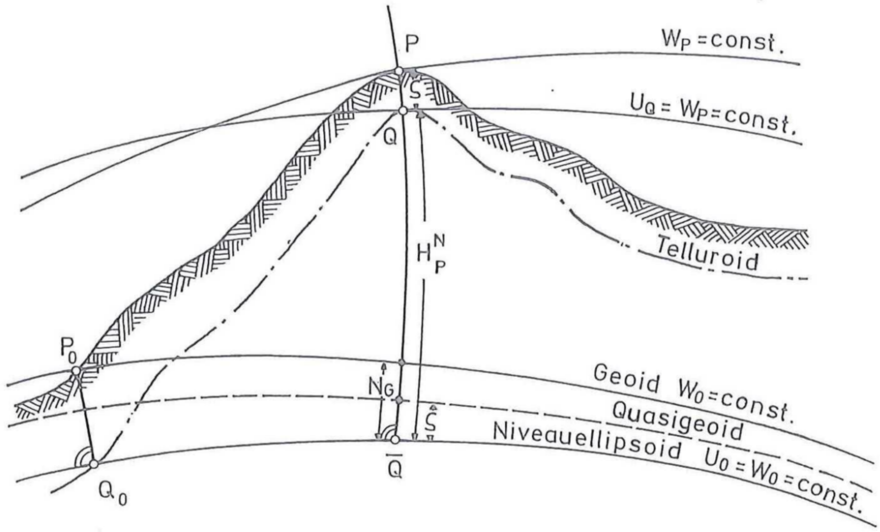

Figure B.1: Schematic illustration of the relations between Geoid, Ellipsoid, Quasi-geoid and Normal Heights [Leismann et al., 1992, Figure 3.3]. Note in the text $\bar{Q}$ is referred to as Q'.

B.2. Surface Gravity Anomalies

As has been mentioned several times throughout the report, gravity interpolation is performed on surface gravity anomalies (SGA). For SGAs the height dependency of the observed gravity is removed. SGA is defined as:

$$\Delta g = g(P) - \gamma(Q) \tag{2.3 revisited}$$

Here, $\gamma(Q)$ is the normal gravity at the telluroid and $g(P)$ the observed gravity at the Earth's surface, both illustrated in Figure B.1. How height dependency is removed from observed gravity by subtracting $\gamma(Q)$ is clarified below.
Starting by approximating the normal gravity on the telluroid (Q) by a Taylor series expansion on the ellipsoid (Q'):

$$\gamma(Q) = \gamma(Q') + \left.\frac{\partial \gamma}{\partial h}\right|_{Q'} H^\star + \mathcal{O}(H^{\star 2}), \tag{B.3}$$

where, $H^\star$ is the normal height. Substituting this into Equation 2.3 results in:

$$\Delta g = g(P) - \left.\frac{\partial \gamma}{\partial h}\right|_{Q'} H^\star - \gamma(Q') \tag{B.4}$$

Subtracting the normal gravity gradient times the normal height being removes the height dependency by reducing the observed gravity. This effect is also clearly seen in the results of Appendix D. Subtracting the normal gravity at the ellipsoid, further removes the large latitude dependency.

When approximating the normal gravity gradient by a representative value of the free-air gravity gradient, α, and the normal height by the orthometric height the definition of free-air anomalies (FAA) emerges:

$$\Delta g_{faa} = g(P) - \alpha H - \gamma(Q'), \tag{B.5}$$

where H is the orthometric height of point P and

$$\alpha = -0.3086\, mGal/m \tag{B.6}$$

is a representative value of the free-air gravity gradient.
The difference between FAA and SGA depends on the difference between orthometric (H) and normal height ($H^{\star}$), which is even in mountainous regions typically in the order of only a few decimeters [Flury and Rummel, 2009]. This results in an error not exceeding 0.1 $mGal$. [Slobbe, 2013, Appendix A]
Some gravity data sets were provided as FAAs. Given their small differences, in this project FAA and SGA were assumed equal and used interchangeably. This also relates to an assumption which was stated previously in is Chapter 2.1.1: *"For the height of point Q the NAP height of point P is used"*.

NAP heights are realized through levelling only, they correspond neither to normal nor to orthometric heights. However, the difference between the geoid and NAP in the Netherlands is in the order of centimeters Bruijne and Brand [2005]. Thus, for the computation of gravity reductions NAP, normal and orthometric heights are assumed equal, and are also used interchangeably:

$$H_{NAP} = H^{\star} = H \tag{B.7}$$

This assumed relation is only applicable for computing gravity corrections. It is important to define height unambiguously. Markers in the NAP network can be transformed into normal heights via geopotential numbers. This procedure is shown in Figure 2.1 and is also implemented in the software.

C

Additional Discretization Validation

In Chapter 2.1, the definition of geopotential differences was given:

$$\Delta W_{AB} = W_B - W_A = -\int_A^B g dh \tag{2.1 revisited}$$

There, it was also discussed that the following discretization was necessary for practical use:

$$\Delta W_{AB} = W_B - W_A \approx -\sum_{i=1}^{N} g_i \delta n_i \tag{2.2 revisited}$$

Besides studies on the impact of this approximation by Ramsayer [1965], which were already discussed in Chapter 2.1, additional validation was performed on the specific data used in this project. This validation will be discussed here. Figure C.1 shows the part of the process which is considered here.

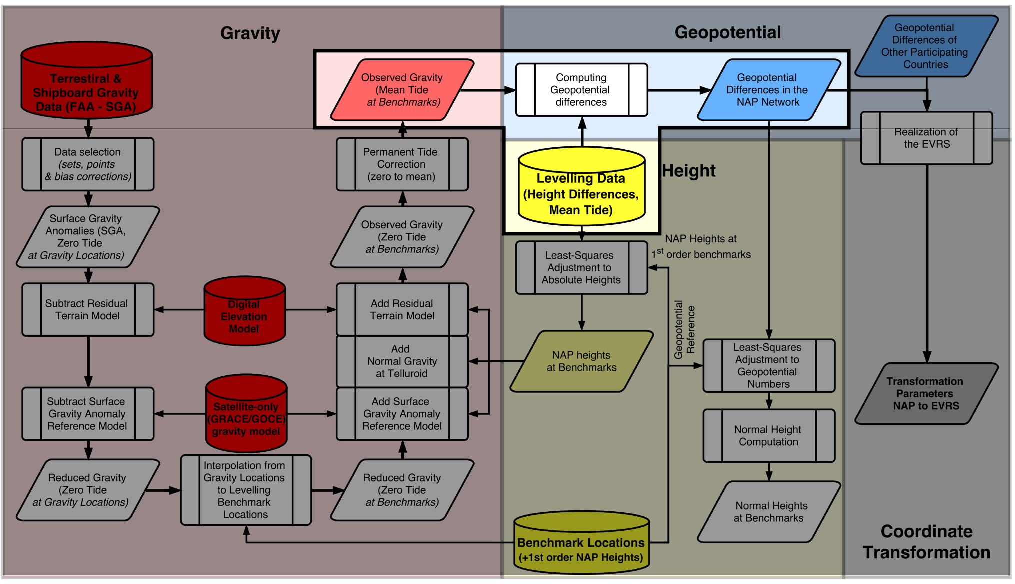

Figure C.1: Overview of the workflow (Figure 2.1) in which the computation of geopotential differences is highlighted.

C.1. Research Set-up

As was mentioned in Section 2.1.1, the provided levelling connections are the combined result of many levelling set-ups. By combining consecutive levelling connections new and coarser levelling connections can be created. These newly synthesized observations connect two benchmarks with a single height observations which were previously only connected through several, indirectly. Figure C.2 provides a schematic illustration of such a construction.

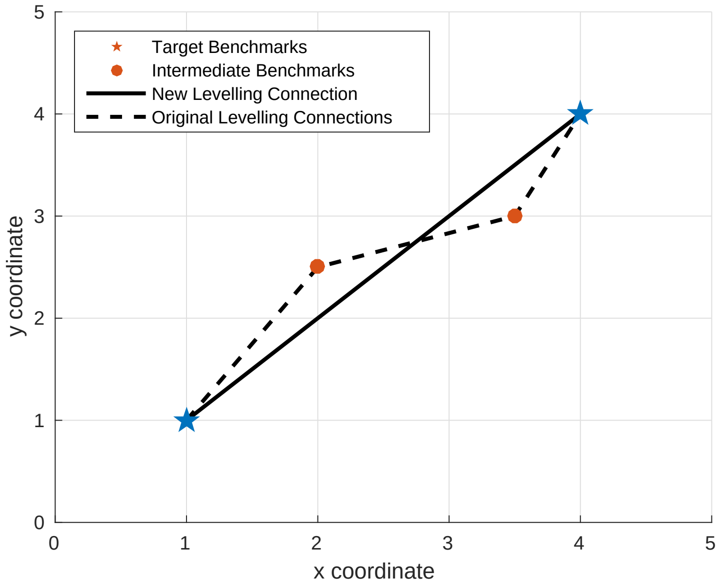

Figure C.2: Schematic illustration, in planar view, of creating a new and coarser levelling connection from several levelling connections.

Computing the geopotential difference between these two target benchmarks can now be performed in two ways:

- by taking the path via the intermediate benchmarks. Using the levelled height difference for each step and computing g_i for each step. The final result is the sum of all steps taken.
- by taking less steps, skipping intermediate benchmarks and using the height difference between the target benchmarks directly with the average gravity between these benchmarks.

The only difference between these methods is the coarseness of the discretization. Comparing the obtained geopotential differences of both methods, illustrates the impact of the discretization coarseness on the geopotential result.

As a reference ideally the true geopotential differences between the target benchmarks would be used. However, as it is not possible to evaluate the line integral in Equation 2.1 exactly the true geopotential difference is unknown.
Smaller steps in the approximation yield more accurate computed geopotential difference. The original levelling data provide the finest discretization available here and therewith the best possible result obtainable given the provided data.

The methods which are tested here are all based on utilizing different step sizes to examine the discretization effect of Equation 2.1 on the computed geopotential differences. The geopotential differences computed via existing paths through the data are taken as reference and the computational procedure described in Chapter 2.4 was used.

C.1.1. Coarsening Lines

For three long levelling lines, crossing the whole of the Netherlands, the geopotential difference between the first and last benchmark was computed using a variable number of intermediate benchmarks. Each line consists of about 500 observations from the original levelling data. The lines are shown in Figure C.3.

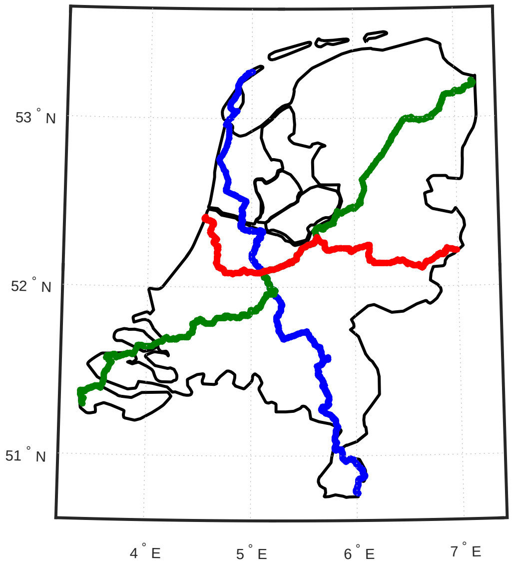

Figure C.3: Overview of the long lines tested with a different number of intermediate steps.

When examining such a long line only a single geopotential discrepancy is obtained, which then is representative for the whole length of the line. This provides a good measure for the average effect. However, regional features would blend into this single result. To be able to visualize possible regional features, several shorter lines were investigated separately. Ten lines evenly distributed over the Netherlands were selected for this purpose. Five additional lines were selected in southern Limburg to specifically look at topographic influences. The locations of these lines are shown in Figure C.4. Each of these lines consist of about 70 observations from the original levelling data.
The shortest path between two benchmarks through the provided levelling network was identified with MATLAB's "graphsearch" algorithms, located in the Bioinformatics Toolbox [MAT, 2015].

After having established the original shortest path (Figures C.3 and C.4), the selection of the intermediate benchmarks for coarser discretizations were chosen equidistant along the original path. An example of the selection of equidistant intermediate benchmarks is shown in Figure C.5.

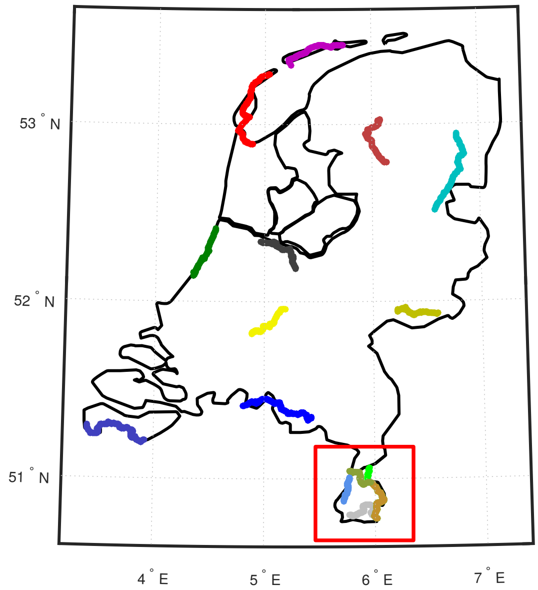

Figure C.4: Overview of the short lines tested with different number of intermediate steps. The five lines in the red square in Southern Limburg are examined separately from the ten lines in the rest of the Netherlands.

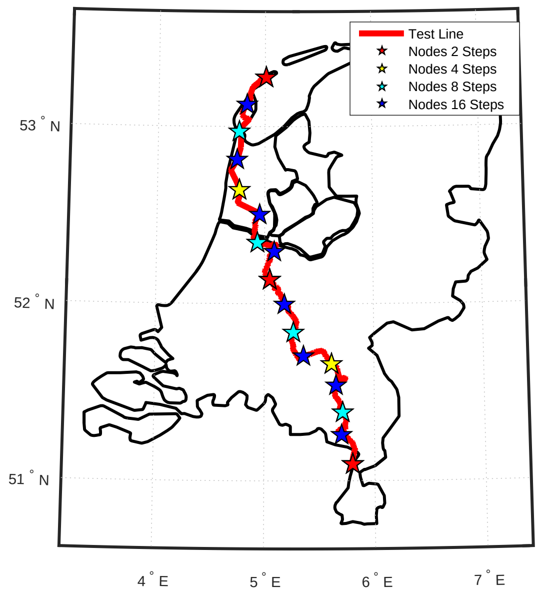

Figure C.5: Example of selection of intermediate benchmarks for a levelling line discretized into 2, 4, 8 and 16 steps. The coarser discretization benchmarks are also used for the finer discretizations, because the number of steps used in this example is a sequence with a factor of 2. E.g. the red star in the middle, used for the 2 steps, is also used for the discretization into 4 steps, together with the yellow stars, etc.

C.1.2. Direct vs. Path-wise

Utilizing the previously explained concept enables the computation of the geopotential difference between any two benchmarks in a single step. A single step is the coarsest discretization possible and should in theory result in the largest discrepancy.
The discrepancy between the geopotential difference, computed with a single step or via the shortest path through the original network, is computed for all possible connection combinations between the 8890 benchmarks.

This creates almost 80 million results. To make this interpretable, the individual results are binned in order to visualize the general trend.

C.1.3. Discretezation Refinement

Ramsayer [1965] showed that Equation 2.1 can be approximated by Equation 2.2 with sufficient accuracy for lines shorter than 10 km in areas with topography similar or smoother to that of the Black Forest.
The Netherlands has very smooth topography and almost all provided levelling lines are shorter than 10 km. However, there are a few lines which exceeded 10 km, which were already addressed in Chapter 2.1 in Figure 2.3.

The previously described methods create larger steps to examine the discretization influence. This is well suited to examine the influence of discretization on levelling lines which initially have small steps. However, this does not provide much information on the lines with already large steps, e.g. larger than 10 km.
As these long lines are actually the main concern for the justification of the discretization, they will be examined separately as well.

So instead of coarsening the discretization for these lines, they will be refined. The geopotential difference over these lines can be computed in smaller steps by assuming an evenly distributed height difference along these lines. Especially for the lines crossing ”Het IJselmeer” this is a plausible approximation. These lines were levelled over ice when the lake was frozen [Brand and Damme, 2004].
The influence of refining the discretization into step sizes of 3 and 5 km was tested. The refined discretization steps were made equidistant.

C.2. Results

The results in this section are the differences between the geopotential difference obtained via the original path and the alternative path of tested methods. These results, the differences in geopotential differences, will hereafter be referred to as (geopotential) discrepancies and are expressed as absolute values.

C.2.1. Coarsening Lines

The discrepancy as a function of the number of steps for the levelling lines discussed above, is given in Figure C.6. The colors in these plots correspond to the colors of the levelling lines in Figures C.3

and C.4.
Note, the axis of the sub-figures in Figure C.6 do not have the same upper limits. The maximum values of the x- and y-axis for the long lines are obviously larger than for the short lines.

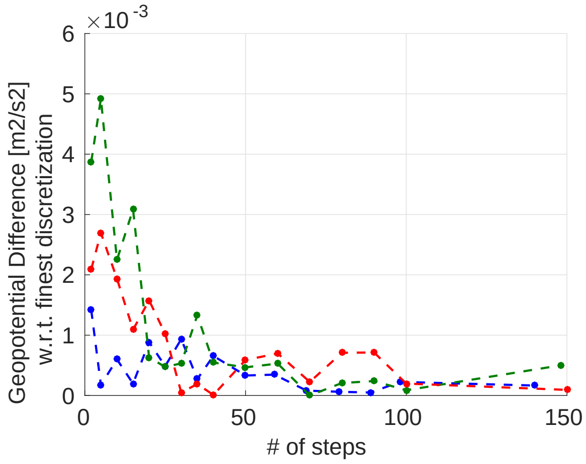

(a) Long lines (spatial overview in Figure C.3).

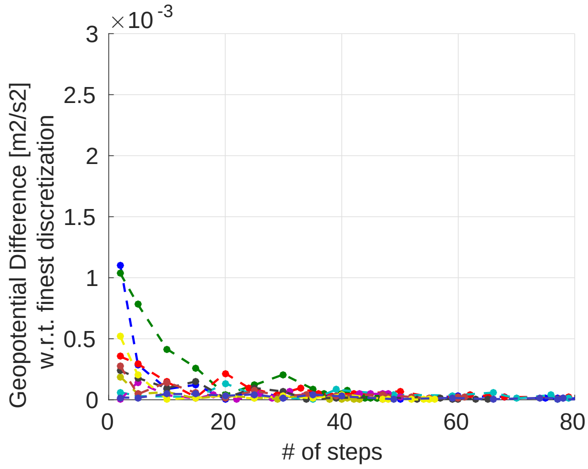

(b) Short lines (spatial overview in Figure C.4).

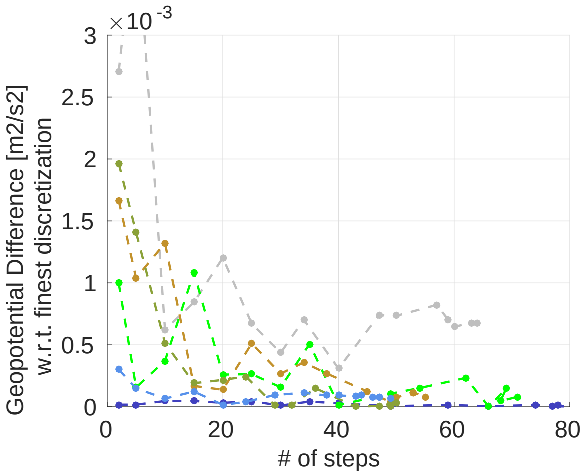

(c) Short lines Southern Limburg (spatial overview in Figure C.4).

Figure C.6: The discrepancy computed via the original path through the levelling network and a coarser discretized version. The colors of the lines correspond to the colors of the levelling paths in Figures C.3 and C.4.

C.2.2. Direct vs. Path-wise

The discrepancies between direct, a single step, and stepwise geopotential difference between all benchmarks are shown in Figure C.7b. The maximum benchmark separation plotted is 400 km. This is about the maximum spatial separation possible within the Netherlands. Over this range 50 bins were created, for which the average value and the 2σ interval are plotted on top of the scatter of individual observations.

The absolute benchmark heights were obtained via a LSQ adjustment, see Chapter 2.1.1. Therefore, the height differences computed directly from the benchmark data does not correspond exactly to

the levelled height differences obtained via any given path.
Figure C.7a shows the difference in height difference, i.e. height discrepancy, between heights via the levelled route and directly from the benchmark data. In this figure also the expected difference is plotted, assuming a levelling error of 1 $mm/\sqrt{km}$ [Brand and Damme, 2004].

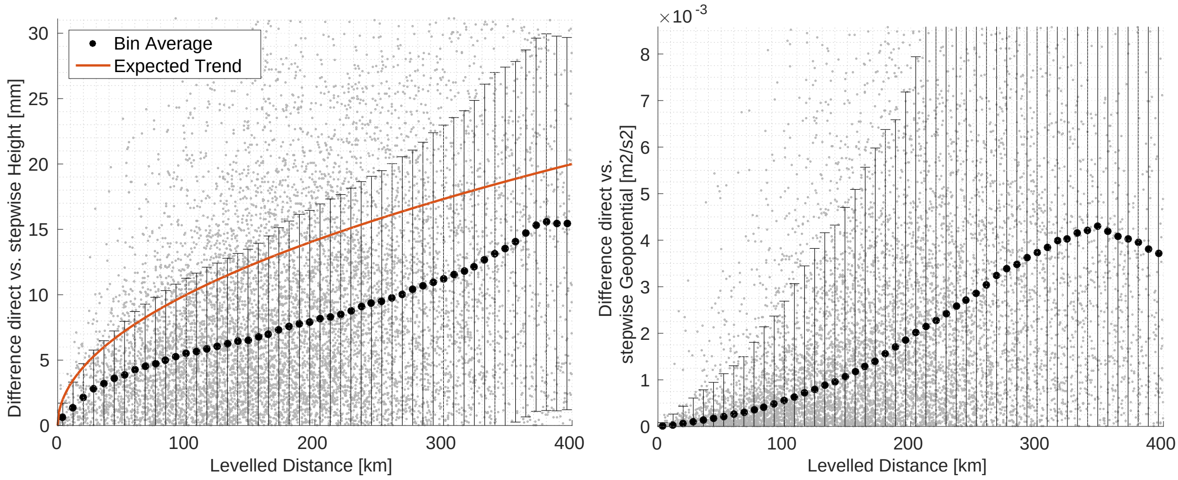

(a) Height discrepancy.

(b) Geopotential discrepancy.

Figure C.7: Geopotential and height discrepancy between the results computed directly and via the shortest levelling path through the original data.

C.2.3. Discretization Refinement

Figure C.8a shows the same long lines as presented previously in Figure 2.3. The discrepancy between the original long line and the finer discretization, with maximum steps of 5 km, is visualized as the color of the levelling lines.
The values of the discrepancies in Figure C.8a are hard to read. Therefore, Figure C.8b shows the discrepancy for the same lines in a plot. The results are sorted in ascending order with respect to the 3 km results. Note, the y-axis is logarithmic, the discrepancies are in the range of $10^{-4} - 10^{-9} m^2/s^2$.

Table C.1: Overview of the length and maximum observed geopotential discrepancies for the different tested lines.

Tested Lines	**Length**	**Maximum Discrep.**
Short lines	$\pm$ 50 km	$1 \cdot 10^{-3}\, m^2/s^2$
Short lines Southern Limburg	$\pm$ 40 km	$3 \cdot 10^{-3}\, m^2/s^2$
Long lines	$\pm$ 400 km	$5 \cdot 10^{-3}\, m^2/s^2$

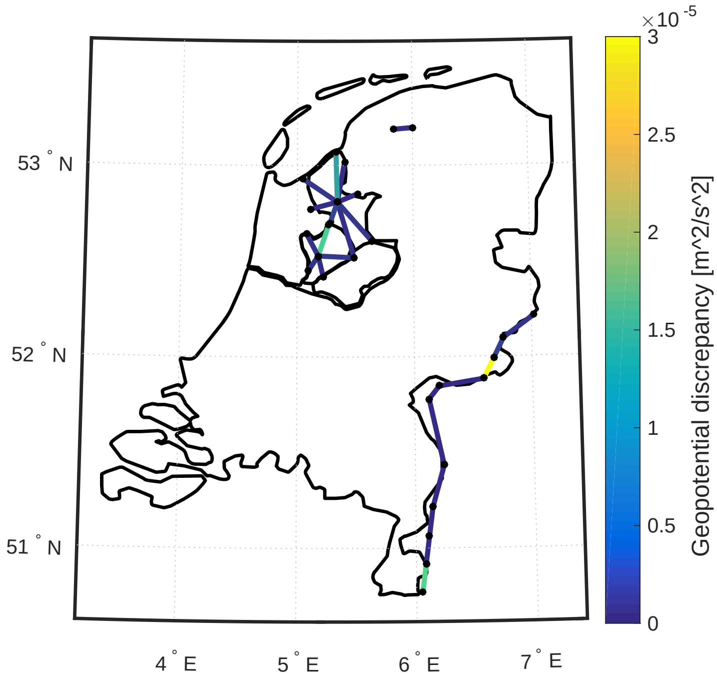

(a) Discrepancy between the original connection and a finer discretization, with a maximum step size of 5 km.

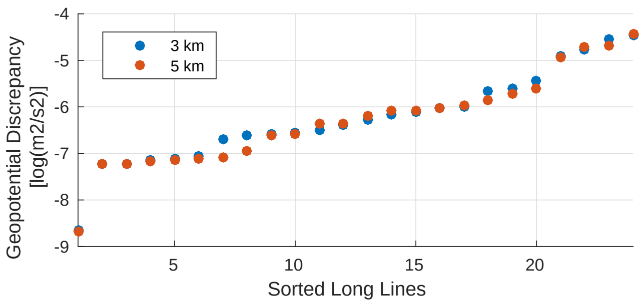

(b) Discrepancy for the refinement of the long lines shown in Figure C.8a. Refinement for maximum step sizes of 3 and 5 km were tested.

Figure C.8: Discretization refinement results for the long lines.

C.3. Discussion

C.3.1. Coarsening Lines

The plots in Figure C.6 are obtained with a small number of different discretizations. The particular benchmarks which are used, or skipped, in a certain realization determine how well this result resembles the original path result. Only a few realizations were examined, resulting in a large scatter of the obtained discrepancies.

However, the coarsening of the lines shows for all lines the same trend. The discrepancy declines when more steps are used. By approximating a levelling line with more steps, less steps will be skipped, making the possibilities of introducing discrepancies smaller. This is expected behaviour.

A longer line has larger steps for the same amount of steps, making the discretization relatively coarser. This explains the higher discrepancy for the longer lines at the same amount of steps.

The discrepancies for the short lines in southern Limburg show a much slower decline than the other short lines, respectively Figure C.6c and C.6b.
Equation 2.2 illustrates that geopotential difference is directly proportional to height difference. With more topography there can be more height difference over a smaller lateral distance. Southern Limburg is the area in the Netherlands with the most topography. This clearly illustrates the topography sensitivity of the discretization approximation, which Ramsayer [1965] showed quantitatively, in a qualitative way.

It is not possible to interpret the impact of the discretization quantitatively, to define a minimum step size or even get a correlation with average step sizes, from these qualitative results. However, these results do give a feeling for the expected magnitude of the error introduced by the discretization. Table C.1 shows an overview of the tested lines, their approximate length and the maximum observed discrepancy.
These maximum observed discrepancies correspond to height differences of respectively 0.1, 0.3 and 0.5 mm. Whereas the corresponding expected levelling error with 1 $mm/\sqrt{km}$ is about 7, 6 and 20 mm respectively. Showing that for these tested lines the differences in computed geopotential differences, due to coarser discretizations, are not significant with respect to the expected levelling errors.

C.3.2. Direct vs. Path-wise

Firstly looking at the height misfit in Figure C.7a, shows that the average height misfit is less than the theoretically expected trend of 1 $mm/\sqrt{km}$. The 95^{th} (2σ) confidence interval fits the expected trend up to about 150 km.
The values of the height errors are relatively big compared to the geopotential discrepancies. 1 mm roughly corresponds to $10^{-2}m^2/s^2$. Hence, the height related geopotential discrepancy would be in the order of $0.1m^2/s^2$. The geopotential discrepancy due to discretization is two orders of magnitude smaller. Due to this difference the height discrepancy would have hidden the discretization influence. Using the height difference as observed with the original path, prevents contaminating the geopotential result with height discrepancy. This allows to see the influence of discretization on the results.

The largest discrepancies for the lines previously studied, should approximately corresponds with the geopotential discrepancy observed here. For the long lines, with a length of about 400 km, this corresponds to the peak of the geopotential discrepancy in Figure C.7b. The maximum value for the long lines, given in Table C.1, corresponds nicely with the maximum average discrepancy of $5 \cdot 10^{-3}\, m^2/s^2$ observed at 350 km in Figure C.7b. The decline observed after 350 km is caused by a decreasing number of observations due to the maximum spatial separation possible within the Netherlands.
Considering the short lines; the 95^{th} percentile expected discrepancy at a distance of 50 km, matches the maximum observed discrepancy observed previously.
However, the discrepancies for the short lines in southern Limburg are bigger than the 95% confidence interval. Again, illustrating the big influence of topography which is much more present in the southern part of the Netherlands.

The distribution of levelling line distances in the provided data was already discussed in Chapter 2.1.1 and shown in Figure 2.2. Almost all lines are shorter than 5 km and even the longest connection is

less than 50 km.
Considering the extreme case of a connection of 50 km, this would suggest that in 95% of the cases the error in the geopotential computation due to discretization in the Netherlands is below $10^{-3}\,m^2/s^2$, roughly corresponding to a 0.1 mm levelling error.
As the height error in Figure C.7a is about two orders of magnitude larger, the current discretization of the NAP network is more than sufficient for the computation of geopotential differences.

C.3.3. Discretization Refinement

Figure C.8b shows very small differences between the 3 and 5 km steps size results. This small influence of discretization steps size could be due to either, a smooth gravity field, or an evenly distributed height difference along these lines, as was assumed.

The discrepancies for refining the long lines are in the range of $10^{-4} - 10^{-9} m^2/s^2$. This corresponds roughly to a maximum levelling error of 0.01 mm. The expected levelling error for lines longer than 10 km is about 3.2 mm. From this, it is concluded that also the discretization error for the long lines is negligible.

C.4. Conclusion

With more topography there can be more height difference over a smaller distance. Therefore, geopotential computation becomes more sensitive to a coarse discretization in areas with irregular terrain or a lot of topography.

In order to visualize the influence of discretization on the computed geopotential differences, it is necessary to use the same height differences as provided along the original levelling line. In other words, within the Netherlands the influence of discretization on the computed geopotential differences is negligible with respect to the height errors made by levelling.

Considering the worst-case scenario of a 50 km levelling connection in the NAP network, this would have an expected maximum error due to discretization of $10^{-3}\,m^2/s^2$. This is roughly equivalent to a 0.1 mm levelling error. Given the lengths of the levelling connection in the NAP network, Figure 2.2, and an expected levelling error of 1 $mm/\sqrt{km}$, the expected levelling error is 2.2 mm. Again, this justifies the usage of Equation 2.1 for the provided NAP levelling connections.

D

Gravity Field Smoothness

In Chapter 2.3, the influence of RTM correction on the interpolation performance was examined straightforward by looking at the difference in interpolation results.
It has also been briefly mentioned that a smooth field facilitates interpolation performance. Therefore, in this appendix the influences of the different corrections on the smoothness of the gravity field will be investigated. Figure D.1 highlights the reductions and restore steps for all tested corrections in the workflow.

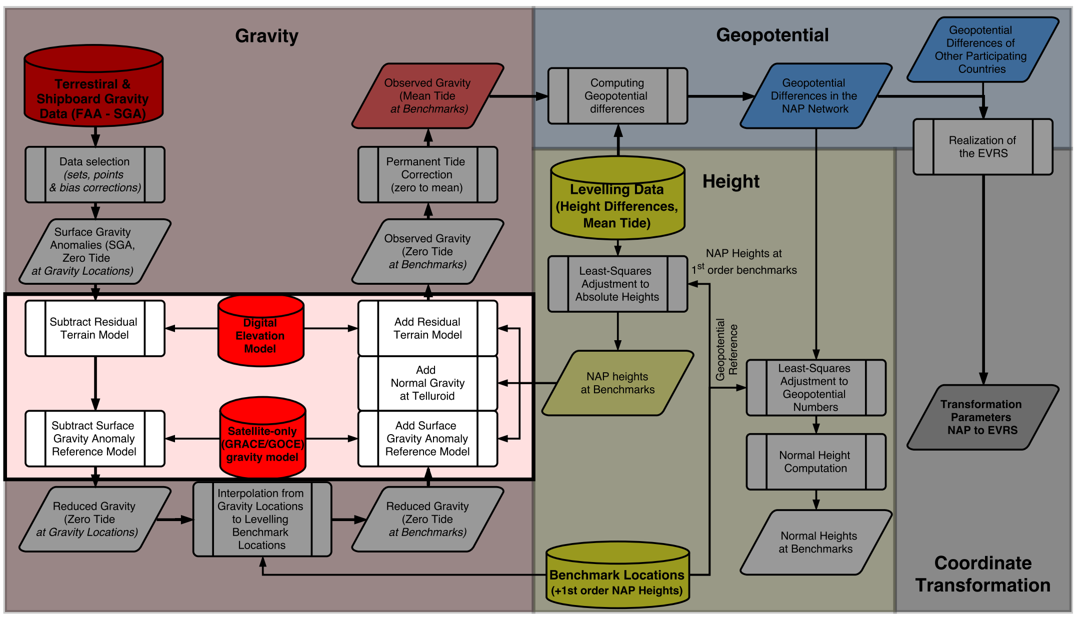

Figure D.1: Overview of the workflow(Figure 2.1) in which the gravity reduction and restore steps, discussed in this appendix, are highlighted.

D.1. Research Set-up

From the corrections shown in Figure D.1, only residual terrain modelling is actually applied to smooth the gravity field. However, the influence of the reduction to SGAs and the subtraction of the reference field will be also examined, just for comparison. Also in this analysis, the same standard input dataset was used (Figure 2.8).

Since the smoothness of the field influences the interpolation performance, the measure to express the smoothness of the field should be obtained without interpolation. Many well known smoothness/roughness measures, i.e. Fourier Analysis or fractal theory, have to be performed on regularly sampled data. Unfortunately, the input data is not sampled in regular intervals and may not be interpolated. Therefore, three separate smoothness measures, which can handle scattered data, will be discussed below.

D.1.1. Standard Deviation (StDev)

As the most common measure for variability the standard deviation (StDev) of a dataset can be used, which for discrete data is:

$$\sigma = \sqrt{\frac{1}{N}\sum_{i=1}^{N}(g_i - \mu)^2}, \quad where \quad \mu = \frac{1}{N}\sum_{i=1}^{N} g_i \tag{D.1}$$

Here, g_i is an single measurement, N the total number of measurements and μ the mean of all measurements. The StDev expresses the global variability of the values within a dataset. However, it does not really measure smoothness as the location of the measurements is not taken into account. A simple example to illustrate this is provided in Figure D.2. Here, two datasets both have the values 1, 2 and 4 at locations 1, 2 and 4. On the left the data is arranged in a linear fashion, on the right two data points are swapped. Thus, both datasets have the same StDev, of about 1.5. However, one can see that interpolating the value at location 3 appears to be more straightforward for the left example than for the right one.

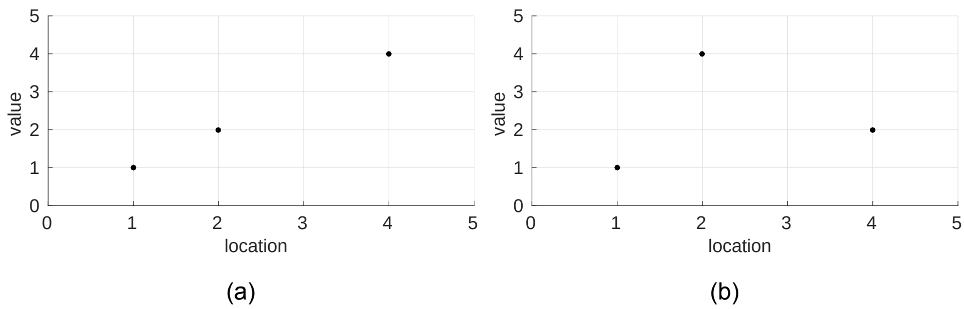

Figure D.2: Two datasets with the same values at the same locations, resulting in the same standard deviation of about 1.5. On left arranged in a linear fashion, on the right the values at location 2 and 4 are interchanged. Resulting in a ”field” harder to interpolate while having the same standard deviation.

Even though the StDev does not really measure smoothness, a smaller StDev does imply smaller deviations from the mean value of the dataset. This makes it not a completely useless measure for expressing smoothness. Also because of its familiarity, the StDev is included here, but is mainly considered as a reference measure.

D.1.2. Local Plane Misfit (LPM)

If all observations would lie in a single plane, which can be simply expressed analytically, i.e. linearly or low order polynomials, one could consider the data to be smooth. Thus, a way of expressing smoothness is the average distance to a certain reference plane. The StDev is actually defined as such. The StDev's reference plane is the mean value of the dataset, which is constant global reference. Because its reference is global the ordering of the data is not taken into account, as illustrated previously.
So, by substituting the global reference by a local reference plane this issue would be solved. It is proposed here to use a local linear plane which is LSQ fitted through the neighbouring observations. This is done by solving a linear system for each target point:

$$\begin{bmatrix} 1 & x_1 & y_1 \\ 1 & x_2 & y_2 \\ \vdots & \vdots & \vdots \\ 1 & x_n & y_n \end{bmatrix} \cdot \begin{bmatrix} a \\ b \\ c \end{bmatrix} = \begin{bmatrix} g_1 \\ g_2 \\ \vdots \\ g_n \end{bmatrix} \tag{D.2}$$

$$g_{ref,i} = a + bx_i + cy_i \tag{D.3}$$

Here, n is the number of neighbours, $g_{ref,i}$ the gravity value of the LSQ local reference plane at the 2-D location, (x_i, y_i), of the target point g_i. The Local Plane Misfit (LPM), a sort of localized StDev, can be defined as the root mean square misfit to this local plane for all observations:

$$\sigma_{LPM} = \sqrt{\frac{1}{N}\sum_{i=1}^{N}[g_i - g_{ref,i}]^2} \tag{D.4}$$

Figure D.3 gives a 3D visualization of the LPM.

Coming back to the StDev example given in Figure D.2, the left plot would have a LPM of 0 while the right examle would have a LPM of about 2.33. This clearly shows the difference in smoothness, remember both had the same StDev.

Neighbour Determination

There would be several ways of determining neighbours for a target point. It was chosen to identify the neighbouring points via Delaunay Triangulation (DT), using RD coordinates. The criteria for DT, which also keep the angles of the triangles as large as possible, ensures close neighbours in all directions of the target point.
Figure D.4 shows an example of a DT of five points.

A drawback of this method for determining neighbours is that there is no control over the maximum distance to certain neighbour. At the edge of the data domain, or in unevenly distributed regions, this could lead to very stretched and thin triangles. However, for the data used here this does not seem to be an issue. The data is evenly distributed and there are relatively few border observations compared with the vast amount of internal observations.

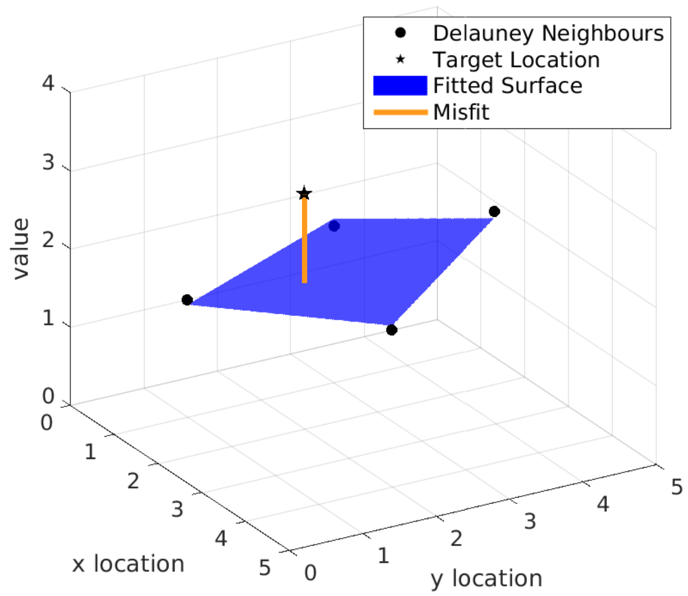

Figure D.3: 3D visualization of the computation of the Local Plane Misfit of the Delaunay Triangulation given in Figure D.4.

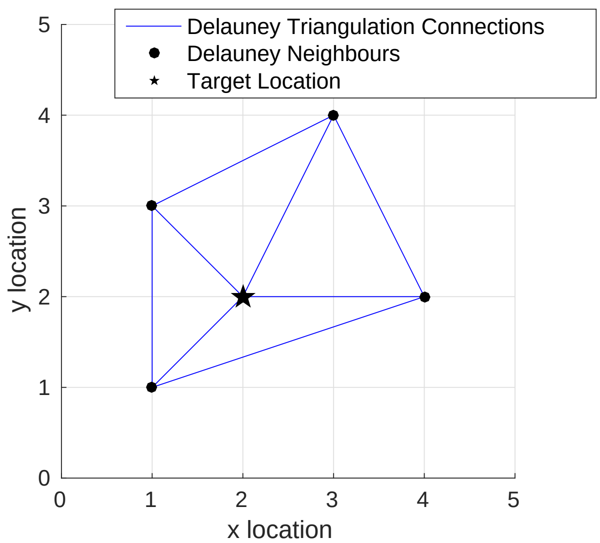

Figure D.4: A Delaunay triangulation of five example points. The four outer points on the convex hull are used to determine the local smoothness of the target location.

D.1.3. Absolute Local Mean Gradient (ALMG)

For this method, the concept of distance to a plane is abandoned. By taking distance between observations directly into account, gradients within a data set may also provide a measure of smoothness. The smoothness measure proposed here is the average of the absolute smoothness values of all points. These individual smoothness values are obtained by taking the mean of the gradients to all Delaunay neighbours for the target points:

$$\sigma_{ALMG} = \frac{1}{N}\sum_{i=1}^{N}\left|\frac{1}{n}\sum_{k=1}^{n}\frac{g_i - g_k}{\sqrt{(x_i - x_k)^2 + (y_i - y_k)^2}}\right| \tag{D.5}$$

Here, g is the value of a point with RD coordinates x and y, averaged over all n Delaunay neighbours for all N target points. Since this method also expresses smoothness, just as the two methods described previously, it is chosen to use the same symbol (σ) even though it has the units of $mGal/m$ instead of $mGal$.

Figure D.5 gives a 3D visualization of the Absolute Local Mean Gradient (ALMG). Once again coming back to the StDev example given in Figure D.2; the left plot has a ALMG of 1 while the right plot has a ALMG of 2.

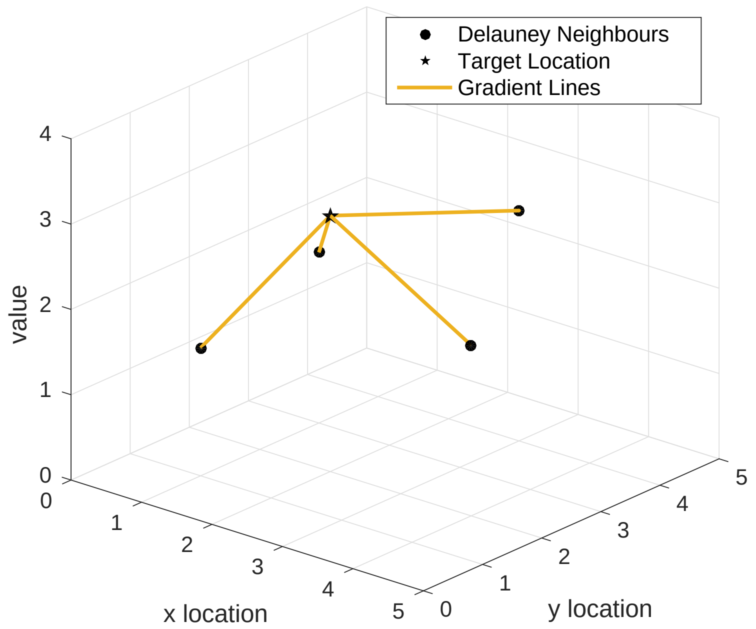

Figure D.5: 3D visualization of the computation of the Local Mean Absolute Gradient of the Delaunay Triangulation given in Figure D.4.

D.2. Results

Table D.1 shows the values obtained with the different smoothness measures. The smoothness of the corrections are first given separately. Then the observed gravity with the influences of the different corrections are given. Smaller values indicate a smoother field. Note, order of magnitude are set equal per column for easier comparison.

Table D.1: Overview of the different smoothness measures for the different gravity corrections and reduced gravity fields.

Field Type	$\sigma[mGal]$	$\sigma_{LPM}[mGal]$	$\sigma_{ALMG}[mGal/m]$
Normal Gravity (on Ellipsoid)	$60.60 \cdot 10^{-5}$	$0.03 \cdot 10^{-6}$	$0.24 \cdot 10^{-7}$
Normal Gravity (on Telluroid)	$63.49 \cdot 10^{-5}$	$13.40 \cdot 10^{-6}$	$24.35 \cdot 10^{-6}$
SGA Reference (SGA_ref)	$8.83 \cdot 10^{-5}$	$0.85 \cdot 10^{-6}$	$2.10 \cdot 10^{-7}$
RTM	$0.92 \cdot 10^{-5}$	$4.61 \cdot 10^{-6}$	$7.18 \cdot 10^{-7}$
Observed Gravity	$61.58 \cdot 10^{-5}$	$11.48 \cdot 10^{-6}$	$30.77 \cdot 10^{-7}$
SGA	$7.67 \cdot 10^{-5}$	$6.53 \cdot 10^{-6}$	$20.14 \cdot 10^{-7}$
SGA - RTM	$7.65 \cdot 10^{-5}$	$5.40 \cdot 10^{-6}$	$19.69 \cdot 10^{-7}$
SGA - SGA_Ref	$6.81 \cdot 10^{-5}$	$6.53 \cdot 10^{-6}$	$20.20 \cdot 10^{-7}$
SGA - SGA_Ref - RTM	$6.66 \cdot 10^{-5}$	$5.41 \cdot 10^{-6}$	$19.76 \cdot 10^{-7}$

D.3. Discussion

As the numbers in Table D.1 are hard to interpret individually, in absolute sence, they will be interpreted with respect to each other. First, the separate corrections are examined after which the influence on the observed gravity will be discussed.

The normal gravity field (at constant height, i.e. the ellipsoid) is known to be a very smooth field. This is also reflected in the local measures, i.e. LPM and ALMG. However, its StDev is almost an order of magnitude larger than that of the SGA reference field and about two orders of magnitude larger than the RTM correction. This is due to the large latitude dependency and therewith large trend in the normal gravity field. This has been illustrated in the StDev example in Figure D.2.
Taking the normal gravity on the telluroid includes height dependency of the data. This can be clearly seen in the very large increase in the local smoothness measures.

Following the same reasoning, it can be seen from the local measures that the SGA reference field is smoother than the RTM corrections. And the StDev shows that the SGA reference field also contains a larger trend than the RTM corrections. This is expected, considering the different purposes of both corrections, discussed in Chapters 2.2 and 2.3.

The observed gravity field has values most similar to the normal gravity at the telluroid. By subtracting this field, the major trends and height dependency are removed. This can be seen in the drop in StDev and local measures respectively.

The RTM corrections hardly change the StDev but slightly improves the local smoothness measures.

The SGA reference field does the opposite, hardly changing the local smoothness measures while decreasing the StDev slightly. These results illustrate the de-trending effect of the SGA reference field and the smoothing effect of the RTM corrections.
Applying both corrections shows the combined effect of de-trending and smoothing.

D.4. Conclusion

The StDev alone is not able to express the smoothness of a data set. The use of a global reference in the StDev makes it sensitive to trends in the data. This sensitivity can be removed by the use of local reference, as in the LMP method.
The interpretation of the local measures in an absolute sense is difficult. Therefore, relative interpretation of the smoothness of the fields was performed. As both measures show the same behaviour the interpreted smoothness effects seems consistent and reliable.

By combining the StDev and the local measures, the differences between trend removal and smoothing effects of the various corrections could be verified. E.g. the large trend removal of the normal gravity and its smoothing effect for height corrections to SGAs, as well as the de-trending of the SGA reference field and smoothing of the RTM corrections.

E

Software: Miscellaneous and Support Routines

The routines described in this appendix are not meant for direct use. The descriptions are supplementary to the MATLAB help of the routines themselves.

E.1. Input Support

Figure 3.1 showed the input support scripts and functions for *ComputeNAPGeopotential*. These scripts are used to pre-process the input for the rest of the function.

E.1.1. CNG_InputPrep

CNG_InputPrep pre-processes the variable input of *ComputeNAPGeopotential*. Extracting the necessary information from the variable input and storing it as the correct arrays. It also handles the optional input arguments and computes the RD coordinates, using the RDNAPTRANS functions which is discussed below.

E.1.2. CNG_InputCheck

CNG_InputCheck verifies if the input is of the right format, class and length. It also validates if all benchmark IDs used in LevelData are provided by BenchData.

E.1.3. CNG_GravPrep

CNG_GravPrep selects the gravity subset used for the interpolation in *ComputeNAPGeopotential*.
The input consists of:

1. the gravity data (”./Data/GravDATA_input.mat”),
2. the benchmark coordinates [Lat, Lon],
3. a desired maximum interpolation distance (set to 10 km by default) and
4. a flag for optional plotting (by default no plots are made).

For the selection of the gravity subset it is attempted to satisfy the following criteria:

- The observations have to be located within the area in which RD coordinates can be computed accurately with the RDNAPTRANS routines.
- The observations have to be located within the convex hull of the benchmarks, extended with a buffer zone. This buffer has a width equal to the desired maximum interpolation distance.
- Starting with the Dutch terrestrial gravity observations it is attempted to satisfy the desired maximum interpolation distance by incorporating the necessary gravity subsets, these subsets have been presented in Figure 2.6 and Table 2.1.

The distribution of interpolation distances between the used gravity measurements and the levelling benchmarks can be plotted by this function when flagged.

E.2. RDNAPTRANS

For the coordinate transformation between ETRS89 and RD coordinates RDNAPTRANS was used, found in ”misc/rdnaptrans”. The whole package consist of many routines from which only *nap2etrs* and *etrs2rdnap* were used here. More information can be found in Bruijne and Brand [2005] or in the help of the individual functions.

E.2.1. etrs2rdnap

The purpose of *etrs2rdnap* is to convert Cartesian ETRS89 coordinates into RD coordinates and NAP heights.

E.2.2. nap2etrs

The purpose of *nap2etrs* is to convert NAP height into ellipsoidal ETRS89 height.

E.2.3. Example

Because *etrs2rdnap* requires ellipsoidal heights as input while only NAP heights are provided in the data, *nap2etrs* is used to convert these into ellipsoidal heights.
Provide below is an example on how both routines are implemented together to compute RD coordinates from the provided ETRS89 latitude and longitude and NAP heights.

```
hell  = nap2etrs(pointLat, pointLon, pointNAP);
rdnap = etrs2rdnap([pointLat*pi/180 pointLon*pi/180 hell] ,'PLH');
```

E.3. Gravity Corrections

The following functions were provided (or inspired) by Cornelis Slobbe.

E.3.1. ComputeNormalGravityAboveEll

ComputeNormalGravityAboveEll computes the normal gravity for a given ellipsoidal geodetic latitude, ellipsoidal height and reference ellipsoid.

E.3.2. ComputeMeanNormalGravity

ComputeMeanNormalGravity computes the mean normal gravity between the ellipsoid and a given ellipsoidal height, for a given ellipsoidal geodetic latitude and reference ellipsoid.
This function is a slightly adjusted version of *ComputeNormalGravityAboveEll*.

E.3.3. TransformPermanentTideSystems

TransformPermanentTideSystems is used in *ComputeNAPGeopotential* to transform gravity from zero to mean tidal system.

However, the function is much more versatile, being able to transform between tide-free, mean and zero tidal systems for:

- Geoid heights,
- Deflection of vertical (in north-south direction),
- GNSS heights,
- Orthometric or normal heights and
- Gravity.

More information and reference is found in the function help.

E.3.4. Gravity Support Scripts

In the previous described functions *defval* is a small function used to assign default values to variables. *RefEllipsoidParam* returns the parameters of a references ellipsoid. Here, only GRS80 was used.

E.4. Output Support

These functions are used for the generation of the *ComputeNAPGeopotential* output plots and spreadsheet. They are located in the corresponding folders in the 'misc' folder. These functions were taken from Mathworks File Exchange.

E.4.1. borders

The base map, including the outline of the Netherlands, for the location plots was created with borders [Greene, 2015].

Note, MATLAB's Mapping Toolbox is needed for the creation of location plots with ComputeNAPGeopotential. Even though it is not necessary for borders, no alternative for scatterm and plotm were found.

E.4.2. xlwrite

The writing of the output spreadsheet in *ComputeNAPGeopotential* is performed by *xlwrite*. This is a robust routine which does not relying on Microsoft Excel. Making it possible to create the output spreadsheet in case a Linux system or Windows without Microsoft Excel is used [de Zegher, 2012].

Bibliography

(2015). *MATLAB version 8.6.0.267246 (R2015b)*. The Mathworks, Inc., Natick, Massachusetts.

Blais, J. (2010). Least squares for practitioners. *Mathematical Problems in Engineering*, 2010.

Bohling, G. (2005). Introduction to geostatistics and variogram analysis. *Kansas geological survey, 20p*.

Brand, G. and Damme, J. (2004). De waterpasmetingen van de 5e NWP. *Ministerie van Verkeer en Waterstaat, AGI-CAP-2004-15 Versie 1.0*.

Bruijne, A. d. and Brand, G. (2005). Geodetic reference frames in the Netherlands: definition and specification of ETRS89, RD and NAP and their mutural relationships. *Nederlandse Commissie voor Geodesie*.

de Min, E. (1995). Zwaartekracht in Nederland, Interpolatie van het 2e order zwaartekrachtnetwerk. `http://www.rijkswaterstaat.nl/zakelijk/open-data/normaal-amsterdams-peil/documenten.aspx`, Retrieved: Jul 2016.

de Zegher, A. (2012). xlwrite: Generate XLS(X) files without Excel on Mac/Linux/Win. `http://nl.mathworks.com/matlabcentral/fileexchange/38591`, Retrieved: Jul 2016.

EurogeoGraphics (2008). EuroDEM Specification Overview. `http://www.eurogeographics.org/content/products-services-eurodem`, Visited: 2016-06-29.

Farahani, H., Slobbe, D., Klees, R., and Seitz, K. (2016). Impact of accounting for coloured noise in radar altimetry data on a regional quasi-geoid model. *Journal of Geodesy*, pages 1–16.

Flury, J. and Rummel, R. (2009). On the geoid–quasigeoid separation in mountain areas. *Journal of Geodesy*, 83(9):829–847.

Forsberg, R. (1984). A study of terrain reductions, density anomalies and geophysical inversion methods in gravity field modelling. Technical report, DTIC Document.

Greene, C. (2015). borders: Simply plot national and US state borders. `https://nl.mathworks.com/matlabcentral/fileexchange/50390`, Retrieved: Jun 2016.

Grombein, T., Seitz, K., and Heck, B. (2013). Optimized formulas for the gravitational field of a tesseroid. *Journal of Geodesy*, 87(7):645–660.

Heck, B. (1990). An evaluation of some systematic error sources affecting terrestrial gravity anomalies. *Bulletin Géodésique*, 64(1):88–108.

Heck, B. and Seitz, K. (2007). A comparison of the tesseroid, prism and point-mass approaches for mass reductions in gravity field modelling. *Journal of Geodesy*, 81(2):121–136.

Hofmann-Wellenhof, B. and Moritz, H. (2006). *Physical geodesy*. Springer Science & Business Media.

Ihde, J., Mäkinen, J., and Sacher, M. (2008). Conventions for the Definition and Realization of a European Vertical Reference System (EVRS)–EVRS Conventions 2007. *EVRS conventions*, 5.

Leismann, M., Klees, R., and Beckers, H. (1992). *Untersuchungen verschiedener Höhensysteme, dargestellt an einer Testschleife in Rheinland-Pfalz*. Beck.

Mäkinen, J. and Ihde, J. (2009). The permanent tide in height systems. In *Observing our changing earth*, pages 81–87. Springer.

Mayer-Guerr, T. (2015). The combined satellite gravity field model GOCO05s. In *EGU General Assembly Conference Abstracts*, volume 17 of *EGU General Assembly Conference Abstracts*.

Menz, A., Benndorf, J., and Wambeke, J. (2015). Signal-controlled least square collocation: A new quality in geostatistical estimation and simulation? *Spatial Statistics*.

Moritz, H. (1978). Least-squares collocation. *Reviews of geophysics*, 16(3):421–430.

Moritz, H. (1980). Geodetic reference system 1980. *Journal of Geodesy*, 54(3):395–405.

Pyrcz, M. and Deutsch, C. (2003). The whole story on the hole effect. *Geostatistical Association of Australasia, Newsletter*, 18:3–5.

Ramsayer, K. (1965). The admissible distances of the gravity points for the determination of geopotential numbers in high mountains, medium high mountains and flat countries. *Bulletin Géodésique (1946-1975)*, 76(1):145–154.

Rülke, A., Liebsch, G., Sacher, M., Schäfer, U., Schirmer, U., and Ihde, J. (2012). Unification of European height system realizations. *Journal of Geodetic Science*, 2(4):343–354.

Sacher, M., Ihde, J., Liebsch, G., and Mäkinen, J. (2009). EVRF2007 as realization of the European Vertical Reference System. *B Geod Sci Aff*, 68(1):35–50.

Sacher, M., Ihde, J., and Svensson, R. (2006). Status of UELN and steps on the way to EVRS 2007. In *Report on the Symposium of the IAG Subcommission for Europe (EUREF), Riga*, pages 14–17.

Sandwell, D. T. (1987). Biharmonic spline interpolation of GEOS-3 and SEASAT altimeter data. *Geophysical research letters*, 14(2):139–142.

Slobbe, D. C. (2013). *Roadmap to a mutually consistent set of offshore vertical reference frames*. PhD thesis, TU Delft, Delft University of Technology.

Tscherning, C., Forsberg, R., and Knudsen, P. (1992). The GRAVSOFT package for geoid determination. In *Proc. 1. continental workshop on the geoid in Europe, Prague*, pages 327–334.

Tscherning, C. C. (1994). Geoid determination by least-squares collocation using GRAVSOFT. *Lecture Notes for the International School for the Determination and use of the Geoid, Milan, October*.

Tscherning, C. C. and Rapp, R. H. (1974). Closed covariance expressions for gravity anomalies, geoid undulations, and deflections of the vertical implied by anomaly degree variance models. *Scientific Interim Report Ohio State Univ., Columbus. Dept. of Geodetic Science.*, 1.

Watson, D. (1992). *Contouring : a guide to the analysis and display of spatial data : with programs on diskette*. Pergamon Press, Oxford New York.

Yang, T. Y. (1986). *Finite element structural analysis*. Prentice-Hall, Englewood Cliffs, N.J.